The nickel-catalyzed hydrocyanation of vinylarenes and dienes : mechanism and appplication

The Nickel-Catalyzed Hydrocyanation of Vinylarenes and Dienes

Mechanism and Application

Jos Wilting

The Nickel-Catalyzed Hydrocyanation of Vinylarenes and Dienes

Mechanism and Application

The Nickel-Catalyzed Hydrocyanation of Vinylarenes and Dienes

Mechanism and Application

PROEFSCHRIFT

ter verkrijging van de graad van doctor aan de
Technische Universiteit Eindhoven, op gezag van de
Rector Magnificus, prof.dr.ir. C.J. van Duijn, voor een
commissie aangewezen door het College voor
Promoties in het openbaar te verdedigen
op woensdag 13 december 2006 om 16.00 uur

door

Jos Bernard Martin Wilting

geboren te Hoogeloon

Dit proefschrift is goedgekeurd door de promotor:

prof.dr. D. Vogt

Copromotor:
dr. C. Müller

Omslag: Jos Wilting, foto door Bart van Overbeeke ©

Druk: Universiteitsdrukkerij, Technische Universiteit Eindhoven

A catalogue record is available from the Library Eindhoven University of Technology

ISBN-10: 90-386-3008-5
ISBN-13: 978-90-386-3008-3

Dit proefschrift is goedgekeurd door de manuscript commissie:

prof.dr. Dieter Vogt (Technische Universiteit Eindhoven)
dr. Christian Müller (Technische Universiteit Eindhoven)
prof.dr. L.A. Hulshof (Technische Universiteit Eindhoven)
prof.dr. B.L. Feringa (Rijksuniversiteit Groningen)
prof.dr. W.D. Jones (University of Rochester, USA)

Contents

Contents

Chapter 1

Nickel-Catalyzed Hydrocyanation of Carbon-Carbon Double Bonds

An Introduction

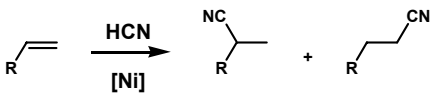

In the catalytic carbon-carbon bond formation toolbox, the hydrocyanation of alkenes has especially great potential since the obtained nitriles can be converted into a variety of products. A short overview will be given on the hydrocyanation of carbon-carbon double bonds: the adiponitrile process, all substrate classes, the mechanism, scope and limitations and the objectives of this thesis will be discussed.

Parts of this Chapter have been published:

Jos Wilting and Dieter Vogt. Asymmetric hydrocyanation of alkenes. In *Handbook of C-H transformations*, 1st ed.; Dyker, G., Ed.; Wiley-VCH: Weinheim, **2005**; Vol. 1 pp 87-96

§ 1.1 Introduction

The hydrocyanation of alkenes [1] is a catalytic carbon-carbon bond formation reaction (Figure 1). The obtained nitriles can be converted into a variety of products (Figure 2) [2]. Although the cyanation of aryl halides [3] and carbon-heteroatom double bonds (aldehydes, ketones, and imines) [4] are well studied, the hydrocyanation of alkenes has mainly focused on the DuPont adiponitrile process [5].

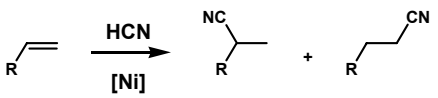

Figure 1 *Nickel-catalyzed hydrocyanation of carbon-carbon double bonds*

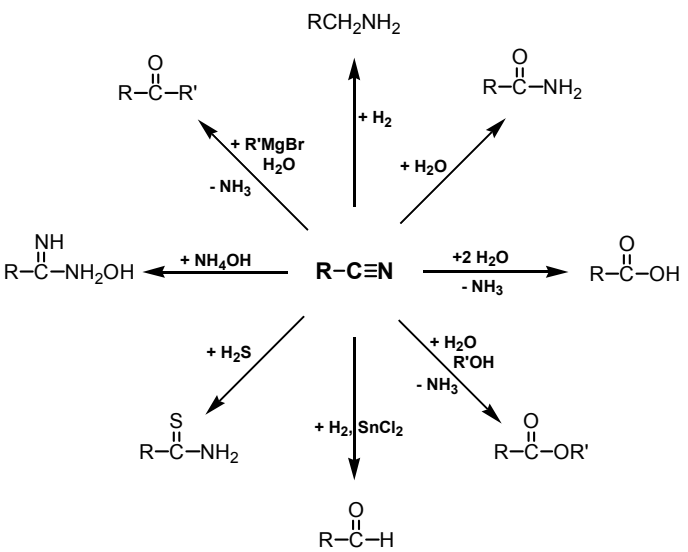

Figure 2 *Nitriles as versatile compounds in organic synthesis*

Adiponitrile is produced from butadiene in a 3-step process via hydrocyanation, isomerization, and a subsequent second hydrocyanation step. This process was developed in the 1970s using a monodentate phosphite-based zerovalent nickel catalyst [6].

Although a number of enzymes are able to enantioselectively catalyze the hydrocyanation of $R_2C=O$ and $R_2C=NR$ bonds [7], (asymmetric) hydrocyanation of carbon-carbon double bonds is unprecedented in biology. In homogeneous catalysis (asymmetric) hydrocyanation is still underdeveloped as can be seen from the relatively few reports in literature. In the following paragraphs a short overview will be given on the hydrocyanation of carbon-carbon double bonds: the adiponitrile process, all substrate classes, the mechanism, scope and limitations and the scope of this thesis will be discussed.

§ 1.2 The adiponitrile process

In 1951 Paul Arthur, Jr. and Burt Carlton Pratt filed a patent on behalf of E.I. du Pont de Nemours regarding the nickel-catalyzed hydrocyanation of conjugated diolefinic compounds. [8] This discovery, using $Ni(CO)_4/PPh_3$ as catalytic system, ultimately led, after 20 years of research, to the adiponitrile process, which has been commercialized in the 70s. [9] Adiponitrile is a precursor for hexane-1,6-diamine which is used to produce Nylon(6,6). Hexane-1,6-diamine is produced mainly via the adiponitrile route (Figure 3).

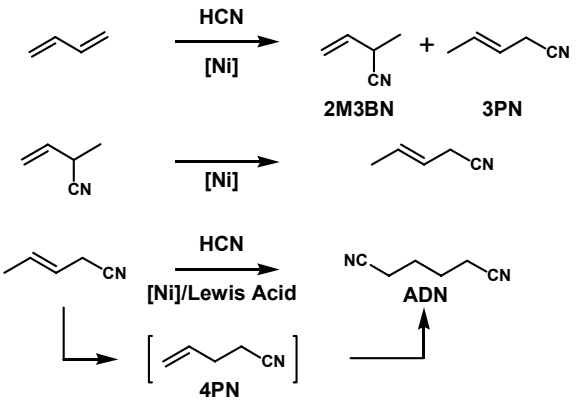

Figure 3 *The 3-step adiponitrile process*

In this process adiponitrile (ADN) is produced in a 3-step process. The first step consists of a single hydrocyanation of 1,3-butadiene. Two products are formed as HCN gives 1,2- and 1,4-addition over the diene, leading to the 1,2-product 2-methyl-3-butenenitrile (2M3BN) and the 1,4-product 3-pentenenitrile (3PN). The ratio depends on the catalyst employed. Reported values for formation of 2M3BN

in the hydrocyanation of butadiene with mono- and bidentate phosphite ligands range between 30-88 % (2M3BN/(2M3BN+3PN). [10] The branched 1,2-product is then converted into the linear 1,4-product in an isomerization reaction involving a carbon-carbon bond activation reaction, which is the second step of the process. The last step is the hydrocyanation of the *in situ* formed 4-pentenenitrile (4PN) to produce ADN. 4PN is formed by isomerization of 3PN by the catalyst system Ligand/Nickel(0)/Lewis acid that also catalyzes the hydrocyanation. These 3 steps are all nickel(0)-catalyzed with a phosphorus ligand system based on triphenylphosphite ($P(OPh)_3$), and the preferred Lewis acid is $ZnCl_2$.

In the 90s the monodentate phosphites were replaced by bidentate ligands, which are superior in terms of activity and efficiency, as only 3 equivalents of bidentate ligand have to be used instead of 15 equivalents of monodentate ligand. [10]

§ 1.3 Substrates used in hydrocyanation reactions

§ 1.3.1 Aliphatic olefins

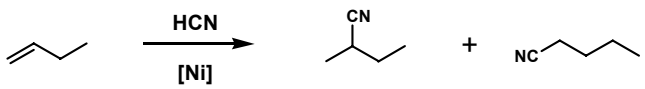

Figure 4 *Nickel-catalyzed hydrocyanation of 1-butene*

In the 50s olefins have been hydrocyanated very selectively towards branched nitriles (the linear products were not observed) with dicobalt octacarbonyl/PPh_3 as catalyst. [11] The reactions were performed in autoclaves at 130 ˚C with substrate/metal ratios of 30-40, which resulted in TON's up to 20. Substrates used in this study were: ethylene, propylene, 1- and 2-butene, 1-octene, 3-pentenenitrile, 4-hexenenitrile, styrene as well as several cyclic olefins. This catalytic system has not received much attention as industry was mainly interested in linear products. The group of Santini studied the possibilities of cobalt-catalyzed isomerization of 2M3BN to 3PN, and although carbon-carbon bond activation was observed, the system was not applicable for the isomerization of 2M3BN. [12]

Taylor reported on the hydrocyanation of α-olefins with NiL_4/L/Lewis Acid as catalytic system (L = P(O-*p*-tol)$_3$) and found that the linear/branched ratio of the obtained products was dependent on the steric properties of the substrate: propylene (1.5), 1-hexene (19-2.3) [13], isobutene (>99), 2,3-dimethyl-1-butene (>99) and 3,3-dimethyl-1-butene (>99). Furthermore, the linear/branched ratio also depended on the Lewis acid used for the hydrocyanation of 1-hexene with $ZnCl_2$ (78 %), $TiCl_3$ (75 %) and $AlCl_3$ (69 %). [14] The position of the double bond in octenes had almost no effect on the linear/branched ratio in the hydrocyanation of octenes with $P(OPh)_3$ and P(O-*p*-^{t}BuPh)$_3$ as ligands. As with 1-hexene, 1-octene isomerized to an equilibrium mixture of octenes, which resulted in similar linear/branched ratios of 87% for 1-octene and 79% for 4-octene. In this study the effect of the Lewis acid on activity (mol product/mol nickel) was investigated: $ZnCl_2$ (3), BPh_3 (5), $AlCl_3$ (10), $AlEtCl_2$ (250). [15]

McKinney investigated the hydrocyanation of ethylene as a model reaction for the hydrocyanation of other olefins and carried out kinetic measurements. The proposed mechanism will be discussed further on in this chapter. [16]

Addition of HCN to vinyltriethoxysilane, vinylmethyldiethoxysilane, vinyl-dimethylethoxysilane and 1,3-divinyltetramethyldisiloxane with $Pd(0)(P(OPh)_3)_4$ afforded the corresponding (cyanoethyl)silanes in 30-80% yield, the (2-cyanoethyl)-silane isomer being the major addition product. [17]

Buchwald developed a convenient stoichiometric method for the anti-Markovnikov hydrocyanation of olefins (Figure 5) utilizing organozirconium chemistry. It has been shown that these systems tolerate a wide range of substrate functionalities. The isocyanide CN^{t}Bu as well as TMSCN are used instead of HCN followed by a workup with I_2. [18]

Figure 5 *Hydrocyanation of olefins with the (anti)-Markovnikov products*

Unfortunately, no follow-up studies have been undertaken. So far, only Ni(0) with bidentate phosphine ligand systems are known to catalyze this reaction, the hydrocyanation of 1-octene and methyl-9-dec-1-enoate, with TON's up to 10. [19]

To summarize, the hydrocyanation of aliphatic olefins is far from an established catalytic reaction as the TON's are between 5 and 20 with substrate/metal ratios up to 40. Still, this reaction has a lot of potential and should be investigated in more detail.

§ 1.3.2 Conjugated dienes

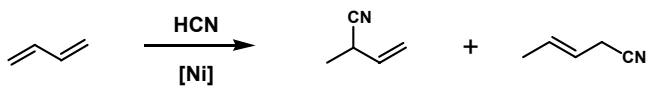

Figure 6 *Nickel-catalyzed hydrocyanation of 1,3-butadiene*

Addition of hydrogen cyanide to dienes results in a 1,2- and a 1,4-product. The most studied reaction of a conjugated diene is the hydrocyanation of 1,3-butadiene as this is the first step in the adiponitrile process, giving 2M3BN (1,2-product) and 3PN (1,4-product) as a mixture. The 1,2- and 1,4-products are identical for systems that react via a symmetrical allyl intermediate (Chapters 4 and 5 of this thesis). This is for instance the case for 1,3-cyclohexadiene and piperylene. Keim and Jackson studied the hydrocyanation of a variety of (conjugated) dienes: 1,3-butadiene, isoprene, piperylene, 1,4-pentadiene, 1,5-hexadiene, 1,7-octadiene and 1,3,7-octatriene. [20,21] Unfortunately, attempted applications of similar hydrocyanation conditions to more complex dienes, e.g. geraniol acetate, geraniol methyl ether, limonene, or 4-phenylpenta-1,3-diene gave only traces of nitriles.

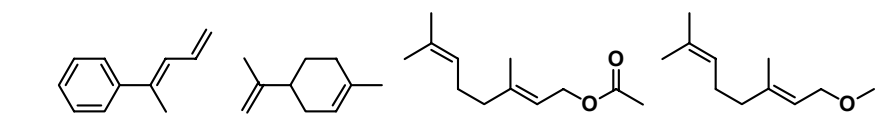

4-phenylpenta-1,3-diene limonene geraniolacetate geraniolmethylether

Figure 7 *Dienes tested unsuccessfully in the nickel-catalyzed hydrocyanation reaction*

Tolman demonstrated that insertion of cyclopentadiene into $DNiL_4^+$ results in a deuterated (π-allyl)nickel complex in which the nickel center and deuterium atom are located on the same side of the ring. [22] Bäckvall and Andell showed *cis* addition of DCN over the diene in 1,3-cyclohexadiene with $Ni(P(OPh)_3)_4$ as catalyst system. [23]

Hydrocyanation of dienes, which are sterically hindered on one side of the diene [24], gives 1,2-addition with high regioselectivity, in which case high enantioselectivities can be achieved. [25] The catalytic system $Ni(0)(DIOP)_2$, reported by Jackson gave low enantioselectivities (<5 %) for 1-phenylbuta-1,3-diene and penta-1,4-diene. [21]

The copper-catalyzed hydrocyanation of conjugated olefins with CuBr and $CuBr_2$ as catalysts with an HCN/Cu ratio of 5 and gave 1,4-addition with high selectivity. [26]

§ 1.3.3 Cyclic (di)enes

The cobalt-catalyzed hydrocyanation of norbornene-like compounds has been reported in the 50s with $Co_2(CO)_8/PPh_3$ as catalytic system. [11] The substrates were the Diels-Alder products of cyclopentadiene with cyclopentadiene, maleic anhydride and acrylonitrile.

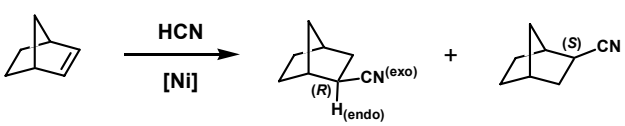

Figure 8 *Nickel-catalyzed hydrocyanation of norbornene*

In 1979 Elmes and Jackson [27-29] described the asymmetric hydrocyanation of norbornene and norbornadiene with $Pd(DIOP)_2$ as the catalyst precursor, resulting in *exo*-2-cyano-norbornane as the product. Parker *et al.* [30,31] looked in more detail into this reaction and studied the coordination chemistry of $(DIOP)Pd(C_2H_4)$ in the presence of HCN. Under these conditions a hydrido cyano and an alkyl cyano palladium complex were detected by NMR. Takaya *et al.* [32] applied the phosphine-phosphite ligand BINAPHOS with palladium and nickel and obtained ee's (enantiomeric excess) of 48%(Pd) and 40%(Ni) with yields of up to 50%. Pringle and Baker [33,34] investigated the diphosphite ligand **1** based on (*R*)-2,2'-binaphthol with nickel, resulting in isolated yields of 40-70% with ee's of 28-38% (M/L/S/ACH [metal / ligand / substrate / acetone cyanohydrine] 1/2/700/350) at different temperatures. Chan *et al.* [35] used the diphosphite ligand **2** based on (*S*)-binaphthol with nickel and found the highest ee for the hydrocyanation of norbornene, 55.0% in 89% yield (M/L/S/ACH 1/7/100/110).

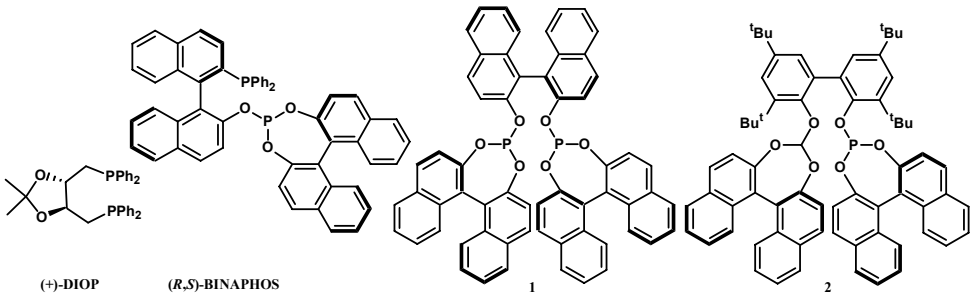

Figure 9 *Chiral ligands used in the asymmetric hydrocyanation of norbornene*

Jackson has shown spectroscopically, by using DCN, that the addition of HCN to norbornene and 4-(^{t}bu)cyclohexene proceeds in a completely stereospecific *cis* fashion over the carbon-carbon double bond with DIOP/Pd^0 as catalyst. [29]

§ 1.3.4 Vinylarenes

Vinylarenes usually react in the hydrocyanation reaction with high regioselectivities (> 98%) to the branched product. Few reports show lower regioselectivity. [18,36] This is an advantage over hydroformylation, where regioselectivity can be a matter of concern.

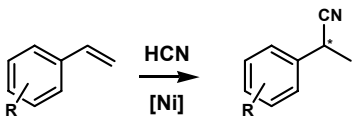

Figure 10 *Hydrocyanation of vinylarenes*

Chan *et al.* tested the Ni(ligand **2**) system also with vinylarenes, and found 50% ee (89% yield) in the hydrocyanation of styrene [35]. With $Ni(cod)_2$ (nickel(0)bis-[1,5-cyclooctadiene]) in the presence of ligand **3** Babin *et al.* observed an ee of 64% for styrene as substrate, however this system has a modest regioselectivity (~65%) [36]. Vogt *et al.* investigated diphosphonite ligands with an achiral xanthene backbone and (*S*)-binaphthyl substituents. [37] These resulted in ee's of 42% (styrene), 63% (4-isobutylstyrene), and 29% (MVN [6-methoxy-2-vinylnaphthalene]) with ligand **4**.

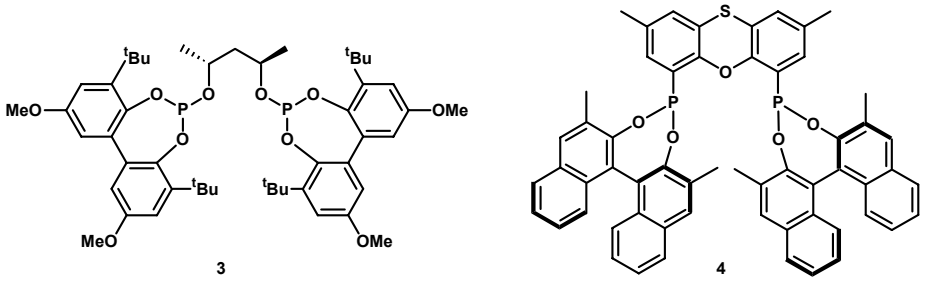

Figure 11 *Ligands studied in the asymmetric hydrocyanation of vinylarenes*

RajanBabu and Casalnuovo [38,39] tested diphosphinite ligand systems (**5** and **6** in Figure 12) based on carbohydrate backbones. The steric and electronic properties were controlled by the substituents on the aryl groups at the phosphorus atoms. The use of different chlorophosphine precursors led to the electronically asymmetric ligand **6**. This approach resulted in both enantiomers of naproxen nitrile from MVN in 91% ee (*S*)-nitrile (ligand **5**) and 95% ee (*R*)-nitrile (ligand **6**) at 0 °C.

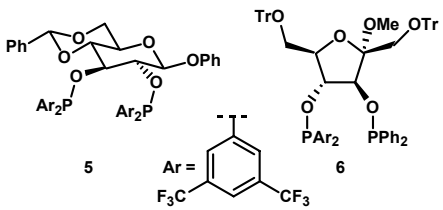

Figure 12 *Ligands used by RajanBabu and coworkers*

§ 1.4 Mechanism

Tolman, Druliner, and McKinney [5] were the pioneers in the nickel-catalyzed hydrocyanation using monodentate phosphites, mainly to understand and improve the adiponitrile process. Although bidentate ligands give better results in the adiponitrile process [40], mechanistic studies with these systems are rare; bidentate phosphinites have been studied in the asymmetric hydrocyanation of MVN [38].

The rate law of the promoted hydrocyanation of 3-pentenenitrile (3PN) to adiponitrile with Ni(P(O-*p*-tol)$_3$)$_4$ has been established to be first order in HCN, Ni, Lewis acid and 3PN and a negative order of 2 for L, by monitoring the temperature after injecting small portions of HCN into a pulse reactor. [5]

$$v = k_{obs} \frac{[Ni]^1[HCN]^1[3PN]^1[LA]^1}{[L]^2} \qquad (1)$$

The unpromoted hydrocyanation of ethylene with Ni(P(O-*o*-tol)$_3$)$_4$ has shown to have zero order rates in substrate and in HCN but first order in catalyst and ligand [16].

$$v = \frac{d[EtCN]}{dt} = k_1[Ni]^1[L]^1 \qquad (2)$$

Furthermore, the possible intermediate [(L)Ni(CN)(C_2H_5)(C_2H_4)] has been characterized by NMR, which led to the conclusion that the reductive elimination of the product is the rate-determining and most important step. During this step an additional ligand would need to recombine with this nickel species resulting in a second order rate law. This is based on the fact that five-coordinated nickel complexes are more effective in the reductive elimination compared to four-coordinated nickel complexes [41].

The rate laws for hydrocyanation of 3PN (Eq. 1) and ethylene (Eq. 2) are inconsistent. This is explainable by the fact that the equilibrium constant for binding ethylene is ~70 times greater than for binding 4PN, whereas P(O-*p*-tol)$_3$ is preferred over P(O-*o*-tol)$_3$ by a factor 10^8. [5]

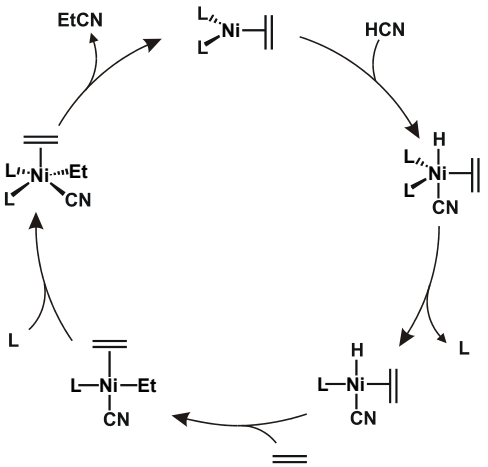

Figure 13 *Catalytic cycle for the nickel-catalyzed hydrocyanation of ethylene with monodentate ligands*

According to the mechanism for hydrocyanation of ethylene, it seems plausible that the reductive elimination step in the catalytic cycle with bidentate ligands, $(PP)Ni^{II}(CN)R$ to $(PP)Ni^{0}(S)$, follows an associative mechanism in which first a substrate molecule or nitrile (S in Eq. 3) coordinates to the nickel, hereby stabilizing the zero valent complex, which is formed during the reductive elimination. The zero valent complex would then be able to exchange S for HCN (resulting in oxidative addition) or the substrate. This would result in a second order rate law.

$$v = \frac{d[RCN]}{dt} = k_1[Ni]^1[S]^1 \tag{3}$$

However, the kinetic model for the hydrocyanation of MVN with bidentate phosphinites is more consistent with the experimental data when both, the rate law for product formation (Eq. 4), which is zero order in substrate, product and HCN, and for catalyst-deactivation (Eq. 5), are combined as displayed by model 1 in Figure 14.

$$v = \frac{d[P]}{dt} = k_1[Ni]^1 \tag{4}$$

$$-\frac{d[Ni]}{dt} = k_2[Ni]^1[HCN]^1 \tag{5}$$

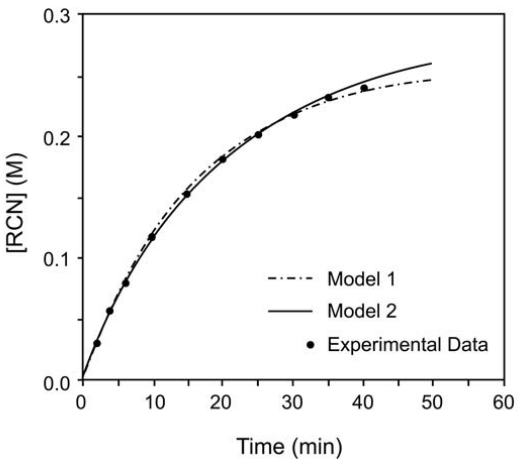

Figure 14 *The hydrocyanation of MVN, kinetic model 1: $d(RCN)/dt=k_1[Ni]$ and $-d[Ni]/dt=k_2[HCN][Ni]$ with $k_1=27\ min^{-1}$ and $k_2=0.15\ M^{-1}min^{-1}$, this figure is reprinted from ref. [38]. Copyright 1994 American Chemical Society.*

Therefore, the reductive elimination cannot follow an associative mechanism as proposed in Eq. 3, as the rate law for the hydrocyanation with a monodentate phosphite (Eq. 2). It should be noted here, that Eq. 2 is based on the substrate ethylene, which is not capable of forming a η^3-intermediate, whereas MVN (Eq. 4) can form an η^3-intermediate. The mechanism for hydrocyanation of vinylarenes with bidentate phosphorus ligands can be proposed as follows.

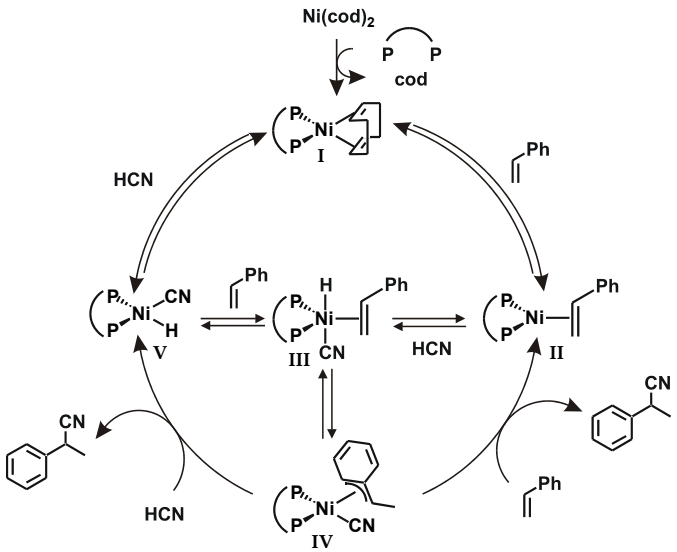

Figure 15 *Catalytic cycle for the hydrocyanation of styrene*

For vinylarenes the proton migration (III to IV) is favored to the branched species by the η^1-η^3 equilibrium, which is not possible for the linear species. Although several η^3-benzylic complexes have been characterized [42,43], the (α-methyl)benzylic cyano nickel complex could not be isolated or even observed. The η^3-η^1 equilibrium has been investigated for an aliphatic allyl cyano nickel(II) complex [44]. Labeling studies with deuterated MVN [38] and 2M3BN [45] revealed an equilibrium for the proton migration. Moreover, the relative rate of reductive elimination over β-hydride elimination increases when the electron density on phosphorus is reduced by introducing electron withdrawing groups on the ligand.

The catalyst deactivates in time through the formation of insoluble cyanonickel complexes $[Ni(CN)_x]^{(2-x)}$, making the deactivation of the catalyst an important issue. The molecular structure of $(PP)Ni(CN)_2$, formed during a hydrocyanation reaction, where PP is a diphosphine ligand, has been reported (Figure 16). [46]

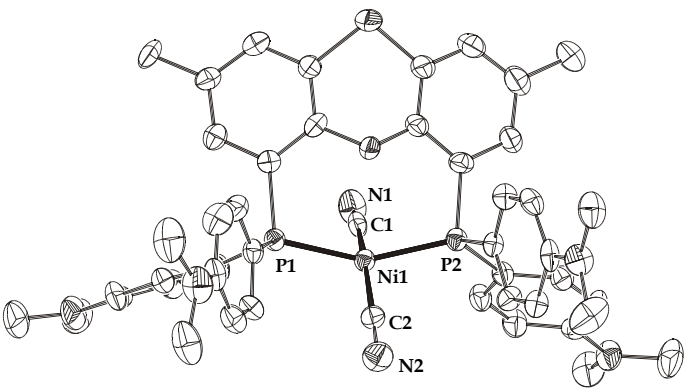

Ni-P(1)	2.208(1)
Ni-P(2)	2.197(1)
Ni-CN(1)	1.863(5)
Ni-CN(2)	1.861(5)
C(1)-N(1)	1.154(6)
C(2)-N(2)	1.145(6)
P-Ni-P	151.51(5)
NC-Ni-CN	161.0(2)

Figure 16 *Molecular structure of $LNi(CN)_2$, hydrogen atoms have been omitted for clarity, thermal ellipsoids are shown at 50 % probability level. Selected bond lengths (Å) and angles (°) with standard deviations in parentheses*

Several other interesting effects have been observed in reductive elimination reactions and in the hydrocyanation reaction. The bite angle [47] induces a significant effect in the reductive elimination. A 10^4 fold rate increase was observed progressing from a small bite angle (~85 °) to a larger bite angle in (DIOP)Pd(CH_2TMS)CN (~100 °, TMS = trimethylsilyl) [48]. The rate shows a dependency on the alkyl group, causing it to vary by orders of magnitude (CH_2CMe_3 ~10 x CH_2TMS >> CH_3). The addition of the Lewis acid $AlPh_3$ increases the rate by a factor 50 [49].

The most commonly used Lewis acid in the last step of the adiponitrile process, the hydrocyanation of 3PN to ADN via 4PN, is $ZnCl_2$. Undoubtedly, other Lewis acids outperform $ZnCl_2$ but no detailed study is present in literature on this topic. Keim reported on $EtAlCl_2$ as Lewis acid for the hydrocyanation of 1-octene. [15] For the hydrocyanation of propene and 1-hexene it has been shown that the Lewis acid, particularly aryl boranes, also influences the linear/branched ratio. [5]

The electronic properties of the phosphorus groups influence the activity and stability of the catalyst during the hydrocyanation. Diphosphine and diphosphinite

catalyst systems benefit greatly from electron withdrawing substituents on the aryl groups [38,46]. Benzene, toluene, and hexane [50] are usually the solvents of choice, while coordinating solvents, such as CH_3CN, have been shown to have a negative influence, resulting in a dramatic drop in yield and ee. The effect of the HCN source (either directly as HCN or *in situ* via acetone cyanohydrin (ACH)), has not been studied carefully. The concentration of free HCN is much lower using ACH leading to less deactivation. However, the role of the acetone formed during the reaction has not been determined. On the other hand a low concentration of HCN can also be achieved by slowly bubbling HCN through the reaction mixture or by adding an HCN solution by syringe pump.

The reductive elimination of the product seems to be the key reaction step and has been studied extensively in other catalytic systems. The influence of the electronic properties of the ligand system is usually of more importance than the steric properties. [51,52] Also computational studies have appeared recently concerning the reductive elimination. [41,53] It remains unclear, which exact ligand properties are required for the catalyst system in the hydrocyanation reaction.

Studies concerning (fundamental) nickel chemistry have been very important for the nickel-catalyzed hydrocyanation reaction as well as inspiring, *i.e.* the work of Wilke [54], and Tolman [5,55,56].

§ 1.5 Scope and limitations

In asymmetric hydrocyanation reactions only the chiral branched products are the desired isomers. Good regioselectivity towards the branched product (>98%) is limited to vinylarenes. Hydrocyanation of 1,3-dienes gives various mixtures depending on the catalyst and conditions; whereas 1-alkenes give the linear nitrile as major product [19]. Both are seen in the adiponitrile process in which the unwanted branched 2M3BN (hydrocyanation product from 1,3-butadiene) is isomerized to the linear product 3-pentenenitrile, which is then hydrocyanated *via* an *in situ* isomerization to 4-pentenenitrile resulting in the linear adiponitrile. Thus vinylarenes and (strained) cyclic alkenes (mainly norbornene) are usually the substrates of choice for the asymmetric hydrocyanation.

Hopefully 1,3-dienes will become feasible substrates in the near future for asymmetric hydrocyanation. Jackson tested $Ni(DIOP)_2$ as catalyst for the asymmetric addition of HCN to pentadiene and 4-phenylbuta-1-3-diene. [21]

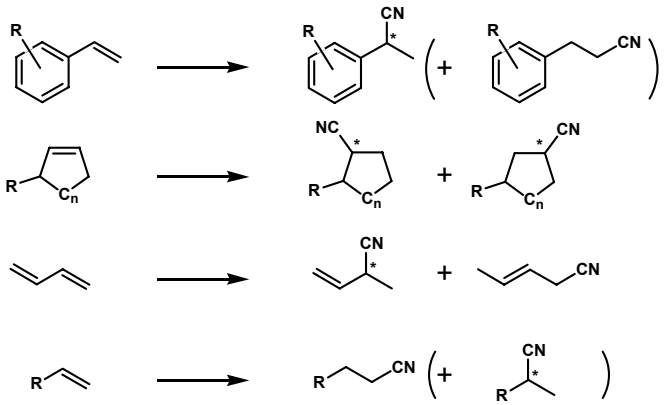

Figure 17 *Substrate variations in the asymmetric hydrocyanation (minor products between brackets)*

The poor turnover numbers (TON) in the hydrocyanation reactions are another limitation, due to catalyst degradation, which still has to be overcome. The maximum TON reached until now have been in the order of 500-750, which is extremely low compared to other homogeneous catalytic reactions, such as hydroformylation and hydrogenation reactions. Nevertheless, the adiponitrile process in the United States has an estimated annual consumption of ~250 kiloton HCN.

An overview of the substrates applied in the hydrocyanation as well as their corresponding products and references is given in Table 1.

Table 1 *Substrates applied in the hydrocyanation reaction*

Entry	Substrate	Main Product(s)	Ref.
1			[11,16]
2		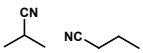	[11,14]
3			[11]
4		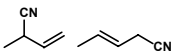	[5,21]
5		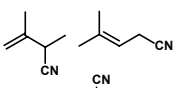	[20,21]
6			[20]
7			[20,21]
8	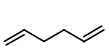	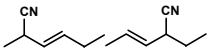	[20,21]
9	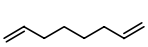	mononitriles	[20,21]
10	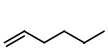	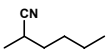	[11]
11	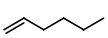	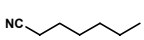	[14]
12	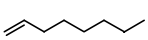	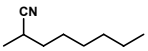	[11]
13	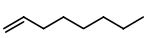	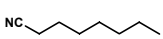	[15,19]
14	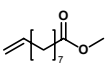	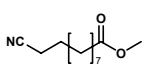	[19]
15		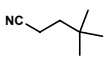	[14,23,29]
16			[14]
17	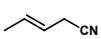	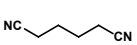	[5,45]
18			[35]
19			[17]
20		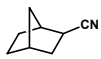	[27-32,34,35]
21			[27,29]
22[a]			[11]
23[a]			[11]
24[a]			[11]
25			[28]
26			[35-38,46]
27			[35,37-39]
28			[23]
29			[11]
30			[29]
31			[21]

[a] exo/endo ratio has not been determined

§ 1.6 Towards improved hydrocyanation reactions

The performance of existing catalysts for the Ni-catalyzed hydrocyanation can be improved on many important points such as: activity, stability and selectivity. In order to improve the hydrocyanation reaction we need to have a better understanding of the reaction mechanism and new catalytic systems have to be developed to give a variety examples where hydrocyanation is successfully employed, so that hydrocyanation becomes one of the tools in the toolbox of synthetic chemists. These new catalytic systems should ideally be systems suitable for systematic variation and not just random hits.

Industry continues to improve the adiponitrile process and filed the first patents on heterogeneous hydrocyanation. [57] In these patents a copper based catalyst system is used in combination with the substrate 1,3-butadiene.

In this thesis, activity and selectivity were given a higher priority than stability, thus no detailed study about deactivation pathways of the catalyst was undertaken. From the 4 substrate classes (Figure 17) vinyl arenes and 1,3-dienes were selected because these substrates can form η^3-intermediates. Moreover, hydrocyanation of these substrates can be performed without the use of a Lewis acid. The research presented in this thesis focused on the understanding of the mechanism of the nickel-catalyzed hydrocyanation reaction for vinylarenes and 1,3-dienes with bidentate phosphorus based ligands. The 3 main aspects studied are coordination chemistry, kinetics and applications (asymmetric hydrocyanation and kinetic resolution).

In Chapter 2 the isomerization of 2M3BN to 3PN catalyzed by a (DPEphos)Ni-species is studied spectroscopically. A kinetic investigation of the isomerization reaction (2M3BN to 3PN) is described in Chapter 3 by applying a variety of bidentate phosphorus based ligands. Chapter 4 describes the preparation of a series of chiral (*R*)-binaphthol based diphosphite ligands with different substituents and their application in the asymmetric hydrocyanation of styrene and 1,3-cyclohexadiene, to investigate the influence of the steric properties of the ligand. The rather unique features of the nickel-catalyzed hydrocyanation of 1,3-cyclohexadiene, identical product formation for 1,2- and 1,4-addition, *cis*-addition over the diene and high enantiomeric excess, were exploited in chapter 5 to determine the enantioselective step. And finally, the kinetic resolution of allylic nitriles using chiral phosphorus based ligands with $Ni(cod)_2$ is discussed in chapter 6.

§ 1.7 References

[1] Huthmacher, K. and Krill, S. Reactions with hydrogen cyanide (hydrocyanation). In *Applied Homogeneous Catalysis with Organometallic Compounds*, 2nd ed.; Cornils, B., Hermann, W. A., Eds.; Wiley-VCH: Weinheim, 2002; Vol. 1 pp 465-486.

[2] Pollak, P., Romeder, G., Hagedorn, F. and Gelbke, H. Nitriles. In *Ullman's encyclopedia of industrial chemistry*, 5th compl. rev. ed.; Wiley-VCH: Weinheim, 1985; Vol. A17 pp 363-376.

[3] Sundermeier, M., Zapf, A. and Beller, M. *Eur. J. Inorg. Chem.* **2003**, (19), 3513-3526.

[4] Groger, H. *Chem. Eur. J.* **2001**, *7* (24), 5246-5251.

[5] Tolman, C. A., McKinney, R. J., Seidel, W. C., Druliner, J. D. and Stevens, W. R. *Adv. Catal.* **1985**, *33*, 1-46.

[6] Drinkard, W. C. Hydrocyanation of olefins using selected nickel phosphite catalysts. US 3,496,215, **1970.**

[7] Gregory, R. J. H. *Chem. Rev.* **1999**, *99* (12), 3649-3682.

[8] Arthur, P., Jr. and Pratt, B. C. Hydrocyanation of conjugated diolefinic compounds. US 2,571,099, **1951.** *Chem. Abstr.* **1952,** *46*, 3068.

[9] Tolman, C. A. *J. Chem. Educ.* **1986**, *63* (3), 199-201.

[10] Foo, T., Garner, J. M. and Tam, W. Hydrocyanation of diolefins and isomerization of nonconjugated 2-alkyl-3-monoalkenenitriles. WO 99/06357, **1999.** *Chem. Abstr.* **1999,** *130*, 169815.

[11] Arthur, P., Jr., England, D. C., Pratt, B. C., and Whitman, G. M. *J. Am. Chem. Soc.* **1954**, *76*, 5364-5367.

[12] Lecocq, V., Santini, C. C., Chauvin, Y., Basset, J. M., and Galland, J. C. *J. Mol. Catal. A: Chem.* **2006**, *246* (1-2), 242-247.

[13] Under catalytic conditions, 1-hexene isomerizes and the equilibrium mixture of hexenes gives a linear/branched ratio of 2.3, pure 1-hexene gives a ratio of 19.

[14] Taylor, B. W. and Swift, H. E. *J. Catal.* **1972**, *26* (2), 254-260.

[15] Keim, W., Behr, A., Bioul, J. P., and Weisser, J. *Erdöl Kohle, Erdgas, Petrochem.* **1982**, *35* (9), 436.

[16] McKinney, R. J. and Roe, D. C. *J. Am. Chem. Soc.* **1985**, *107* (1), 261-262.

[17] Brown, E. S., Rick, E. A., and Mendicino, F. D. *J. Organomet. Chem.* **1972**, *38* (1), 37-42.

[18] Buchwald, S. L. and LaMaire, S. J. *Tetrahedron Lett.* **1987**, *28* (3), 295-298.

[19] Goertz, W., Kamer, P. C. J., Van Leeuwen, P. W. N. M. and Vogt, D. *Chem. Commun.* **1997**, (16), 1521-1522.

[20] Keim, W., Behr, A., Lühr, H. O., and Weisser, J. *J. Catal.* **1982**, *78* (1), 209-216.

[21] Campi, E. M., Elmes, P. S., Jackson, W. R., Lovel, C. G., and Probert, M. K. S. *Aust. J. Chem.* **1987**, *40* (6), 1053-1061.

[22] Tolman, C. A. *J. Am. Chem. Soc.* **1970**, *92* (23), 6785-6790.

[23] Bäckvall, J. E. and Andell, O. S. *Organometallics* **1986**, *5* (11), 2350-2355.

[24] Zhang, A. and RajanBabu, T. V. *J. Am. Chem. Soc.* **2006**, *128* (1), 54-55.
[25] Saha, B. and RajanBabu, T.V. *Org.Lett.* **2006** *In Press*.
[26] Puentes, E., Mamalis, I., Noels, A. F., Hubert, A. J., Teyssie, P., and Waddan, D. Y. *J. Catal.* **1983**, *82* (2), 365-372.
[27] Elmes, P. S. and Jackson, W. R. *J. Am. Chem. Soc.* **1979**, *101* (20), 6128-6129.
[28] Elmes, P. S. and Jackson, W. R. *Aust. J. Chem.* **1982**, *35* (10), 2041-2051.
[29] Jackson, W. R. and Lovel, C. G. *Aust. J. Chem.* **1982**, *35* (10), 2053-2067.
[30] Hodgson, M. and Parker, D. *J. Organomet. Chem.* **1987**, *325* (1-2), C27-C30.
[31] Hodgson, M., Parker, D., Taylor, R. J. and Ferguson, G. *Organometallics* **1988**, *7* (8), 1761-1766.
[32] Horiuchi, T., Shirakawa, E., Nozaki, K. and Takaya, H. *Tetrahedron: Asymmetry* **1997**, *8* (1), 57-63.
[33] Baker, M. J., Harrison, K. N., Orpen, A. G., Pringle, P. G. and Shaw, G. *J. Chem. Soc., Chem. Commun.* **1991**, (12), 803-804.
[34] Baker, M. J. and Pringle, P. G. *J. Chem. Soc., Chem. Commun.* **1991**, (18), 1292-1293.
[35] Yan, M., Xu, Q. Y. and Chan, A. S. C. *Tetrahedron: Asymmetry* **2000**, *11* (4), 845-849.
[36] Babin, J. E. and Whiteker, G. T. Asymmetric syntheses using optically active metal-ligand complex catalysts. US 5,360,938, **1994.** *Chem. Abstr.* **1995,** *122*, 186609.
[37] Goertz, W., Kamer, P. C. J., Van Leeuwen, P. W. N. M. and Vogt, D. *Chem. Eur. J.* **2001**, *7* (8), 1614-1618.
[38] Casalnuovo, A. L., RajanBabu, T. V., Ayers, T. A. and Warren, T. H. *J. Am. Chem. Soc.* **1994**, *116* (22), 9869-9882.
[39] RajanBabu, T. V. and Casalnuovo, A. L. *J. Am. Chem. Soc.* **1996**, *118* (26), 6325-6326.
[40] Kreutzer, K. A. and Tam, W. Hydrocyanation process and multidentate phosphite and nickel catalyst composition therefor. WO 9611182, **1996.** *Chem. Abstr.* **1996,** *125*, 114851.
[41] Tatsumi, K., Nakamura, A., Komiya, S., Yamamoto, A. and Yamamoto, T. *J. Am. Chem. Soc.* **1984**, *106* (26), 8181-8188.
[42] Gatti, G., Lopez, J. A., Mealli, C. and Musco, A. *J. Organomet. Chem.* **1994**, *483* (1-2), 77-89.
[43] Albers, I., Alvarez, E., Campora, J., Maya, C. M., Palma, P., Sanchez, L. J. and Passaglia, E. *J. Organomet. Chem.* **2004**, *689* (4), 833-839.
[44] Brunkan, N. M. and Jones, W. D. *J. Organomet. Chem.* **2003**, *683* (1), 77-82.
[45] Druliner, J. D. *Organometallics* **1984**, *3* (2), 205-208.
[46] Goertz, W., Keim, W., Vogt, D., Englert, U., Boele, M. D. K., Van der Veen, L. A., Kamer, P. C. J. and Van Leeuwen, P. W. N. M. *J. Chem. Soc., Dalton Trans.* **1998**, (18), 2981-2988.
[47] Casey, C. P. and Whiteker, G. T. *Isr. J. Chem.* **1990**, *30* (4), 299-304.
[48] Marcone, J. E. and Moloy, K. G. *J. Am. Chem. Soc.* **1998**, *120* (33), 8527-8528.

[49] Huang, J., Haar, C. M., Nolan, S. P., Marcone, J. E. and Moloy, K. G. *Organometallics* **1999**, *18* (3), 297-299.
[50] The catalyst precursor is not very soluble in hexane and gives a slurry which becomes homogeneous during catalysis.
[51] Culkin, D. A. and Hartwig, J. F. *Organometallics* **2004**, *23* (14), 3398-3416.
[52] Caporali, M., Müller, C., Staal, B. B. P., Tooke, D. M., Spek, A. L., and Van Leeuwen, P. W. N. M. *Chem. Commun.* **2005**, (27), 3478-3480.
[53] Zuidema, E., Van Leeuwen, P. W. N. M., and Bo, C. *Organometallics* **2005**, *24* (15), 3703-3710.
[54] Wilke, G. *J. Organomet. Chem.* **1980**, *200* (1), 349-364.
[55] Tolman, C. A. *Chem. Soc. Rev.* **1972**, *1* (3), 337-353.
[56] Tolman, C. A. *Chem. Rev.* **1977**, *77* (3), 313-348.
[57] Druliner, J. D., Herron, N. and Lecloux, D. Copper-catalyzed, vapor-phase hydrocyanation process for the conversion of diolefinic compounds with hydrogen cyanide into unsaturated nitriles. WO 2002092551, **2002.** *Chem. Abstr.* **2004,** *137*, 371731.

Chapter 2

Nickel-Catalyzed Isomerization of 2−Methyl−3−Butenenitrile

A Spectroscopic Study

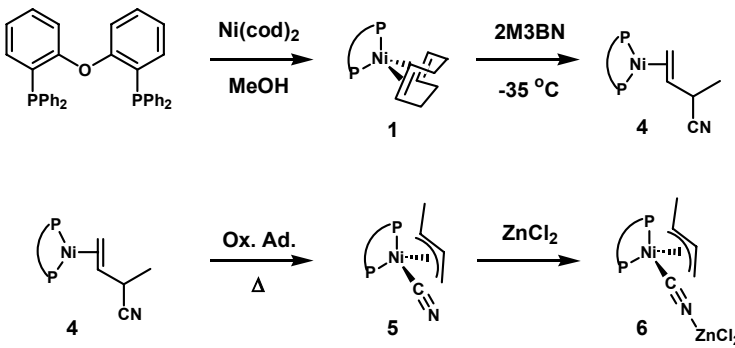

The isomerization of the branched 2M3BN to the linear 3PN by a DPEphosNi-species has been investigated by means of variable temperature NMR spectroscopy. The catalyst precursor DPEphosNi(cod) has been characterized by X-ray diffraction and its reactivity has been investigated. An intermediate in this reaction, which is formed via carbon-carbon bond activation, could be trapped by addition of $ZnCl_2$ and the molecular structure of the corresponding Ni(II) complex has been determined crystallographically. A range of diphosphine ligands was applied in the isomerization of 2M3BN and in the hydrocyanation of styrene.

Parts of the work described in this chapter have been published:

Jos Wilting, Christian Müller, Alison C. Hewat, Dianne D. Ellis, Duncan M. Tooke, Anthony L. Spek, and Dieter Vogt. Nickel-Catalyzed Isomerization of 2-Methyl-3-butenenitrile, *Organometallics* **2005**, *24* (1), 13-15.

Duncan M. Tooke, Jos Wilting, Dieter Vogt, and Anthony L. Spek. 2-(Diphenylphosphino)-phenyl 2-(diphenylphosphinoyl)phenyl ether, *Acta Crystallographica, Section E: Structure Reports Online* **2005**, *E61* (8), o2406-o2407.

§ 2.1 Introduction

Among carbon-carbon bond formation reactions, the hydrocyanation of alkenes is an attractive, yet challenging route for the functionalization of carbon-carbon double bonds. [1] The Ni-catalyzed isomerization of 2−methyl−3−butenenitrile (2M3BN) to 3−pentenenitrile (3PN), for example, is closely related to the hydrocyanation, and is at the same time an important step in the industrial adiponitrile process. [2]

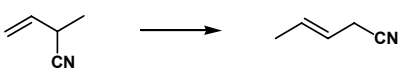

Figure 1 *The Ni-catalyzed isomerization of 2M3BN to 3PN*

In combination with $Ni(cod)_2$, all classes of bidentate phosphorus ligands (phosphines [3,4], phosphinites [5], phosphonites [6], and phosphites [7]) catalyze the isomerization, without the addition of Lewis-acids. However, the influence of ligand parameters on this conversion still remains unknown. The isomerization is in fact a suitable reaction to study the reductive elimination to the final product 3PN without the deactivation of the catalyst usually caused by HCN during hydrocyanations. [8] Goertz *et al.* obtained a dicyano nickel complex, which precipitated during catalysis (Figure 16 in Chapter 1). [9] In this chapter a spectroscopic investigation is described of the isomerization of 2M3BN to 3PN catalyzed by DPEphos/$Ni(cod)_2$ to study the reductive elimination of nitriles, which is believed to be the crucial step in catalytic hydrocyanation reactions.

§ 2.2 Coordination of DPEphos to Ni(0) and Ni(II)

Addition of 2,2′-bis(diphenylphosphine)diphenylether (DPEphos) to $Ni(cod)_2$ in MeOH gives DPEphosNi(cod) as orange powder in almost quantitative yield (Figure 2). The ^{31}P NMR signal shifts from –16.5 ppm for the free ligand to 33.1 ppm for **1**. Crystals suitable for X-ray diffraction were grown from a saturated toluene solution layered with *n*-hexanes (Figure 3). The molecular structure shows a distorted pseudo tetrahedral coordination around nickel as is known for other (PP)Ni(cod) complexes. [10,11]

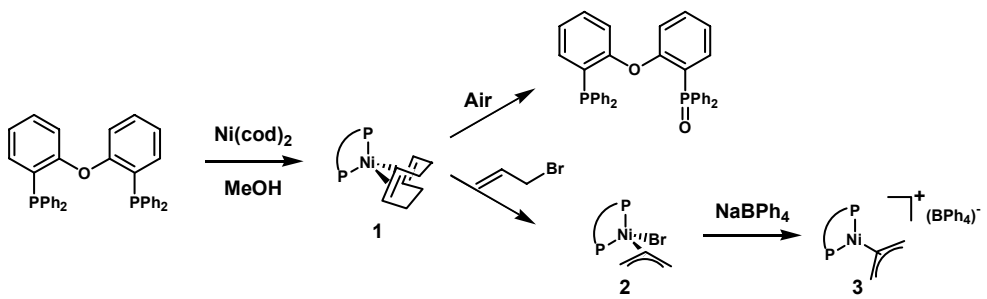

Figure 2 *Reaction of DPEphos with $Ni(cod)_2$, followed by reaction with air and allylbromide and $NaBPh_4$.*

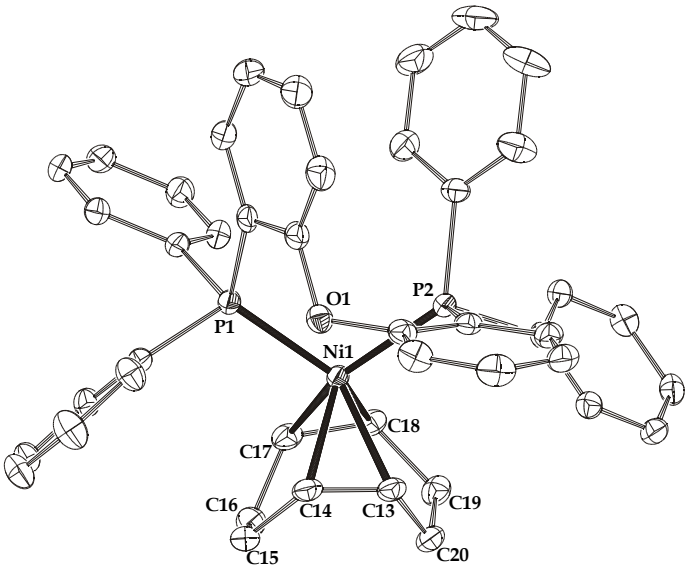

Figure 3 *Molecular structure of DPEphosNi(cod) (**1**). Hydrogen atoms have been omitted for clarity, thermal ellipsoids are shown at 50 % probability level. Selected bond lengths for (**1**) with estimated errors between parentheses: Ni-C13=2.1210(2), Ni-C14=2.124(3), Ni-C17=2.100(2), Ni-C18=2.095(2)*

Treatment of a THF/pentane solution of **1** with air causes decomposition of the complex and to mono oxidation of the ligand DPEphos. Crystals suitable for X-ray diffraction were obtained from this solution after 2 weeks at –30 ^{o}C (Figure 4).

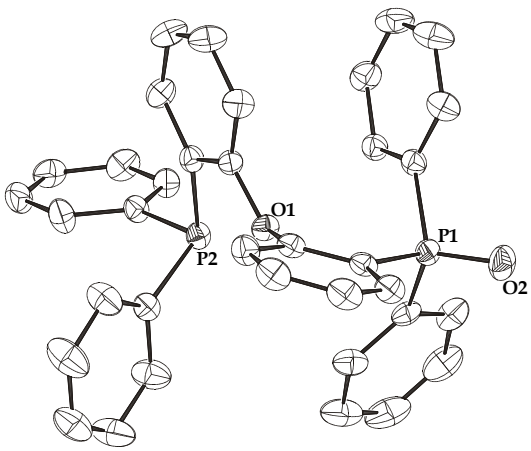

Figure 4 *Molecular structure of DPEphos mono oxide. Hydrogen atoms have been omitted for clarity, thermal ellipsoids are shown at 50 % probability level. Selected bond lengths for DPEphos mono oxide with estimated errors between parentheses: P(1)-O(1)=1.4832(14)*

Oxidative addition of 1 equivalent of allylbromide to **1** gives **2** *in situ*. Consecutive anion exchange with $NaBPh_4$ results in formation of **3** (Figure 2). Crystals suitable for X-ray diffraction were obtained by slow diffusion of methanol in to a CH_2Cl_2 solution of **3** (Figure 5). The center carbon atom of the allyl fragment is distorted as the allyl fragment can be positioned in two conformations (only one conformation is shown in Figure 5, in the second conformation the allyl fragment is rotated 180°). Reaction of **3** with KCN did not result in formation of (DPEphos)Ni(C_3H_5)CN.

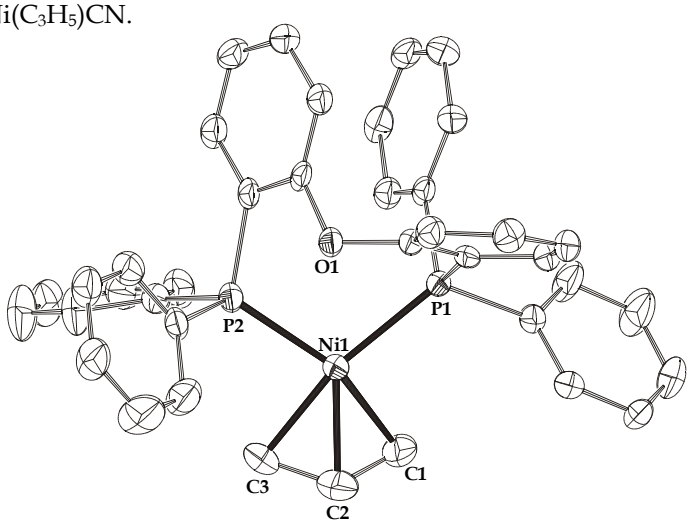

Figure 5 *Molecular structure of [DPEphosNi(C_3H_5)][BPh_4] (**3**), anion and hydrogen atoms have been omitted for clarity, thermal ellipsoids are shown at 50 % probability level. Selected bond lengths for (**3**) with estimated errors between parentheses: Ni-C1=2.041(3), Ni-C2=2.014(4), Ni-C3=2.049(3)*

Typical for DPEphos is the π-stacking of two phenyl rings, with one of the two being a phenyl ring of the diphenyl ether backbone. Other ligands in this class of bidentate phosphine ligands (Xantphos, Sixantphos, etc.) show no π-stacking because they have a rigid backbone, which changes the 'bite angle' [12] but also the steric pocket where the actual catalysis takes place. This Xantphos type of ligands has been applied in a variety of catalytic reactions and for each reaction a specific bite angle and/or steric pocket is required to give the best results.

Addition of another equivalent of DPEphos to DPEphosNi(cod) (**1**) gives formation of Ni(DPEphos)$_2$. Unfortunately no crystals suitable for X-ray analysis were obtained. The $^{31}P\{^1H\}$ signal shifts to 14.9 ppm (broad signal). These Xantphos

type bis-chelates have been studied by Goertz *et al.* in more detail, and have been shown to be still active in hydrocyanation reactions. [9] Other bis-chelate complexes are more stable and are less active or inactive in catalysis. [13] This can be rationalized since the nickel center is shielded by the two ligands, and is, in this configuration, not accessible (a space filling model of $Ni(dppb)_2$ [14] is shown in Figure 6).

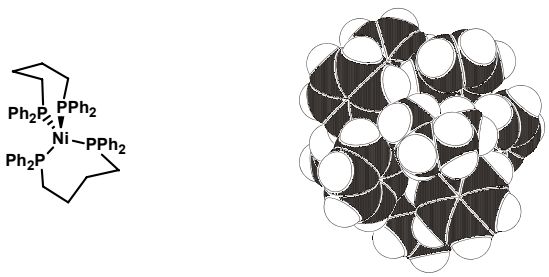

Figure 6 *The molecular structure of $Ni(dppb)_2$ from ref. [14] displayed as chemical structure, and as space filling model*

However, with the Xantphos type ligands the bis-chelates can easily lose one ligand to form a nickel complex, which is active in catalysis. The catalyst system DPEphos/Ni(0) was tested in the isomerization of 2M3BN to 3PN. The rate of isomerization increases for this system going from 1 to 3 equivalents of DPEphos (TOF = 198 and 334 h^{-1} respectively), which clearly indicates that no stable bis-chelates are formed. The increase in TOF arises probably from a change in the equilibrium between mono-chelate and bis-chelate species. Both NMR and UVvis spectroscopy measurements were undertaken in order to quantify the change in equilibrium but gave inconclusive results.

Upon adding 1 equiv. DPEphos to $Ni(cod)_2$ in toluene-d_8 the ^{31}P NMR displays a singlet at $\delta = 33.1$ ppm for the species (DPEphos)Ni^0(cod) (**1**) (Figure 7). This signal disappears on addition of approximately 3 equiv. of 2M3BN at −35 °C, and two doublets appear at $\delta = 21.3$ and 24.2 ppm, with $^2J_{pp} = 38$ Hz. These resonances correspond to (DPEphos)Ni^0(2M3BN) (**4**) with 2M3BN most likely coordinating through its carbon-carbon double bond. The η^2−alkene complex (DPEphos)Ni^0(styrene), which can be prepared via addition of styrene to (**1**) or by reduction of $DPEphosNiCl_2$ with Zn dust in the presence of styrene, gives a very similar ^{31}P NMR spectrum (Figure 8), which shows two doublets at δ=20.2 and 22.9 ppm with $^2J_{pp} = 44$ Hz. Upon warming to +25 °C, the two doublets of **4** disappear and no signal could be detected anymore in the ^{31}P NMR spectrum. The ^1H NMR

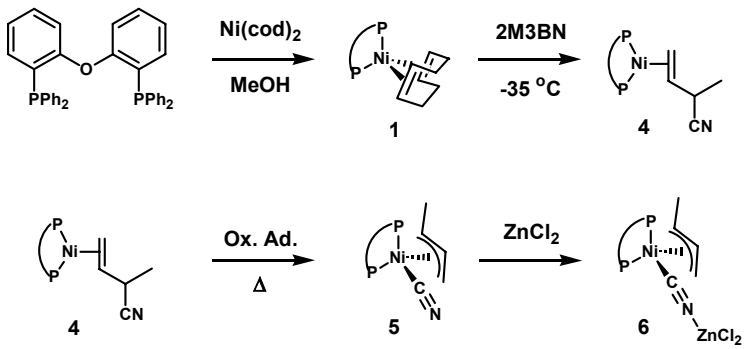

Figure 7 *Reaction of **1** with 2M3BN*

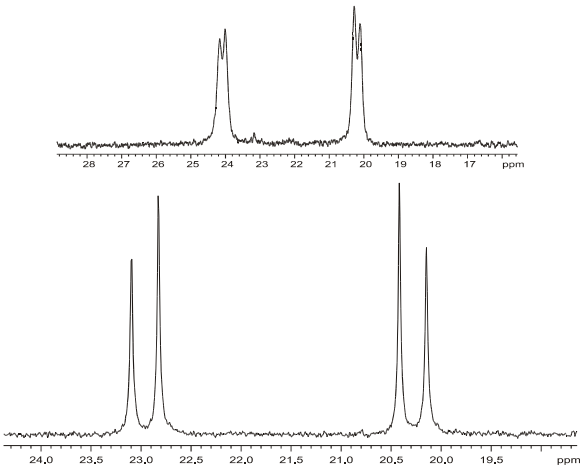

Figure 8 *$^{31}P\{^{1}H\}$ NMR spectra of **1** + 2M3BN at –35 °C (upper) and **1** + styrene at 20 °C (lower)*

spectrum shows broad signals at δ = 4.5 (C*H*CH_2), 3.4 (C*H*CH_3), 2.4 (1H, C$H^{syn}H^{anti}$), 1.6 (CH_3) and 1.2 (1H, $CH^{syn}H^{anti}$) ppm. Increasing the temperature to +35 °C causes slow isomerization of 2M3BN to 3PN, indicated by the methyl signals in the ^{1}H NMR spectrum. The 3PN analogue (DPEphos)Ni^{0}(3PN) could not be detected by variable temperature NMR spectroscopy when approximately 5 equiv. of 3PN were added to **1**. However, **1** disappears and the same broad signals in the ^{1}H NMR spectrum occur, which were detected upon warming of **4**. This spectrum can be ascribed to (DPEphos)$Ni^{II}(C_4H_7)$(CN) (**5**), which is formed by oxidative addition of 2M3BN or 3PN to the Ni(0)-center (Figure 7). Chaudret *et al*. reported similar

^{1}H NMR data for (dppb)Ni^{II}(C_4H_7)(CN). [4] Both complexes display distinct signals for the *syn* and *anti* protons. The substitution of 1,5-cyclooctadiene by 2M3BN occurs faster compared to the substitution by 3PN as is expected for a terminal versus an internal alkene. [15]

Cooling the NMR tube from +35 to −85 °C gave 3 sets of signals as displayed in Figure 9. [16] One set of very low intensity is similar to the signals of **4**. The other two sets most likely correspond to the *syn* and *anti* isomers of **5** (Figure 10), with $^2J_{pp}$ = 49 Hz and 64 Hz. Isomerization between *syn* and *anti* is indeed possible via the η^1−methylallyl species **I** and **II**, which can undergo rotation of the C2-C3 bond without exchange of the *syn* and *anti* protons of the CH_2 group. [17] The other η^1−methylallyl species **III** and **IV** would give interconversion of the *syn* and *anti* protons upon rotation of the C1-C2 bond. Although this interconversion is not observed, the formation of 3PN is likely to proceed via **III** and **IV**. Slowly warming the NMR tube shows the dynamic behavior: first the two sets of doublets become one set of broad signals (−40 °C) indicating fast exchange between the *syn* and *anti* isomers without rotation of the allyl group. Only one position seems to be favored as only 2 species were detected at low temperature. Rotation of the allyl group, indicated by one broad signal, is observed at 0 °C. This signal disappears after warming the NMR tube to temperatures above 20 °C. At these temperatures the complex becomes catalytically active, *i.e.* reductive elimination to form the isomerized product occurs.

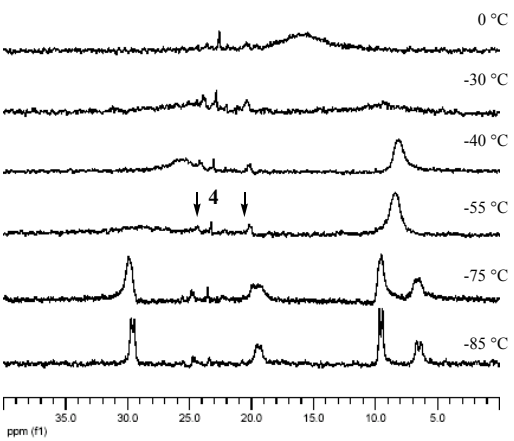

Figure 9 $^{31}P\{^1H\}$ VT NMR spectra on a sample of 1 equiv. of DPEphos and $Ni(cod)_2$ in toluene-d_8 to which 3 equiv. of 2M3BN were added at -78 ºC

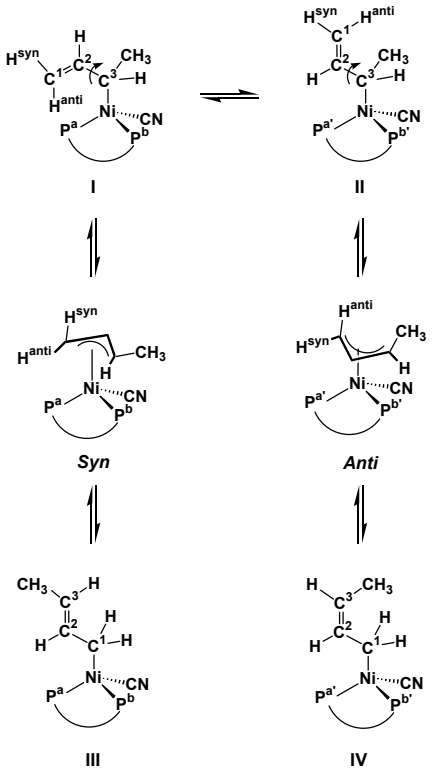

Figure 10 *The η^1-η^3 equilibrium of complex* **5**

The addition of $ZnCl_2$ to **5** caused precipitation of complex **6**. The ^1H NMR spectrum is similar to the spectrum of **5**. An alternative route to complex **6** is addition of either 2M3BN or 3PN to $DPEphosNiCl_2$ in the presence of zinc dust. However, from a mixture of 2M3BN and 3PN (1:1) only 2M3BN gave oxidative addition to Ni(0) at 20 ^oC, no isomerization is observed due to precipitation of complex **6**. This demonstrates the large difference in reaction rate for coordination of 2M3BN over 3PN to the Ni-center (*vide infra*). [15]

Single crystals of **6** suitable for X-ray diffraction could be obtained. The molecular structure of **6** is shown in Figure 11. Selected bond lengths and distances are reported in Figure 11 and Table 1. It is best described as pseudo tetrahedral around the nickel center, which has also been observed in the recently reported structures for (dppb)$Ni^{II}(C_4H_7)(CN)$ [4] and (dppf)$Ni^{II}(C_4H_7)(CNBEt_3)$ [18], which are described as trigonal pyramidal. The molecular structures are very similar and without any noteworthy difference in bond lengths, *i.e.* the Ni-CN bond length is 1.895±3 Å in all structures, thus the Lewis acid $ZnCl_2$ has little influence. This is also observed during catalysis, which shows similar rates for 0, 1, and 2 equiv. of $ZnCl_2$ in DMSO. However, the molecular structure reported for (dippe)$Ni^{II}(C_3H_5)(CN)$ has a square pyramidal geometry with the CN in the apical position. [19] The structural difference originates from the short bridge between the phosphorus atoms resulting in different P-Ni-P angles (105.9 ° in **6** vs. 88.7 ° in (dippe)$Ni^{II}(C_3H_5)(CN)$).

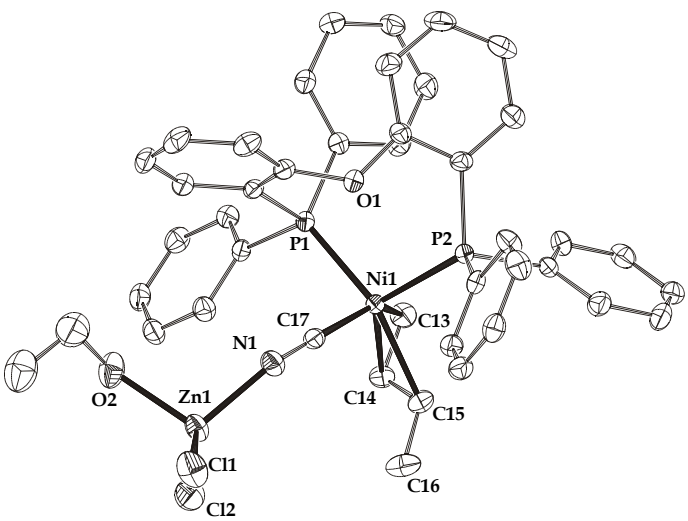

Figure 11 *Molecular structure of* **6**, *hydrogens and the additional solvent molecule (benzene) of crystallization have been omitted for clarity. Thermal ellipsoids are shown at 50 % probability level, selected bond lengths (Å) and angles (°): Ni(1)-C(17) = 1.893(2), C(17)-N(1) = 1.150(3), Ni(1)-C(13) = 2.067(3), Ni(1)-C(14) = 2.000(3), Ni(1)-C(15) = 2.148(3), N(1)-Zn(1) = 1.985(2)*

Table 1 *Selected bond lengths (Å) and angles (°) for the X-ray structures*

Bond/Angle	DPEphosO	**1**	**3**	$Ni(dppb)_2$	**6**
$P\text{-}C_{(av)}$	1.802	1.840	1.823	1.860	1.834
$OP\text{-}C_{(av)}$	1.830	-	-	-	-
P1-Ni	-	2.1560(7)	2.2482(7)	2.208	2.3080(6)
P2-Ni	-	2.1728(7)	2.2060(8)	2.201	2.2031(6)
Ni···O	-	3.1758(16)	3.3076(18)	-	3.3266(18)
π-stack (dist.)	3.8289(10)	3.8258(16)	3.6380(14)	-	3.6198(14)
π-stack (α)	17.80	23.61	16.70	-	13.89
P-Ni-P	-	105.54	105.24(3)	105.05[a]	105.89(2)

[a] Average angle of chelating ligand with Ni

Warming up a sample of compound **6** results in reductive elimination of 2M3BN and 3PN as well as isomerization of 2M3BN to 3PN. At 50 °C approximately equal amounts of 2M3BN and 3PN are formed, predominantly 3PN is observed upon heating the NMR tube to 75 °C, most likely due to isomerization.

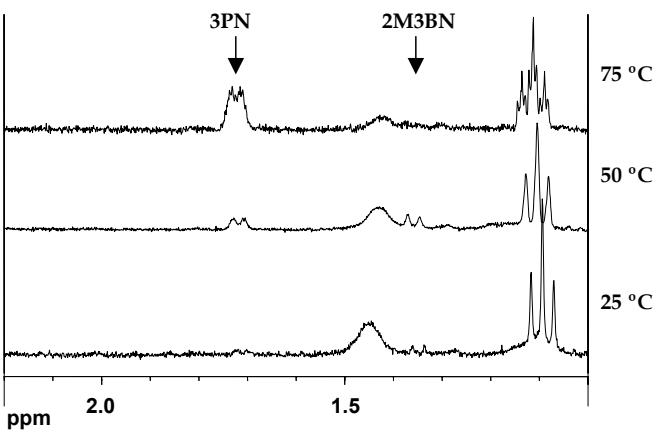

Figure 12 *VT ^{1}H NMR spectra of the reductive elimination from* **6** *in DMSO-d_6*

§ 2.3 Diphosphine ligands applied in hydrocyanation and isomerization

A range of diphosphine ligands (Figure 13) was tested under equal reaction conditions in the nickel-catalyzed isomerization of 2M3BN to 3PN and in the nickel-catalyzed hydrocyanation of styrene. The result of the reaction is likely to be dependent on structural properties such as the P-Ni-P angle [20,21], the rigidity of the ligand as well as the steric properties.

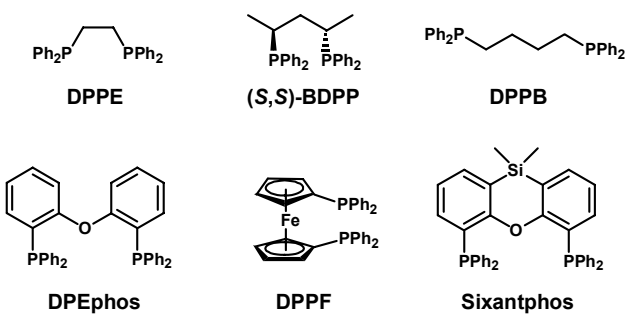

Figure 13 *Chemical structures of the diphosphine ligands*

The isomerization reaction was performed in 2 mL of toluene with 0.5 mL of substrate (2M3BN) at 100 °C with a nickel concentration of 0.0073 M. The substrate to metal ratio was 285, and the reaction was followed by means of GC analysis. The hydrocyanation of styrene was performed starting with 1.0 mL of toluene with a 0.018 M nickel concentration to which was added 1.0 mL with ~2.5 equivalents of HCN by syringe pump at 60 °C with a styrene to nickel ratio of 100.

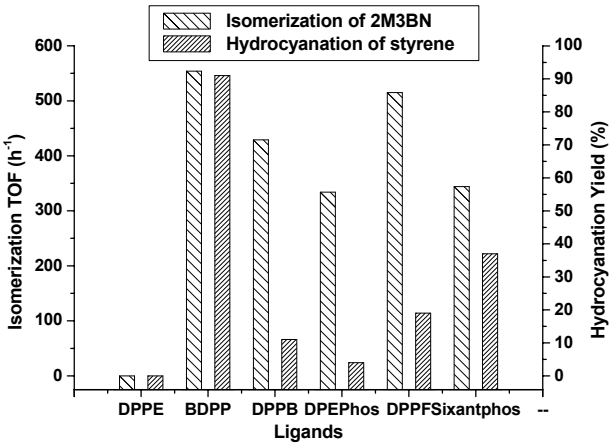

Figure 14 *Diphosphine ligands in the nickel-catalyzed isomerization and hydrocyanation*

It becomes immediately clear from Figure 14 that one ligand is superior in the hydrocyanation reaction (only BDPP has a yield > 50%) whereas all ligands (except DPPE) show high activity for the isomerization. This is caused by another key reaction pathway in the hydrocyanation reaction that needs to be controlled, which is the deactivation of the catalyst due to HCN and formation of cyano-nickel species. Finding a catalyst stable under hydrocyanation conditions seems of at least equal importance as finding a highly active catalyst for the reductive elimination. Within the six ligands studied here, no trend was observed in the performance in the two catalytic reactions.

§ 2.4 Conclusions

The isomerization of 2M3BN to 3PN can be used as model reaction for the activity in the hydrocyanation of dienes and vinyl arenes. The individual reaction steps were studied by NMR spectroscopy. The reversibility of the reaction was demonstrated and the coordination chemistry of DPEphos with Ni(0) and Ni(II) was studied. The carbon-carbon bond activation product (**6**), characterized by single crystal X-ray diffraction, is an intermediate in the isomerization of 2M3BN to 3PN.

The most active catalytic system in the isomerization is not *per se* the best system for hydrocyanation as the deactivation of the catalyst by HCN is equally important as activity. This was demonstrated by the catalytic system BDPP/Ni(0) and DPPF/Ni(0), which show both high activity (TOF = 554 and 515 h^{-1} respectively) for the isomerization but only BDPP/Ni(0) gives a high yield (91 %) in the hydrocyanation of styrene, while DPPF/Ni(0) only gives 19 % yield. Of the diphosphine ligands tested in this study BDPP proved to be best in the hydrocyanation of styrene as well as the isomerization of 2M3BN to 3PN. A detailed kinetic study will be discussed in Chapter 3.

§ 2.5 Experimental

Chemicals were purchased from Aldrich, Acros or Merck and used as received. Styrene (over CaH_2) and 2-methyl-3-butenenitrile were distilled prior to use. All preparations were carried out under an argon atmosphere using standard Schlenk techniques. $Ni(cod)_2$ [22] and HCN [23] were synthesized according to literature procedures. NMR spectra were recorded on a Varian Unity Inova 500 (VT NMR), Mercury 400 and Mercury 200 spectrometer (^1H, $^{13}C\{^1H\}$, $^{31}P\{^1H\}$). Maldi-TOF mass spectroscopy was performed on a PerSeptive Biosystems Voyager-DE PRO spectrometer. Elemental analysis was performed on a Perkin Elmer 2400 apparatus. IR spectra were recorded on an Avatar 360 FT-IR instrument in ATR mode.

DPEphosNi(cod) (1)
To a 50 mL Schlenk flask, containing 50 mg (0.182 mmol) $Ni(cod)_2$ and 100 mg (0.183 mmol) DPEphos, was added 15 mL of methanol. This suspension was stirred for 45 minutes, after which the product was filtered off, washed with 5 mL methanol and 5 mL of cold pentane. The orange powder was dried *in vacuo*. Crystals suitable for X-ray diffraction were grown from a saturated toluene solution that was layered with *n*-hexanes. Yield: 112 mg (0.16 mmol, 86%)
^1H NMR: (500 MHz, C_7D_8, 298K) δ (ppm): 7.5-6.5 (aromatic signals), 4.54 (br s, 4H, cod), 1.84 (br s, 4H, cod), 1.70 (br s, 4H, cod) $^{31}P\{^1H\}$ NMR: (162 MHz, C_7D_8, 298K) δ (ppm): 33.1 (s)

[DPEphosNi(C_3H_5)][BPh_4] (3)
To a solution of 200 mg (0.28 mmol) DPEphosNi(cod) in 15 mL THF was added 1 equiv. allyl bromide (34.2 mg, 0.28 mmol) at –78 °C. The color turned reddish upon slow warming to room temperature. After addition of 1 equiv. of $NaBPh_4$ (97.4 mg, 0.28 mmol) the flask was gently warmed (~40 °C) until the color changed to yellow. All volatiles were removed *in vacuo* after filtration over celite and **3** was recrystallized by addition of MeOH to a solution of the complex in CH_2Cl_2. Crystals suitable for X-ray diffraction were grown from layering a CH_2Cl_2 solution of **3** with MeOH at room temperature. Yield: 84 mg (0.09 mmol, 31%)
^{31}P NMR (CD_2Cl_2) δ (ppm): 14.1 Maldi TOF: 637.19 [DPEPhosNi(C_3H_5)]$^+$

DPEphos oxide
Treatment of a THF/pentane solution of **1** with air causes decomposition of the complex and mono oxidation of the ligand DPEphos. Crystals suitable for X-ray diffraction were obtained from this solution after 2 weeks at –30 °C.

DPEphosNi(2M3BN) (4)
In a nitrogen filled glovebox 5 mg (0.018 mmol) $Ni(cod)_2$ and 10 mg (0.018 mmol) DPEphos were dissolved in 0.7 mL toluene-d_7 and transferred to a NMR tube. The NMR tube was cooled to –78 °C (dry ice/acetone) and 50 µL (0.52 mmol) of 2M3BN were added. The cooled NMR tube was placed in a cooled NMR spectrometer.
^{1}H NMR: (500 MHz, C_7D_8, 238K) δ (ppm): 8.3-6.2 (aromatic signals), 2.90 (br d, 1H, $^3J_{HH}$=8 Hz), 2.53 (br s, 1H), 2.38 (br s, 1H), 1.71 (br s, 1H), 1.07 (br d, 3H, CH_3, $^3J_{HH}$=8 Hz) ^{31}P{^{1}H} NMR: (162 MHz, C_7D_8, 238K) δ (ppm): 21.3 (d, 1P, $^2J_{PP}$= 8 Hz), 24.2 (d, 1P, $^2J_{PP}$=38 Hz)

DPEphosNi(C_4H_7)(CN) (5)
In a nitrogen filled glovebox 5 mg (0.018 mmol) $Ni(cod)_2$ and 10 mg (0.036 mmol) DPEphos were dissolved in 0.7 mL toluene-d_7 and transferred to a NMR tube. The NMR tube was cooled to –78 °C (dry ice/acetone) and 50 µL (0.52 mmol) of 2M3BN were added. The cooled NMR tube was placed in a cooled NMR spectrometer, which was warmed up to 25 °C.
^{1}H NMR: (500 MHz, C_7D_8, 298K) δ (ppm): 7.6-6.5 (aromatic signals), 4.5 (1H, C*H*CH_2), 3.4 (1H, C*H*CH_3), 2.4 (1H, CH_2), 1.6 (3H, CH_3) and 1.2 (1H, CH_2) ^{31}P{^{1}H} NMR: (162 MHz, C_7D_8, 198K) δ (ppm): 29.7 (d, $^2J_{PP}$=49 Hz), 19.5 (d, $^2J_{PP}$=64 Hz), 9.5 (d, $^2J_{PP}$=49 Hz), 6.4 (d, $^2J_{PP}$=64 Hz)

DPEphosNi(styrene)
To a mixture of 30 mg DPEphos$NiCl_2$ in 1 mL benzene-d_6 100 µL styrene and 100 mg zinc dust were added and stirred for 2 hours, the mixture was filtered over Celite.
^{31}P{^{1}H} NMR: (162 MHz, C_6D_6) δ (ppm): 22.96 (d, $^2J_{PP}$=43.9 Hz), 20.28 (d, $^2J_{PP}$=43.9 Hz)

DPEphosNi(C_4H_7)($CNZnCl_2$.EtOH) (6)
Method 1: A mixture of 85 mg (0.307 mmol) $Ni(cod)_2$ and 172 mg (0.319 mmol) DPEphos in 10 mL toluene/EtOH (10:1) was stirred for 15 minutes, then 40 µL of 2M3BN or 3PN and 311 µL of a 1 M $ZnCl_2$ solution in diethyl ether was added. The complex precipitated and was filtered off and washed twice with cold EtOH. Yield 164 mg (0.191 mmol, 63%) of orange crystalline powder.
Method 2: A mixture of 279.8 mg (0.420 mmol) (DPEphos)$NiCl_2$, 120 µL of 2M3BN or 3PN and 100 mg zinc dust in 15 mL toluene/EtOH (2:1) was stirred for 2 hours at 40 °C, then filtered over Celite and cooled down to –30 °C for 4 hours. Afterwards the product was filtered and washed two times with cold ethanol. Yield 172 mg (0.200 mmol, 48%) of orange crystalline powder.

^{1}H NMR: (400 MHz, CD_2Cl_2, 298K) δ (ppm): 7.8-6.6 (m, 28H), 4.6 (br s, 1H, C*H*CH_2), 3.64 (br s, 2H, CH_3C*H*$_2$OH) 3.3 (br s, 1H, C*H*CH_3), 2.7 (br s, 1H, CHC*H*$_2$), 1.66 (br s, 1H, CH_3CH_2O*H*), 1.5 (br s, 3H CHC*H*$_3$), 1.4 (br s, 1H, CHC*H*$_2$), 1.16 (br m, 3H, C*H*$_3$$CH_2OH$) ^{31}P{^{1}H} NMR: (162 MHz, CD_2Cl_2/CD_3OD (1:1), 198K) δ (ppm): 32.4 (s), 29.2 (d, $^{2}J_{pp}$=53 Hz), 11.9 (m, 2 signals) ^{13}C{^{1}H} NMR: (100.6 MHz, CD_2Cl_2/CD_3OD (1:1), 298K) δ (ppm): 158.6 (*C*N), 98.7 (C2), 85.3 (C3), 49.6 (C1), 21.0 (*C*H$_3$) IR (νCN): 2115 cm^{-1}, Maldi-TOF: 651 (M^+ −$CNZnCl_2$.EtOH) Elemental Analysis: calculated for $C_{43}H_{41}N_1O_2P_2Ni_1Zn_1Cl_2$: %C 60.2, %H 4.8, %N 1.6, (found): %C 60.9, %H 4.9, %N 1.4

Isomerization of 2M3BN to 3PN

A solution of 3 equiv. (0.054 mmol) of diphosphine ligand in 2.0 mL of toluene was added to 5 mg (0.018 mmol) $Ni(cod)_2$ in a Schlenk tube and was stirred for 5 minutes. To this solution 0.5 mL (5.20 mmol) 2M3BN was added and the Schlenk tube was placed in an oil bath at 100 ˚C. Samples for GC analysis (see § 3.12 for details) were taken over time to determine the TOF (h^{-1}).

Table 2 *Diphosphine ligands applied in the isomerization of 2M3BN to 3PN*

Ligand	DPPE	BDPP	DPPB	DPEphos	DPPF	Sixantphos
TOF (h^{-1})	0	554	429	334	515	344

Hydrocyanation of styrene

A solution of 3 equiv. (0.054 mmol) of ligand in 500 µL of toluene was added to 5 mg (0.018 mmol) $Ni(cod)_2$ in a glovebox (N_2 atmosphere). From this stock solution 200 µL were added with an Eppendorf pipet to a 15 mL reaction Schlenk tube equipped with a teflon coated stirring bar followed by 100 equiv. (100 µL, 7.2 mmol) of styrene/n-decane (90/10 vol.%) solution. A round bottom Schlenk flask was filled with 1 mL toluene and 100 µL hydrogen cyanide, which was taken up in a 5 mL syringe and added to the reaction mixture by syringe pump in 2 hours (closed system). The reaction was stirred for another hour, after which the reaction mixture was cooled to 0 ˚C and was flushed with a gentle stream of argon for 1 minute to remove traces of HCN. The reaction product was then analyzed by GC (see § 4.6 for details).

Table 3 *Diphosphine ligands applied in the hydrocyanation of styrene*

Ligand	DPPE	BDPP	DPPB	DPEphos	DPPF	Sixantphos
Yield (%)	0	91	11	4	19	37
Conversion (%)		94	16	16	30	45

Table 4 *Selected crystallographic data for complexes* ***1****, DPEphos oxide,* ***3*** *and* ***6***

	1	**DPEphos oxide**	**3**	**6**
Formula	$C_{44}H_{40}Ni_1O_1P_2$	$C_{36}H_{28}O_2P_2$	$C_{39}H_{33}Ni_1O_1P_2$. $C_{24}H_{20}B_1$	$C_{43}H_{41}Cl_2Ni_1O_2P_2Zn_1$.$0.5C_6H_6$
FW ($g \cdot mol^{-1}$)	705.41	554.52	957.51	899.74
Crystal size (mm)	0.18x0.18x0.18	0.30x0.30x0.15	0.18x0.18x0.32	0.18x0.12x0.08
Crystal system	Monoclinic	Triclinic	Triclinic	Monoclinic
Space group	P_{21}/c (no.14)	$P\bar{1}$ (no. 2)	$P\bar{1}$ (no. 2)	P_{21}/c (no.14)
a (Å)	11.3799(6)	9.9316(7)	11.9073(10)	24.9627(4)
b (Å)	15.4065(15)	10.2786(5)	12.4239(14)	12.0804(2)
c (Å)	21.9436(18)	14.5778(10)	19.7748(19)	28.9802(5)
α (°)		75.785(4)	104.640(8)	
β (°)	115.700(5)	83.778(6)	100.072(8)	106.7861(7)
γ (°)		85.529(6)	96.131(8)	
V ($Å^3$)	3466.7(5)	1432.05(16)	2751.6(5)	8366.9(2)
Z	4	2	2	8
d_{calc} ($g\ cm^{-3}$)	1.352	1.286	1.156	1.429
μ (Mo-Kα) (mm^{-1})	0.687	0.184	0.450	1.267
T (K)	150	150	150	150
Total reflections	46617	26296	46005	36646
Unique reflections(R_{int})	7922 (0.058)	6527 (0.044)	10826 (0.055)	9590 (0.049)
wR_2 (F^2) (all data)	0.0908	0.0983	0.1160	0.0881
λ (Å)	0.71073	0.71073	0.71073	0.71073
R_1 (F)	0.0392	0.0389	0.0483	0.0379
F(000)	1480	580	1004	3720

$R_{int} = \sum [\,|F_o^2 - F_{o(mean)}^2|\,] / \sum [F_o^2]$; $wR(F^2) = [\sum [w(F_o^2 - F_c^2)^2] / \sum [w(F_o^2)^2]]^{1/2}$; $R(F) = \sum (||F_o| - |F_c||) / \sum |F_o|$

§ 2.6 References

[1] Huthmacher, K. and Krill, S. Reactions with hydrogen cyanide (hydrocyanation). In *Applied Homogeneous Catalysis with Organometallic Compounds*, 1996; Vol. 1 pp 465-486.

[2] Tolman, C. A., McKinney, R. J., Seidel, W. C., Druliner, J. D. and Stevens, W. R. *Adv. Catal.* **1985**, *33*, 1-46.

[3] van der Vlugt, J. I., Hewat, A. C., Neto, S., Sablong, R., Mills, A. M., Lutz, M., Spek, A. L., Müller, C., and Vogt, D. *Adv. Synth. Catal.* **2004**, *346* (8), 993-1003.

[4] Chaumonnot, A., Lamy, F., Sabo-Etienne, S., Donnadieu, B., Chaudret, B., Barthelat, J. C. and Galland, J. C. *Organometallics* **2004**, *23* (14), 3363-3365.

[5] Bartsch, M., Baumann, R., Kunsmann-Keitel, D. P., Haderlein, G., Jungkamp, T., Altmayer, M., Siegel, W. and Molnar, F. Use of chelating phosphonites with transition metals as catalysts. DE 10150286, **2003.** *Chem. Abstr.* **2005,** *138*, 304408.

[6] Lenges, C. P. Phosphonite ligands and their use in hydrocyanation. WO 03/076394, **2003.** *Chem. Abstr.* **2006,** *139*, 262467.

[7] Foo, T., Garner, J. M. and Tam, W. Hydrocyanation of diolefins and isomerization of nonconjugated 2-alkyl-3-monoalkenenitriles. WO 99/06357, **1999.** *Chem. Abstr.* **1999,** *130*, 169815.

[8] Casalnuovo, A. L., RajanBabu, T. V., Ayers, T. A. and Warren, T. H. *J. Am. Chem. Soc.* **1994**, *116* (22), 9869-9882.

[9] Goertz, W., Keim, W., Vogt, D., Englert, U., Boele, M. D. K., Van der Veen, L. A., Kamer, P. C. J. and Van Leeuwen, P. W. N. M. *J. Chem. Soc., Dalton Trans.* **1998**, (18), 2981-2988.

[10] Kempe, R., Sieler, J., and Walther, D. *Z. Kristallogr.* **1996**, *211* (8), 565-566.

[11] Spielvogel, D. J., Davis, W. M., and Buchwald, S. L. *Organometallics* **2002**, *21* (18), 3833-3836.

[12] Casey, C. P. and Whiteker, G. T. *Isr. J. Chem.* **1990**, *30* (4), 299-304.

[13] Baker, M. J., Harrison, K. N., Orpen, A. G., Pringle, P. G. and Shaw, G. *J. Chem. Soc., Chem. Commun.* **1991**, (12), 803-804.

[14] Edwards, A. J., Retboll, M., and Wenger, E. *Acta Crystallogr., Sect. E: Struct. Rep. Online* **2002**, *E58* (7), m375-m377.

[15] Tolman, C. A. *Organometallics* **1983**, *2* (5), 614-621.

[16] The small sharp singlet at $\delta = 23$ ppm is an impurity

[17] Pregosin, P. S. and Salzmann, R. *Coord. Chem. Rev.* **1996**, *155*, 35-68.

[18] Acosta-Ramirez, A., Munoz-Hernandez, M., Jones, W. D. and Garcia, J. J. *J. Organomet. Chem.* **2006**, *691* (18), 3895-3901.

[19] Brunkan, N. M. and Jones, W. D. *J. Organomet. Chem.* **2003**, *683* (1), 77-82.

[20] Kranenburg, M., Kamer, P. C. J., Van Leeuwen, P. W. N. M., Vogt, D., and Keim, W. *J. Chem. Soc., Chem. Commun.* **1995**, (21), 2177-2178.

[21] Kamer, P. C. J., Van Leeuwen, P. W. N. M., and Reek, J. N. H. *Acc. Chem. Res.* **2001**, *34* (11), 895-904.

[22] Schunn, R. A. *Inorg. Synth.* **1974**, *15*, 5-9.

[23] Slotta, K. H. *Berichte d. D. Chem. Gesellschaft* **1934**, *67B*, 1028-1030.

Chapter 3

Nickel-Catalyzed Isomerization of 2-Methyl-3-Butenenitrile

A Kinetic Study

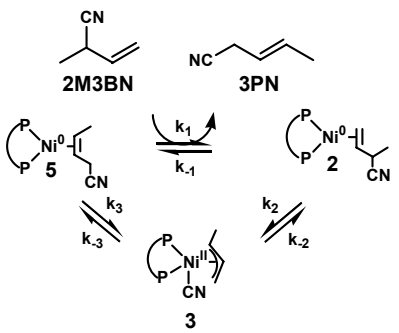

The isomerization of the branched unsaturated nitrile 2M3BN to the linear analogue 3PN has been investigated kinetically, using an automated experimental set-up. The equilibrium of the active catalyst with all other nickel-complexes proved to be important in order to determine the activation parameters $\Delta H^{\ddagger}$, $\Delta S^{\ddagger}$. Unfortunately, the equilibrium constant could not be determined. Therefore, a simplified but still informative parameter was introduced and studied: the combined initial concentration of nickel-precursor and ligand, $[Ni(cod)_2, L]_i$. It is shown that the reaction rate law order in $[Ni(cod)_2, L]_i$ is dependent on the ligand system. This indicates that a two-reaction pathway is more probable than a catalytic cycle based on a mononuclear complex.

Parts of the work described in this chapter have been published:

Jos Wilting, Christian Müller, Alison C. Hewat, Dianne D. Ellis, Duncan M. Tooke, Anthony L. Spek, and Dieter Vogt. Nickel-Catalyzed Isomerization of 2-Methyl-3-butenenitrile, *Organometallics* **2005**, *24* (1), 13-15.

§ 3.1 Introduction

The isomerization of 2-methyl-3-butenenitrile (2M3BN) to 3-pentenenitrile (3PN), displayed in Figure 1, is a model reaction for the hydrocyanation reaction with the advantage that no deactivation of the nickel catalyst, *i.e.* formation of inactive $[Ni(CN)_x]^{(2-x)}$ complexes due to free HCN occurs.

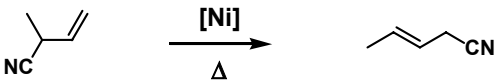

Figure 1 *The isomerization of 2M3BN to 3PN*

The kinetics of this nickel-catalyzed isomerization reaction can be studied easily due to the zero order rate in substrate, as will be shown in § 3.3. In most kinetic studies involving metal based homogeneously catalyzed reactions the emphasis is on the reactants. Examples of homogeneously catalyzed reactions in which the kinetics have been studied are the hydroformylation [1,2], Wacker oxidation [3], and hydrogenation reactions [4].

This study focuses on the role of the catalyst and is aimed to determine the activation parameters $\Delta H^{\ddagger}$ and $\Delta S^{\ddagger}$ in order to compare different catalytic systems, and, if possible, to relate these parameters to activity, stability and selectivity observed for hydrocyanation reactions with these catalyst systems. Such activation parameters are more powerful than for instance IR wave numbers for CN or CO ligands or $^{31}P\{^{1}H\}$ NMR data as the activation parameters describe the transition state.

To relate the data in a computational study could lead to new or improved catalytic systems not only for this model reaction, but also (and more importantly) for the hydrocyanation reaction. However, this is beyond the scope of this thesis and will be part of future studies.

§ 3.2 Ligands

Although many patents and some literature reports cover the isomerization reaction with a broad range of ligands, there is no study available in which ligand systems are directly compared. The ligands used in this study are depicted in Figure 2. These ligands were selected because they cover a broad range in terms of their electronic (Table 1) and sterical characteristics, within the class of phosphorus based bidentate ligands. In order to be able to compare these systems, they should react in a similar manner.

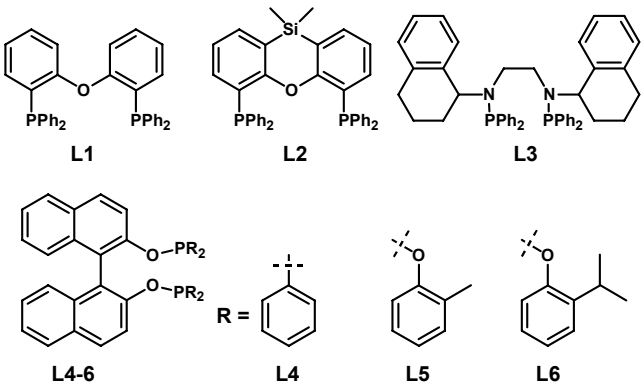

Figure 2 *Overview of ligands used in this kinetic study: DPEphos (**L1**), Sixantphos (**L2**), N,N-bis(diphenylphosphino)-N,N-bis((R)-1,2,3,4-tetrahydronaphtalen-1-yl)-ethane-1,2-diamine (**L3**),(S) -[1,1']-binaphthyl -2,2'-bis(diphenylphosphinite) (**L4**), (R)-[1,1']-binaphthyl-2,2'-bis(di(o-cresol)phosphite) (**L5**) and (R)-[1,1']-binaphthyl-2,2'-bis-(di(o-isopropylphenyl))phosphite (**L6**)*

Table 1 *The electronic parameter (ν) for ligands **L1**-**L6** in (**L**)Ni(CO)$_2$*

Entry	Ligand	A_1 (cm^{-1})	B_1 (cm^{-1})
1	**L1**	1992	1930
2	**L2**	1992	1921
3	**L3**	1996	1987
4	**L4**	2014	1954
5	**L5**	2040	1986
6	**L6**	2041	1987

§ 3.3 Proposed mechanism of the isomerization reaction

Upon analysis by GC, the rate of isomerization of 2M3BN to 3PN was determined to be zero order in substrate (Figure 3 and Eq. 1), which has been observed in the hydrocyanation of 6-methoxy-2-vinylnaphthalene as well. [5]

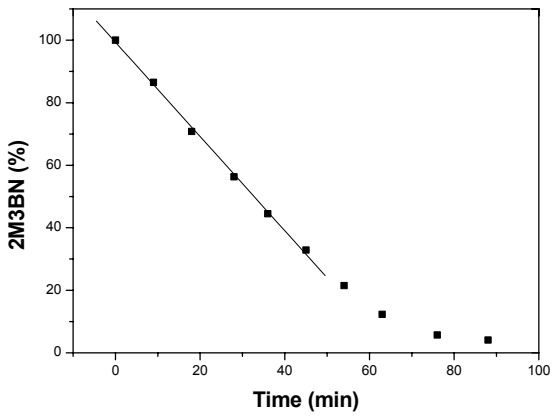

Figure 3 *The nickel-catalyzed isomerization of 2M3BN followed in time by GC-analysis*

$$v = \frac{d[3PN]}{dt} = -\frac{d[2M3BN]}{dt} = k_1[cat]^1[2M3BN]^0 \qquad (1)$$

This result is in clear contrast to the study by Santini *et al.*, in which first order kinetics in substrate were found for the isomerization of 2M3BN to 3PN, conducted in ionic liquids with monodentate phosphines using $Ni(cod)_2$ as the metal precursor [6]. First order kinetics in substrate would suggest an associative mechanism for the reductive elimination, as observed in the hydrocyanation of ethylene. [7] The possibility of a different mechanism for monodentate ligands was considered. However, when performing the isomerization of 2M3BN to 3PN with $Ni(cod)_2$ and 10 equiv. of PPh_3 as catalyst system in toluene, the results clearly indicated zero order kinetics. On closer inspection of the forementioned study, the reported results proved to be consistent with zero order kinetics in substrate.

The data obtained do indicate that reductive elimination of the product is the rate-determining step in the isomerization of 2M3BN, which is in agreement with the results of Chapter 2 of this thesis, where the carbon-carbon activated Ni-complex was isolated. It has been proposed that the allyl species (**3** in Figure 4) is in

equilibrium with its hydrido cyano butadiene species (**6**) with $k_{-4} >> k_4$, which explains the labelling experiments described by Druliner [8] and RajanBabu [5]. This hypothesis was rejected by Chaudret *et al*. on the basis of DFT calculations for a Ni-PH_3 model system without Lewis acid, but no alternative reaction pathway was proposed to explain these experiments. [9] The substitution reaction (**5** to **2**) most likely follows an associative mechanism, thereby avoiding an unstable 14-electron complex.

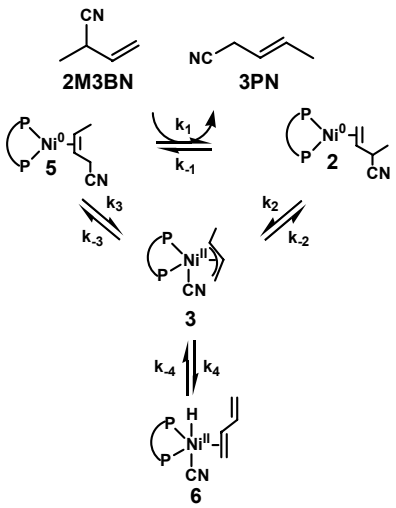

Figure 4 *The proposed catalytic cycle for the nickel(0)-catalyzed isomerization of 2M3BN to 3PN*

The isomerization of 2M3BN to 3PN can be used to study the influence of different ligand parameters on the reductive elimination. It should be mentioned here that the formation of 2M3BN is not included in the rate of isomerization. To be able to compare different catalytic systems it has to be assumed that the selectivity (2M3BN over 3PN) is constant.

§ 3.4 Isomerization of 2M3BN to 2M2BN and 2PN

Unfortunately the isomerization of 2M3BN to 3PN is not completely selective towards 3PN. Isomerization of the double bond of 2M3BN and 3PN occurs and the products 2M2BN and 2PN are formed in small amounts (Figure 5 and Table 2).

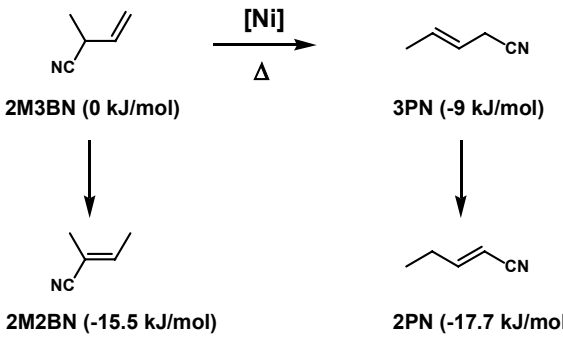

Figure 5 *Isomerization of 2M3BN to 3PN, 2M2BN and 2PN with their calculated relative energies [10]*

Nickel is known for double bond isomerization but also a base can catalyze this reaction [11]. For instance, filtration of 2M3BN over basic alumina gives 2M2BN in an exothermic reaction as the double bond shifts to a conjugated system with the nitrile (~15 kJ/mol difference in energy). Some isomerization to 2M2BN and 2PN occurs in every reaction as the activation energy is much smaller compared to the isomerization to 3PN since no carbon-carbon bond needs to be broken. The results for the isomerization of 2M3BN to 3PN, 2M2BN and 2PN with the diphosphine ligands studied in § 4.3 are summarized in Table 1. In the following paragraphs the results of the isomerization will only focus on the isomerization of 2M3BN to 3PN, the results for the isomerization to 2M2BN and 2PN have been omitted for clarity.

Table 2 *The Ni(0)-catalyzed isomerization of 2M3BN to 3PN with diphosphine ligands*

Entry	Ligand	TOF (h^{-1})[a]	2M2BN (%)[b]	2PN (%)[b]
1	DPPE	0	12.6[c]	<1
2	DPPP	554	4.3	<1
3	DPPB	429	9.9	<1
4	DPEphos	334	3.6	<1
5	DPPF	515	6.5	<1
6	Sixantphos	344	7.6	<1

[a] Defined as $d(3PN/(2M3BN+3PN))/dt$ [b] At 80 % conversion [c] After 1h

§ 3.5 The influence of solvent

For two catalytic systems, Ni(0)/**L1** and Ni(0)/**L6**, the influence of solvent was investigated. The results are summarized in Table 3. Both systems isomerize 2M3BN to 3PN with high activities in toluene, which is the least polar solvent used. However, entry 8 shows that the solvent effect cannot be ascribed solely to a polarity effect. In this particular case, the solvent might react with the ligand as is displayed in Figure 6.

Table 3 *The influence of solvent on the isomerization reaction*

Entry	Ligand	Solvent	TOF (h^{-1})
1	**L1**	toluene	334
2	**L1**	1,4-dioxane	187
3	**L1**	valeronitrile	163
4	**L1**	1-butanol	108
5	**L6**	toluene	123
6	**L6**	1,4-dioxane	106
7	**L6**	valeronitrile	80
8	**L6**	1-butanol	221

Conditions: 0.018 mmol $Ni(cod)_2$, 0.055 mmol **L**, 2 mL solvent and 0.5 mL (5.20 mmol) 2M3BN, 100 ˚C, 1 h.

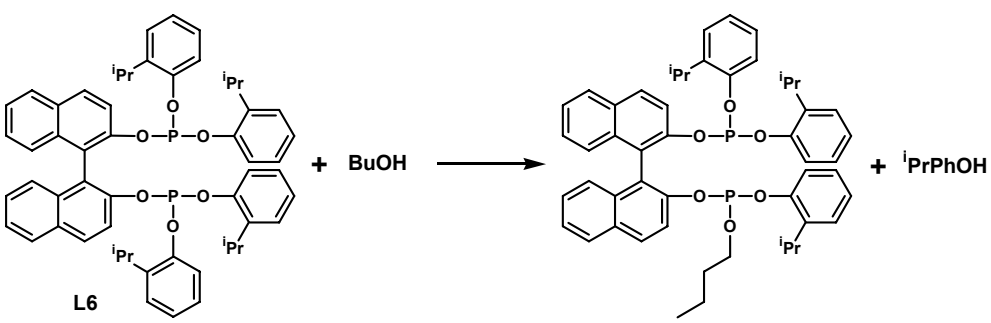

Figure 6 *Possible reaction of 1-butanol with ligand **L6***

§ 3.6 Automated experimentation

To accurately study the kinetics of any reaction requires intensive repetition of the reaction under identical conditions, and therefore automated experimentation is nowadays almost required in order to work within certain error margins. In this kinetic study reactions were either performed with Schlenk techniques, or in an automated fashion using the AMTEC SPR16 or Chemspeed ASW 1000 systems, combined with a GC apparatus equipped with automated sampling system.

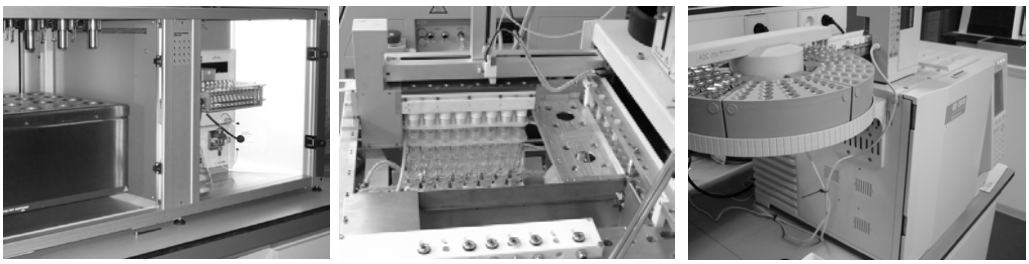

Figure 7 *Pictures of the AMTEC SPR16 (left), Chemspeed ASW1000 (middle) and GC apparatus equipped with automated sampling (right)*

Firstly, new methods were developed for the different experimental automated systems, in order to obtain reproducible and comparable results for the isomerization reaction. Results for the reproducibility tests for the reaction catalyzed by Ni(0)/**L6** are shown in Figure 8. The AMTEC set-up proved to be more reliable (or less problematic to control) in temperature and inert atmosphere, whereas the Chemspeed was more reliable in sampling.

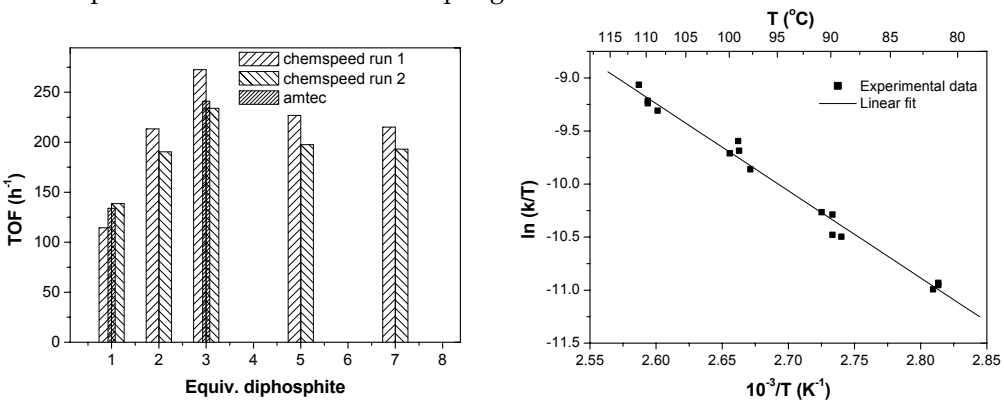

Figure 8 *The isomerization with different Ni(0)/L ratios (left) with AMTEC and Chemspeed, and an Eyring plot (right) from 4x4 AMTEC experiments (64 samples)*

§ 3.7 The rate equation

The rate equation for the isomerization of 2M3BN to 3PN is given by Eq. 1. The turn over frequency (TOF) equals k_1 when [*cat*] = [*Ni*].

$$v = k_1[cat]^1[2M3BN]^0 \tag{1}$$

$$[cat] = [Ni] \tag{2}$$

$$TOF = \frac{v}{[Ni]} = k_1[Ni]^0[2M3BN]^0 = k_1 \quad \{s^{-1}\} \tag{3}$$

If equation 2 is true, the true activation parameters $\Delta H^{\ddagger}$ and $\Delta S^{\ddagger}$ are accessible with relative ease, via the Eyring equation (Eq. 4), since TOF (or k_1) can be determined by GC analysis. This, in combination with a computational study could lead to new insights in order to improve this reaction as well as the hydrocyanation reaction in general.

$$\ln\left(\frac{k}{T}\right) = -\frac{\Delta H^{\ddagger}}{R} \cdot \frac{1}{T} + \ln\left(\frac{k_B}{h}\right) + \frac{\Delta S^{\ddagger}}{R} \tag{4}$$

The definition of v is expressed by Eq. 5 in which the formation of 2M2BN and 2PN is omitted and TOF is defined as in Eq. 6 with units in s^{-1}. In most graphs, however, TOF will be expressed in h^{-1}, and is determined by GC analysis of multiple samples in time.

$$v = \frac{d\left(2M3BN \Big/ (2M3BN + 3PN)\right)}{dt} \tag{5}$$

$$TOF = \frac{v}{[Ni]} \quad \{s^{-1}\} \tag{6}$$

§ 3.8 The assumption [*cat*]=[*Ni*]

For catalytic systems where the ligand easily dissociates from the metal center or when stable, catalytically inactive, bis-chelates are formed, it is obvious that:

$$[cat] \neq [Ni] \tag{7}$$

The catalytic systems were tested to see whether [*cat*] equals [*Ni*] (Eq. 2 and 7) by performing experiments in which the ratio **L**/Ni(cod)$_2$ was varied. The results of these experiments are depicted in Table 4.

Table 4 *The isomerization of 2M3BN with different ratios of* ***L****/Ni(cod)$_2$*

Entry	Ligand	Equiv.	Temp. {°C}	TOF {h^{-1}}	[Ni(cod)$_2$] {mM}
1	**L1**	1	100	198	7.30
2	**L1**	3	100	334	7.30
3	**L5**	1	100	70	7.30
4	**L5**	3	100	35	7.30
5	**L6**	1	110	127	0.91
6	**L6**	2	110	202	0.91
7	**L6**	3	110	254	0.91
8	**L6**	5	110	204	0.91

From the obtained data, it can be concluded that **L6** is not capable of forming bis-chelates (TOF entry 5 < entry 7), whereas **L5** can form bis-chelates (TOF entry 3 > entry 4). However, **L6** is clearly in equilibrium with [*Ni(cod)$_2$*] and [*cat*] as shown in entries 5 and 7. With 3 equiv. of ligand the TOF is approximately 2 times faster as with 1 equiv. This also accounts for **L1**. It is known that **L1** forms bis-chelates but is in fast equilibrium with its mono-chelate form. [12]

This directly affects the main goal of this part of the research, as [*cat*] in Eq. 1 needs to be defined correctly. As a start, a general equation (Eq. 8) can be used in which [*cat*] is dependent on all species in solution (cod, nickel, ligand, bis-chelate, …).

$$v = k_1[cat]^1[2M3BN]^0 \tag{1}$$

$$[cat] = K_n[]^a[]^b[]^c[]^d \tag{8}$$

This results in a somewhat more complicated rate equation:

$$v = k_1 K_n [\,]^a [\,]^b [\,]^c [\,]^d \tag{9}$$

The rate law now has 2 rate constants, that are in principle both temperature dependent. Thus the true activation parameters for the reductive elimination (the rate-determining step) cannot be determined without knowing the exact nature of equation 8. It would be useful to express [*cat*] by the initial (or total) concentrations of [$Ni(cod)_2$] and [*L*] (Eq. 10).

$$[cat] = K[Ni(cod)_2]_i^{\,a} [L]_i^{\,b} \tag{10}$$

Thus extensive kinetic experiments are required for each ligand system to get an expression for [*cat*] before the true activation parameters ($\Delta H^{\ddagger}$ and $\Delta S^{\ddagger}$) for the rate determining step can be determined. As a result, it was decided to pursue a more applied kinetic study.

§ 3.9 The order in $[Ni(cod)_2, L]_i$

As explained in the previous paragraph, changing only $[Ni(cod)_2]$ will not lead to the order in $[Ni(cod)_2]$ for all ligands, due to the formation of other inactive complexes such as bis-chelates. Therefore, a constant ratio was applied between $Ni(cod)_2$ and **L** to determine the order in [*Ni*]. In this way the catalyst precursor does not change, but 1**L**/$Ni(cod)_2$ and 3**L**/$Ni(cod)_2$ are treated as different catalytic systems, and $[Ni(cod)_2]_i$ and $[L]_i$ are combined in $[Ni(cod)_2, L]_i$. This effects the rate equation as is shown by Eq. 11 and 12.

$$v = k_1[cat]^1[2M3BN]^0 \quad (1)$$

$$[cat] = K_2[Ni(cod)_2, L]_i^x \quad (11)$$

$$v = k_1K_2[Ni(cod)_2, L]_i^x \quad (12)$$

The order in $[Ni(cod)_2, L]_i$, given by x, was determined for different catalytic systems with the Chemspeed ASW1000 system (Table 4). The order can be determined (Eq. 14) from the slope of the graph in which ln(TOF) is plotted as function of ln([$Ni(cod)_2$, L]); the slope of the line is the order minus 1.

$$TOF = \frac{v}{[Ni(cod)_2, L]_i} = k_1K_2[Ni(cod)_2, L]_i^{(x-1)} \quad (13)$$

$$\ln(TOF) = (x-1)\ln([Ni(cod)_2, L]_i) + \ln(k_1K_2) \quad (14)$$

Figure 9 displays the determination of the order in nickel with 1 equiv. of diphosphite **L6** and 1 equiv. of diphosphine **L1**.

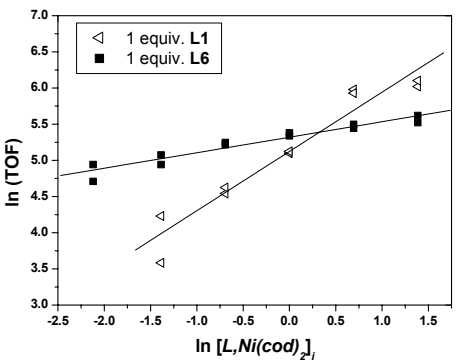

Figure 9 *The order in* $[Ni(cod)_2, L]_i$ for ligands **L1** and **L6**

Table 5 *The order in $[Ni(cod)_2, L]_i$ for ligands **L1**-**L6***

Entry	Ligand	Equiv.	Order in $[Ni(cod)_2, L]_i$	T {°C}
1	**L1**	1	1.8	110
2	**L2**	1	1.4	110
3	**L6**	1	1.2	110
4	**L6**	3	1.2	110

The order in $[Ni(cod)_2, L]_i$ depends on the nature of the ligand, and seems to be predominantly affected by the electronic properties. The order in $[Ni(cod)_2, L]_i$ is for the diphosphine ligand **L1** 1.8 (entry 1) and for the diphosphite ligand **L6** 1.2 (entries 3 and 4). This result demonstrates the possibility of a species with two nickel centers during the rate-determining step. Moreover, the best explanation based on these results is a two reaction pathway system (*i.e.* mononuclear and dinuclear). In Chapter 2 of this thesis a dimetallic complex is described where the cyano group bridged between nickel and zinc. [13] Also dinuclear palladium complexes are known. [14,15] Possible transition states are given in Figure 10.

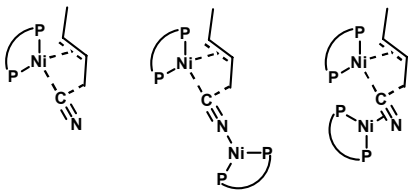

Figure 10 *Proposed transition states during the isomerization of 2M3BN to 3PN for the mononuclear (left) and dinuclear (middle and right) pathways*

It is interesting to note that the observations made by Casalnuovo and RajanBabu, *i.e.* the relative rate of reductive elimination over β-hydride elimination increases when the electron density on phosphorus was reduced by introducing electron withdrawing substituents on the ligand, can be explained by either a one or a two reaction pathway. It would be attractive to study these diphosphinite systems in the isomerization reaction to determine the order in $[Ni(cod)_2, L]_i$ to see whether the rate of reductive elimination over β-hydride elimination is correlated to the order in $[Ni(cod)_2, L]_i$.

§ 3.10 The activation enthalpy

The activation enthalpy ($\Delta H^{\ddagger}$) of the different catalytic systems can be determined as depicted in Figure 11 from the Eyring equation (Eq. 4) with the assumption that K_2 from Eq. 9 is (almost) completely temperature independent. At all temperatures [*cat*] is then in the same way proportional to [$Ni(cod)_2$, $L]_i$ (Eq. 15). And the rate of isomerization (in TOF) can be expressed as a function of the temperature with a constant amount of catalyst. However, it is impossible to determine the activation entropy ($\Delta S^{\ddagger}$) without knowing the exact concentration of catalyst. The activation entropy would give mechanistic insight into the transition state, as it is a measure for the order during the transition state.

$$\ln\left(\frac{k}{T}\right) = -\frac{\Delta H^{\ddagger}}{R}\cdot\frac{1}{T} + \ln\left(\frac{k_B}{h}\right) + \frac{\Delta S^{\ddagger}}{R} \tag{4}$$

$$k \propto TOF \tag{15}$$

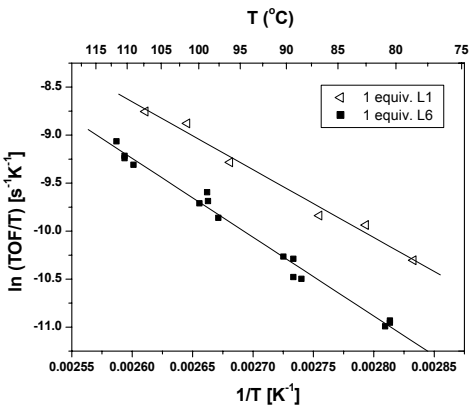

Figure 11 *Eyring plot for ligands **L1** and **L6***

Table 6 *The reaction activation enthalpy for the isomerization of 2M3BN to 3PN*

Entry	Ligand	Equiv.	$\Delta H^{\ddagger}$ (kJ/mol)	[$Ni(cod)_2$, L] {mM}
1	**L1**	1	59	12.8
2	**L2**	1	68	0.94
3	**L3**	1	27	0.78
4	**L4**	1	52	0.46
5	**L6**	1	68	0.46
6	**L6**	3	78	0.50

All systems have an activation enthalpy between 27 and 78 kJ/mol (Table 6), with ligand **L3** being the system with the lowest activation enthalpy. Thus ligand **L3** can be applied with relatively high activity at lower temperatures. At high temperatures, **L2** and **L6** will give high TOFs depending on the concentration.

§ 3.11 Conclusions

The Ni-catalyzed isomerization of 2M3BN to 3PN started as a promising reaction in which different ligand systems could be evaluated with relative ease. However, this kinetic study showed that one should be careful comparing different ligand systems as the exact [*cat*] is not known and different orders were determined for $[Ni(cod)_2, L]_i$. This indicates that a two reaction pathway is more probable than a catalytic cycle based on a mononuclear complex. The initial goal of this study, to compare different catalytic systems by their true activation parameters ($\Delta H^{\ddagger}$ and $\Delta S^{\ddagger}$) proved to be out of scope as extensive kinetic experiments would have required for each ligand system to get an expression for [*cat*] before $\Delta H^{\ddagger}$ and $\Delta S^{\ddagger}$ can be determined.

Nevertheless, the TOF can be determined as function of [*Ni*] and temperature, which made it possible to compare different systems and to decide which system is suitable for the application. In the industrial process a system that operates at low concentration with high TOF and high TON seems best. Of the systems studied in this chapter the diphosphite ligand **L6** fulfils these requirements.

§ 3.12 Experimental

Typical isomerization of 2M3BN to 3PN

A solution of 3 equiv. (0.054 mmol) of ligand in 2.0 mL of toluene was added to 5.0 mg (0.018 mmol) $Ni(cod)_2$ in a Schlenk tube and was stirred for 5 minutes. To this solution 0.5 mL (5.20 mmol) 2M3BN was added and the Schlenk tube was either placed in an oil bath or taken up in a syringe and added to a reactor of the AMTEC or Chemspeed. Samples for GC analysis were taken over time to determine the TOF (h^{-1}).

GC analysis

GC:	Shimadzu GC-2010
Column:	DB1 (30 m, 0.32 mm inner diameter)
Carrier gas:	Helium 58.2 kPa
Temperature program:	80 ˚C (8 min), 25 ˚C/min to 250 ˚C
Injector:	280 ˚C
Detector:	270 ˚C
Split ratio:	200
Injection volume:	1.0 µL

Table 7 *Retention times*

Compound	Retention time (min)
2M3BN	3.77
tr-3PN	5.21
2M2BN	4.20, 5.13
2PN	4.38
1-Butanol	3.47
1,4-Dioxane	4.09
Valeronitrile	5.05
Toluene	5.53

§ 3.13 References

[1] Van Leeuwen, P. W. N. M. Rhodium catalyzed hydroformylation. In *Homogeneous Catalysis: Understanding the Art*, 1st ed.; Kluwer Academic Publishers: 2004; pp 139-147.

[2] Casey, C. P., Martins, S. C. and Fagan, M. A. *J. Am. Chem. Soc.* **2004**, *126* (17), 5585-5592.

[3] Crabtree, R. H. Wacker Process. In *The organometallic chemistry of the transition metals*, 2nd ed.; Wiley Interscience: 1994; pp 193-196.

[4] Landis, C. R. and Halpern, J. *J. Am. Chem. Soc.* **1987**, *109* (6), 1746-1754.

[5] Casalnuovo, A. L., RajanBabu, T. V., Ayers, T. A. and Warren, T. H. *J. Am. Chem. Soc.* **1994**, *116* (22), 9869-9882.

[6] Vallee, C., Valerio, C., Chauvin, Y., Niccolai, G. P., Basset, J. M., Santini, C. C., Galland, J. C. and Didillon, B. *J. Mol. Cat. A: Chem.* **2004**, *214* (1), 71-81.

[7] McKinney, R. J. and Roe, D. C. *J. Am. Chem. Soc.* **1985**, *107* (1), 261-262.

[8] Druliner, J. D. *Organometallics* **1984**, *3* (2), 205-208.

[9] Chaumonnot, A., Lamy, F., Sabo-Etienne, S., Donnadieu, B., Chaudret, B., Barthelat, J. C. and Galland, J. C. *Organometallics* **2004**, *23* (14), 3363-3365.

[10] Gaussian 98, Revision A.9, basis set 3-21G

[11] Prochazka, M., Zelinka, J., Vilim, A., and Cerny, J. V. *Collect. Czech. Chem. Commun.* **1970**, *35* (4), 1224-1234.

[12] Goertz, W., Keim, W., Vogt, D., Englert, U., Boele, M. D. K., Van der Veen, L. A., Kamer, P. C. J. and Van Leeuwen, P. W. N. M. *J. Chem. Soc., Dalton Trans.* **1998**, (18), 2981-2988.

[13] Wilting, J., Müller, C., Hewat, A. C., Ellis, D. D., Tooke, D. M., Spek, A. L. and Vogt, D. *Organometallics* **2005**, *24* (1), 13-15.

[14] Budzelaar, P. H. M., Van Leeuwen, P. W. N. M., Roobeek, C. F., and Orpen, A. G. *Organometallics* **1992**, *11* (1), 23-25.

[15] Tromp, M., Sietsma, J. R. A., van Bokhoven, J. A., van Strijdonck, G. P. F., van Haaren, R. J., van der Eerden, A. M. J., Van Leeuwen, P. W. N. M., and Koningsberger, D. C. *Chem. Commun.* **2003**, (1), 128-129.

Chapter 4

Binaphthol-Based Diphosphite Ligands in Asymmetric Hydrocyanation: Influence of Steric Properties

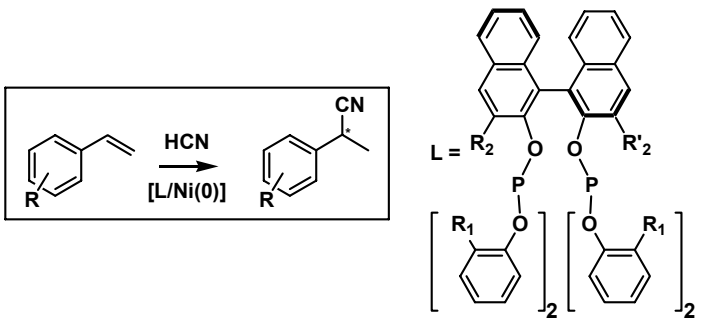

A series of chiral (*R*)-binaphthol-based diphosphite ligands with different substituents were prepared and applied in the asymmetric hydrocyanation of styrene and 1,3-cyclohexadiene, to investigate the influence of their steric properties. The optimal steric properties for the ligands used in the hydrocyanation reaction are defined within a narrow window. With the optimized ligand, hydrocyanation of styrene gave full conversion (Subs/Ni = 100) with 49 % ee, and the TON was determined to be 600. Hydrocyanation of 1,3-cyclohexadiene gave 50 % conversion (Subs/Ni = 500) with an excellent ee of 86 %. This demonstrates that high ee's are not only accessible for vinyl arenes but also for conjugated dienes in the asymmetric nickel-catalyzed hydrocyanation.

Parts of the work described in this chapter have been published:

Jos Wilting, Michèle Janssen, Christian Müller, Martin Lutz, Anthony L. Spek and Dieter Vogt. Binaphthol-Based Diphosphite Ligands in Asymmetric Hydrocyanation of Styrene and 1,3-Cyclohexadiene: Influence of Steric Properties, *Adv. Synth. Catal.* **2006** *accepted for publication*

§ 4.1 Introduction

The production of adiponitrile from butadiene and HCN is an important homogeneous Ni-catalyzed process in industry. [1] Reports on asymmetric hydrocyanation of carbon-carbon double bonds have occasionally appeared since the first report by Elmes and Jackson in 1979 on the asymmetric hydrocyanation of norborn(adi)ene. [2] Table 1 shows an overview regarding the asymmetric hydrocyanation of vinylarenes (Figure 1). [3]

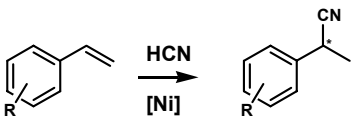

Figure 1 *Asymmetric hydrocyanation of vinylarenes*

Table 1 *Literature overview of the asymmetric hydrocyanation of vinylarenes*

Entry	Substrate	Temp (°C)	Yield (%)	ee (%)	Ref.
1	Styrene	25	nd	65	[4]
2	Styrene	60	22	42	[5]
3	Styrene	100	100	51	[6]
4	Styrene	20	5	65	[6]
5	4-MeStyrene	100	100	41	[6]
6	4-MeStyrene	25	nd	70	[7]
7	4-^{i}BuStyrene	60	40	63 (*S*)	[5]
8	4-^{i}BuStyrene	25	100	57 (*S*)	[7]
9	MVN[a]	60	100	30 (*S*)	[5]
10	MVN[a]	0	100	91 (*S*)	[7]
11	MVN[a]	0	100	95 (*R*)	[8]

[a] MVN = 6-methoxy-2-vinylnaphthalene

RajanBabu and Casalnuovo discussed the importance of the electronic properties of the ligand in the nickel-catalyzed asymmetric hydrocyanation of MVN. [7] It was shown earlier that chelating π-acceptor ligands with a high binding affinity to Ni(0) can lead to very stable nickel bis-chelate complexes, reducing the catalytic activity. [9] All studies show that finding a suitable ligand system is rather tedious and 'fine tuning' is necessary in order to obtain both, high conversion, and high enantioselectivity. Thus a modular ligand design was investigated, that allowed for modification at several positions. In this chapter, the focus is on the

influence of the sterics of (*R*)-binaphthol-derived diphosphite ligands. By adjusting the steric environment, formation of undesirable, catalytically inactive bis-chelate complexes should be suppressed, yielding active catalyst systems.

§ 4.2 Ligand synthesis and catalysis

Binaphthol is a common and relatively cheap chiral building block, and therefore attractive for the synthesis of chiral ligands. (*R*)-[1,1']Binaphthyl-2,2'-bis-(diarylphosphite) is a modular ligand, which has been applied in the asymmetric hydroformylation of vinyl acetate [10] and aryl vinyl ethers. [11] Reaction of 2 equivalents of *ortho* substituted phenols (phenol, 2-methylphenol, 2-isopropyl-phenol, 2-[1,3]-dioxan-2-yl-phenol, 2-*tert*-butylphenol) with PCl_3 in the presence of NEt_3 and subsequently with 0.5 equivalents of (*R*)- [1,1']-binaphthyl-2,2'-diol gave a set of 5 diphosphite ligands **L1**-**L5** (Figure 2).

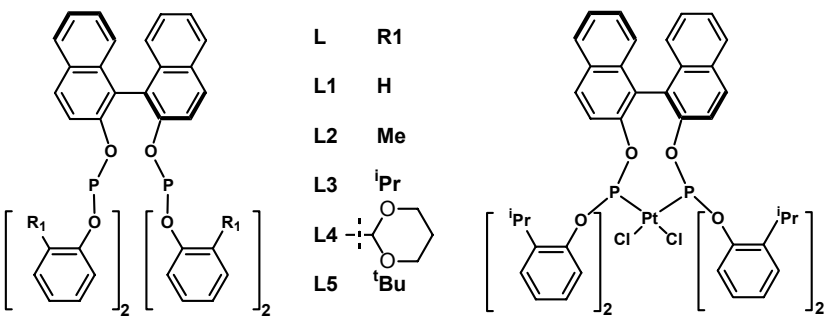

Figure 2 *left: Ligands **L1**-**L5**, right: Chemical structure of **L3**$PtCl_2$*

The complexes **L3**Ni(cod) and **L3**$PtCl_2$ were studied in order to gain insight into the three dimensional structure of the ligand. In solution these complexes show C_2 symmetry as can be seen from the ^{1}H NMR spectra (only 2 sets of signals are observed for the ^{i}Pr groups in Figure 4), as well as from the ^{31}P NMR spectra, which show a singlet at 147.8 ppm for **L3**Ni(cod) and a singlet at 57.2 ppm with platinum satellites ($^1J_{PtP}$ = 5782 Hz, indicating *cis* coordination) for **L3**$PtCl_2$. However, the solid state molecular structure of **L3**$PtCl_2$ shows a distorted C_2 symmetry.

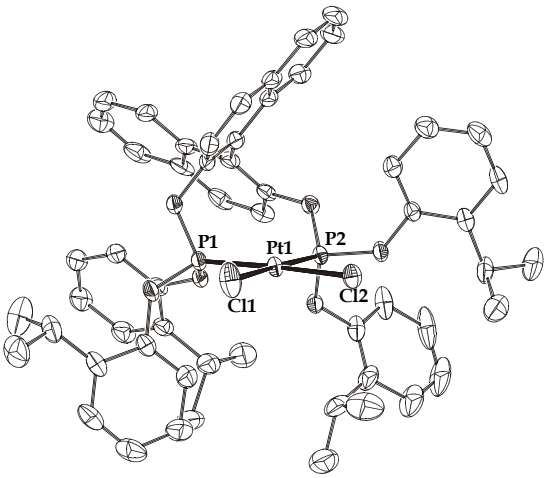

Pt-P1	2.1976(19)
Pt-P2	2.2097(19)
Pt-Cl1	2.336(3)
Pt-Cl2	2.336(3)
P-Pt-P	95.73(7)
Cl-Pt-Cl	88.13(8)

Figure 3 *Molecular structure of* ***L3****$PtCl_2$, hydrogen atoms have been omitted for clarity, thermal ellipsoids are shown at 50 % probability level. Selected bond lengths (Å) and angles (°) with standard deviations between parentheses*

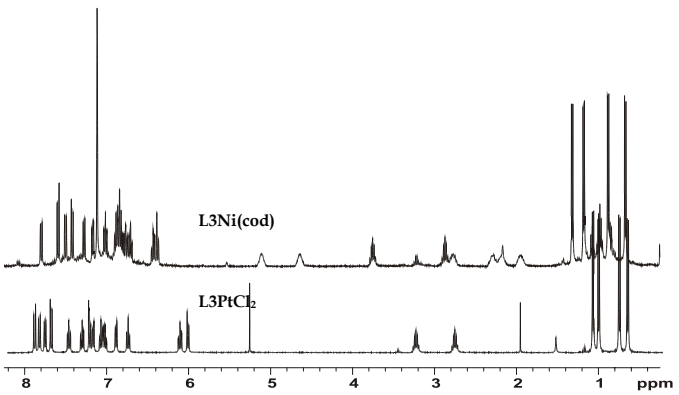

Figure 4 *^1H NMR spectra of* ***L3****$PtCl_2$ ($CDCl_3$) and* ***L3****Ni(cod) (C_6D_6)*

Hydrocyanation of styrene with 1.1 equivalent, with respect to the metal precursor, of ligand and nickel(0)bis-1,5-cyclooctadiene ($Ni(cod)_2$) in toluene at 60 °C with HCN, reveals a difference in conversion of 100 % among these 5 catalyst systems. It was found that Ni/**L3** and Ni/**L4** perform best in terms of conversion and enantioselectivity (Table 2). Interestingly, the most active system is also the most enantioselective and the reaction is completely selective towards the branched product, α-methyl-benzylnitrile. However, the mass balance shows that some polymerization (up to 5%) of styrene occurs as well.

Table 2 *Asymmetric hydrocyanation of styrene with ligands **L1-L5***

Ligand	**L1**	**L2**	**L3**	**L4**	**L5**
R_1	H	Me	^{i}Pr	$C_4H_7O_2$	^{t}Bu
Conv (%)	<1	6	90	100	<1
ee (%)	nd	3	12	43	nd

Conditions: Ni/L/Styrene/HCN: 1/1.1/100/200 in 1.2 mL toluene at 60 ˚C for 4 h, nd = not determined

§ 4.3 Electronic and steric effects

It has been shown that the relative rate of reductive elimination over β-hydride elimination increases when the electron density on phosphorus is reduced by electron withdrawing groups on the ligand. [7] Moreover, the diphosphinite ligand containing electron withdrawing CF_3 groups on the *meta* positions (Figure 12 in Chapter 1) is electronically comparable to diphosphite ligands. This is based on the infrared frequencies of the A_1 (2038 cm^{-1}) and B_1 (1987 cm^{-1}) vibrations of CO in (**L**)Ni(CO)$_2$ complexes. This system performed best in the hydrocyanation of 6-methoxy-2-vinylnaphthalene in terms of activity and enantioselectivity. Ligands **L1** to **L5** show only a small difference in the Tolman electronic parameter (ν) [12] (Table 3), which provides evidence that the differentiation in catalysis should be solely attributed to the steric bulk on the *ortho* positions of the ligands. The five ligands coordinate in a bidentate fashion, as monodentate coordination would form the complexes of the type (**L**)Ni(CO)$_3$, which would give an IR CO vibration at ~2085 cm^{-1}. [12]

Table 3 *ATR IR frequencies of the A_1 and B_1 vibrations of CO in (**L**)Ni(CO)$_2$*

Ligand	**R_1**	**R_2, R'_2**	A_1 (cm^{-1})	B_1 (cm^{-1})
L1	H	H, H	2042	1990
L2	Me	H, H	2040	1986
L3	^{i}Pr	H, H	2041	1987
L4	$C_4H_7O_2$	H, H	2044	1990
L5	^{t}Bu	H, H	2049	2001

10 mg (0.036 mmol) Ni(cod)$_2$ and 1 equiv. (0.036 mmol) **L** were dissolved in 2 mL toluene. The slightly yellow solution was purged with CO for 30 s, during which the solution turned colorless. All volatiles were removed *in vacuo* and the remaining solid was used in the IR measurement in ATR mode.

Furthermore, nickel bis-chelates have been identified as inactive systems in hydrocyanation reactions [7,9,13,14]; the formation of bis-chelates is likely to be dependent on the steric bulk of the ligand. NMR experiments were carried out in which 1 and 3 equiv. of ligand (**L1**-**L5**) were mixed with $Ni(cod)_2$ at 25 °C (Table 4). The bis-chelate complex was only observed for ligands **L1** and **L2**. However, not all bis-chelates are inactive in hydrocyanation reactions; possible ligand exchange for a substrate molecule would give a catalytically active species. Therefore, ligands **L2**, **L3** and **L5** were tested in a closely related reaction, the isomerization of 2-methyl-3-butenenitrile to 3-pentenenitrile (Figure 5) with 1 and 3 equivalents of ligand. [15] Ligands **L2** and **L3** showed comparable rates (TOF = 78, 74 h^{-1} respectively) with 1 equiv. of ligand, whereas **L5** gave no activity. With 3 equiv., **L2** is slower (36 h^{-1}) while the rate of **L3** increased slightly (85 h^{-1}). Thus formation of bis-chelates alone, cannot explain the striking difference observed in the hydrocyanation of styrene.

Table 4 *$^{31}P\{^1H\}$ NMR data of (**L**)Ni(cod) and (**L**)$_2$Ni in C_6D_6*

Ligand	**L1**	**L2**	**L3**	**L4**	**L5**
R_1	H	Me	^{i}Pr	$C_4H_7O_2$	^{t}Bu
(**L**)Ni(cod)[a]	148.0	147.9	147.8	148.0	145.4 (br)
(**L**)$_2$Ni[b]	137.7	133.8	-	-	-

[a] 5 mg (0.018 mmol) $Ni(cod)_2$ and 1 equiv. (0.018 mmol) **L** were dissolved in 0.75 mL C_6D_6

[b] 5 mg (0.018 mmol) $Ni(cod)_2$ and 3 equiv. (0.054 mmol) **L** were dissolved in 0.75 mL C_6D_6

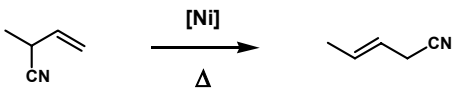

Figure 5 *The nickel-catalyzed isomerization of 2M3BN to 3PN*

Recent studies on the steric and electronic influence on the reductive elimination from palladium complexes show a small steric effect compared to the electronic effect. [16-18] The results indicate that the steric bulk not only prevents the formation of bis-chelates with ligands **L3**-**L5** but also has an effect on either the rate of reductive elimination or on the rate of deactivation. This would explain the fact that these systems become more efficient in the hydrocyanation of styrene (in conversion and enantioselectivity) with increasing steric bulk. However, this system also shows that there is only a small window in steric bulk as too bulky ligands such as **L5** (R_1= ^{t}Bu) are completely inactive in the hydrocyanation of styrene. Different

coordination behavior of **L5** was not observed, which could have explained why the catalytic system Ni/**L5** is inactive. **L**Ni(CO)$_2$ and **L**Ni(styrene) complexes show similar spectroscopic details, see Table 3 and Figure 6.

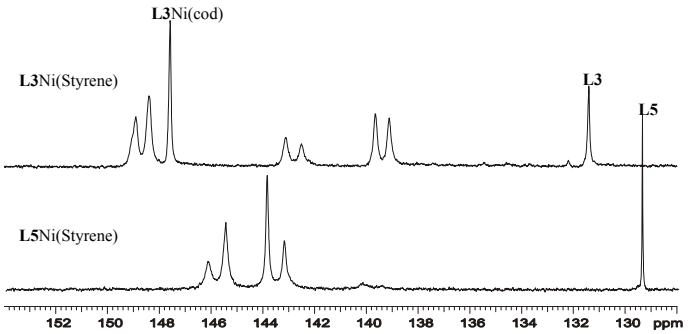

Figure 6 $^{31}P\{^1H\}$NMR of **L3**Ni(Styrene) and **L5**Ni(Styrene)

§ 4.4 Variation on 3 and 3′ position of (*R*)-Binaphthol

To stay within the active window but still change the ligand significantly, modifications can be made in the *para* position of the phenol or in the **3** and **3′** position of the BINOL backbone. The **3** and **3′** positions, **R**$_2$ and **R′**$_2$ (Figure 7) were selected, since the binaphthol unit bears the stereogenic element (atropisomeric axis).

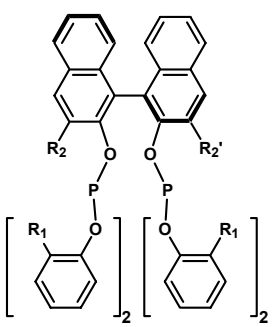

L	R1	R2	R'2
L6	^{i}Pr	Me	H
L7	^{i}Pr	Me	Me
L8		Me	H
L9		Me	Me

Figure 7 *Ligands **L6-L9***

Consecutive protection, lithiation, methylation and deprotection steps were performed in order to obtain the substituted binaphthol derivatives with one or two Me-groups *ortho* to the hydroxyl-functionalities, similar to the route reported by

Dennis and Woodward. [19] These two substituted binaphthols were then converted into the diphosphites **L6-L9** by reaction with the appropriate phosphorochloridites, which were derived *in situ* from PCl_3 and 2-isopropylphenol or 2-[1,3]-dioxan-2-yl-phenol in the presence of NEt_3. Ligands **L6-L9** (Figure 7) were applied in the nickel-catalyzed hydrocyanation of styrene (Table 5).

Table 5 *Asymmetric hydrocyanation of styrene with Ni/(**L6-L8**)*

Ligand	**L6**	**L7**	**L8**	**L9**
$\mathbf{R_1}$	^{i}Pr	^{i}Pr	$C_4H_7O_2$	$C_4H_7O_2$
$\mathbf{R_2}$, $\mathbf{R_{2'}}$	H, Me	Me, Me	H, Me	Me, Me
Conv (%)	19	86	100	100
ee (%)	33	0	34	13

Conditions: Ni/L/Styrene/HCN: 1/1.1/100/200 in 1.2 mL toluene at 60 °C for 4 h

All ligands (**L1-L9**) are C_2 symmetric with the exception of **L6** and **L8**, which are non-symmetric (C_1). Because ligands **L4**, **L8** and **L9** performed best, they were further investigated in additional hydrocyanation experiments, in which temperature and substrate were varied.

Table 6 *Asymmetric hydrocyanation experiments with ligands **L4**, **L8** and **L9***

Entry	Substrate	T (°C)	**L4** (Conv[ee]) %	**L8** (Conv[ee]) %	**L9** (Conv[ee]) %
1	Styrene	60	100 [43]	100 [34]	100 [13]
2	Styrene	0	69 [47]	100 [49]	90 [13]
3	Styrene	-30	nd	9 [53]	nd
4	4-MeStyrene	0	100 [54]	100 [50]	67 [23]
5	tr-β-MeStyrene	60	nd	24 [30]	nd
6	MVN	25	nd	100 [21*S*]	nd
7	Piperylene	60	nd	100 [33]	nd
8[a]	Cyclohexadiene	80	100 [43]	100 [63]	100 [29]
9[b]	Cyclohexadiene	60	nd	53 [71]	nd
10[b]	Cyclohexadiene	0	nd	45 [86]	nd
11	2,3-diMeBuDiene[c]	60	nd	0	nd

Conditions: Ni/L/Substrate/HCN: 1/1.1/100/200 in 1.2 mL toluene for 4 hours
[a] Acetone cyanohydrin was used as HCN source [b] Ni/Substrate: 1/500 [c] 2,3-dimethylbuta-1,3-diene

Hydrocyanation experiments were performed with the best system (**L8**) at 0 °C, and still obtained full conversion of the substrate styrene and 4-methylstyrene; the observed enantioselectivities are promising but need to be improved. The TON at 60 ˚C was determined to be 603 from an experiment with a styrene/nickel ratio of 1000. Trans-β-methylstyrene also reacts with excellent regioselectivity (>99%) towards α-ethylbenzylnitrile.

Hydrocyanation of dienes such as butadiene give different products for the 1,2- and 1,4-addition; hydrocyanation of butadiene results in formation of 2-methyl-3-butenenitrile (1,2-product) and 3-pentenenitrile (1,4-product). However, piperylene [20,21] and 1,3-cyclohexadiene [22] react via a symmetrical allyl system which causes the 1,2- and 1,4-products to be identical. Hydrocyanation of 1,3-cyclohexadiene is selective towards 2-cyclohexene-1-carbonitrile, some isomerization towards 3-cyclohexene-1-carbonitrile is observed after full conversion but no dinitriles were observed. [22] Ligand **L8** gives an excellent enantioselectivity of 86 % in the hydrocyanation of 1,3-cyclohexadiene at 0 °C. Not all cyclic dienes react with high selectivity. When 1,3-cyclooctadiene was applied as substrate, three products were observed in the GC, which were identified by GC-MS and COSY NMR as 1-, 2- and 3-cyclooctene-1-carbonitrile.

Other dienes gave different results, as the hydrocyanation of piperylene is selective but not very enantioselective, while 2,3-dimethylbuta-1,3-diene and α-terpinene gave not even traces of nitriles.

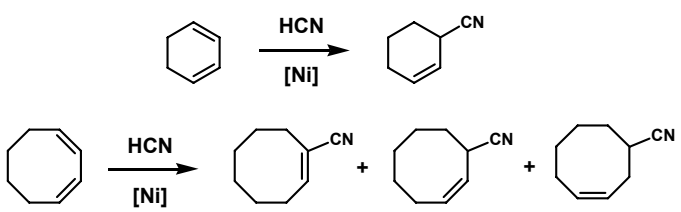

Figure 8: *The hydrocyanation of 1,3-cyclohexadiene and 1,3-cyclooctadiene*

In all hydrocyanation experiments, with active catalyst, cyclooctenenitriles were observed as hydrocyanation products from 1,5-cyclooctadiene using $Ni(cod)_2$ as metal precursor. This observation is different from the report by Casalnuovo and RajanBabu, in which no cyclooctenenitriles were detected. Based on this observation and the fact that their substrate, 6-methoxy-2-vinylnaphthalene, does not exchange with 1,5-cyclooctadiene in (**L**)Ni(cod), they argue that the catalysis proceeds via (**L**)Ni(CN)H (stage **V** in Figure 9).

The catalytic system with ligand **L8** first forms the complex (**L8**)Ni(cod), indicated by two doublets in the ^{31}P NMR spectrum at 149.1 and 145.5 with J_{PP} = 27.8 Hz. Upon addition of 50 equivalents of styrene (**L8**)Ni(Styrene) is formed but (**L8**)Ni(cod) is still present, even at elevated temperatures (Figure 10). These two observations, the hydrocyanation of cyclooctadiene and the presence of (**L**)Ni(styrene), suggests that this reaction proceeds via stage **II**, an η^2-coordinated substrate complex, and not via stage **V** (Figure 9). However, addition of 1,3-cyclohexadiene to (**L8**)Ni(cod) did not result in formation of (**L8**)Ni(1,3-cyclohexadiene) based on the ^{31}P NMR spectrum.

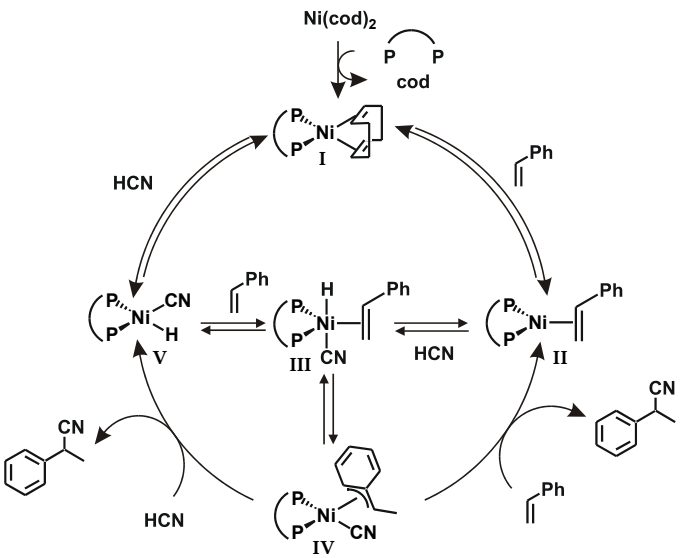

Figure 9 *Catalytic cycle for the hydrocyanation of styrene*

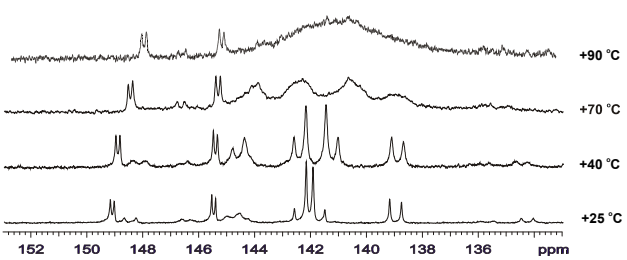

Figure 10 *^{31}P{^{1}H}VT NMR of **L8**Ni(cod) and 50 equiv. styrene in toluene-d8*

§ 4.5 Conclusions

In the hydrocyanation of vinylarenes the steric parameter is equally important as the electronic effect. By controlling the sterics, the ligand can be tuned to the extent that inactive nickel bis-chelate complexes are not formed, leading to active catalysts in the hydrocyanation of vinylarenes and conjugated dienes. Moderate enantioselectivities were obtained for styrene (53%) and 4-methylstyrene (54%). Hydrocyanation of 1,3-cyclohexadiene proved to be selective to 2-cyclohexene-1-carbonitile with 86% ee. In this modular ligand system the catalytic active steric window seems to be narrow. Several modifications to the ligand are possible which ultimately can lead to high enantioselectivities.

§ 4.6 Experimental

Chemicals were purchased from Aldrich, Acros or Merck and used as received. Styrene and 4-methylstyrene were distilled over CaH_2 prior to use. All preparations were carried out under an argon atmosphere using standard Schlenk techniques. $Ni(cod)_2$ [23], $PtCl_2(cod)$ [24] and HCN [25] were synthesized according to literature procedures. NMR spectra were recorded on a Varian Unity Inova 500 (VT NMR), Mercury 400 and Mercury 200 spectrometer (^1H, $^{13}C\{^1H\}$, $^{31}P\{^1H\}$). Maldi-TOF mass spectroscopy was performed on a PerSeptive Biosystems Voyager-DE PRO spectrometer. Elemental analysis was performed on a Perkin Elmer 2400 apparatus. IR spectra were recorded on an Avatar 360 FT-IR instrument in ATR mode.

Caution! HCN is a highly toxic, volatile liquid (bp 27 ˚C) that is also susceptible to explosive polymerization in the presence of base catalysts. It should be handled only in a well-ventilated fume hood by teams of at least two technically qualified persons who have received appropriate medical training for treating HCN poisoning. Sensible precautions include having available proper first aid equipment as well as HCN monitors. Uninhibited HCN should be stored at a temperature lower than its melting point (-13 ˚C). Excess of HCN may be disposed by addition to aqueous sodium hypochlorite, which converts the cyanide to cyanate.

General procedure for ligands L1-L9

The appropriate phenol (14.0 mmol) and Et_3N (6 mL, 43.00 mmol) were added dropwise at –10 ˚C to a solution of PCl_3 (0.95 g, 6.99 mmol) in 200 mL of toluene and the mixture was stirred for 30 minutes. (*R*)-2,2′-binaphthol (1.00 g, 3.50 mmol)

dissolved in 10 mL of THF was added dropwise to the mixture at –10 ºC. The mixture was stirred for 1h at room temperature. Salts were filtered off over a short path of basic alumina (4 cm) and all volatiles were evaporated.

(*R*)-[1,1']Binaphthyl-2,2'-bis(diphenylphosphite) (L1)

PCl_3 (0.95 g, 6.99 mmol), phenol (1.31 g, 13.93 mmol), Et_3N (6 mL, 43.00 mmol), (*R*)-2,2′-binaphthol (1.00 g, 3.50 mmol)

A white paste was obtained after purification by column chromatography (silica 60, hexanes/EtOAc (10:1)). Yield: 1.04 g (1.45 mmol, 41%)

^{1}H NMR: (200 MHz, $CDCl_3$) δ (ppm): 7.89 (dd, ^3J=8.98 Hz, ^4J=3.12 Hz, 4H), 7.50 (d, ^3J=8.98 Hz, 2H), 7.44-7.35 (m, 2H), 7.22 (d, ^3J=4.68 Hz, 4H), 7.12-6.95 (m, 12H), 6.69 (d, ^3J=7.42 Hz, 4H), 6.32 (d, ^3J=7.03 Hz, 4H) ^{13}C NMR: (100 MHz, $CDCl_3$) δ (ppm): 151.30, 151.10, 147.96, 133.85, 130.70, 129.83, 129.62, 129.27, 129.17, 127.91, 126.76, 125.94, 124.91, 123.74, 123.72, 120.60 (m), 120.40 (m) ^{31}P NMR: (162 MHz, C_6D_6) δ (ppm): 127.5 (s) Maldi-TOF: 717.45 (M^+-1), 741.45 (M^++Na) Elemental Analysis: Calculated (Found): %C 73.53 (73.55), %H 4.49 (4.65)

(*R*)-[1,1']Binaphthyl-2,2'-bis(di(*o*-tolyl)phosphite) (L2)

PCl_3 (0.95 g, 6.99 mmol), *o*-cresol (1.51 g, 13.97 mmol), Et_3N (6 mL, 43.00 mmol), (*R*)- 2,2′-binaphthol (1.00 g, 3.50 mmol)

A white paste was obtained after purification by column chromatography (silica 60, hexanes/EtOAc (9:1). Yield: 1.12 g (1.43 mmol, 40 %)

^{1}H NMR: (400 MHz, $CDCl_3$) δ (ppm): 7.82 (d, ^3J=8.79 Hz, 4H), 7.47 (d, ^3J=9.16 Hz, 2H), 7.35 (m, 2H), 7.19 (m, 4H), 7.00 (d, ^3J=7.33 Hz, 4H), 6.87 (t, ^3J=7.33 Hz, 4H), 6.68 (q, ^3J=8.06 Hz, 4H), 6.62 (d, ^3J=7.69 Hz, 2H), 6.57 (d, ^3J=7.69 Hz, 2H), 1.93 (s, 12H^{CH3}) ^{13}C NMR: (100 MHz, $CDCl_3$) δ (ppm): 149.97, 149.92, 147.93, 133.85, 130.87, 130.84, 130.67, 129.72, 129.42, 126.60, 126.49, 126.46, 125.96, 124.85, 123.58, 122.94, 120.9 (m), 120.0 (m), 16.39, 16.37 ^{31}P NMR: (162 MHz, $CDCl_3$) δ (ppm): 130.0 (s) Maldi-TOF: 773.54 (M^+-1) Elemental Analysis: Calculated (Found): %C 74.4 (73.9), %H 5.2 (5.4)

(*R*)-[1,1']Binaphthyl-2,2'-bis(di(*o*-isopropylphenyl)phosphite) (L3)

PCl_3 (0.98 g, 7.21 mmol), 2-(isopropyl)phenol (1.96 g, 14.40 mmol), Et_3N (6 mL, 43.00 mmol), (*R*)- 2,2′-binaphthol (1.03 g, 3.60 mmol)

The product crystallized from 5 mL *n*-heptane at –30 °C as a white crystalline solid. Yield: 2.2 g (2.48 mmol, 69 %)

^{1}H NMR: (400 MHz, $CDCl_3$) δ (ppm): 7.93 (d, ^3J=8.8 Hz, 2H), 7.91 (d, ^3J=6.2 Hz, 2H), 7.62 (d, ^3J=8.8 Hz, 2H), 7.43 (t, ^3J=6.6 Hz, 2H), 7.32-7.26 (m, 4H), 7.19 (d, ^3J=7.7 Hz, 4H), 7.02 (t, ^3J=7.3 Hz, 4H), 6.84 (dt, ^3J=8.1 Hz, 4H), 6.70 (d, ^3J=8.1 Hz, 2H), 6.67 (d,

^{3}J=8.1 Hz, 2H), 3.30 (sept, ^{3}J=6.2 Hz, **H**C(CH_3)$_2$, 4H), 0.97 (m, HC(C**H**$_3$)$_2$, 24H) ^{13}C NMR: (100 MHz, $CDCl_3$) δ (ppm): 148.9, 148.0, 139.41,139.37, 134.0, 130.8, 129.7, 127.9, 126.6, 126.29, 126.25, 126.21, 126.16, 126.10, 124.9, 123.8, 121.24, 121.20, 121.15, 120.07, 120.01, 119.95, 119.91, 119.86, 119.80, 26.64, 26.59, 22.82, 22.78, 22.69
^{31}P NMR: (162 MHz, $CDCl_3$) δ (ppm): 131.4 (s) Maldi-TOF: 885.57 (M^+-1), 919.60 (M^++O_2) Elemental Analysis: Calculated (Found): %C 75.8 (75.0), %H 6.4 (6.5)

(*R*)-[1,1']Binaphthyl-2,2'-bis(di(*o*-[1,3]-dioxan-2-yl-phenyl)phosphite) (L4)

PCl_3 (0.60 g, 4.42 mmol), 2-(1,3-dioxan-2-yl)phenol (1.30 g, 7.22 mmol), Et_3N (3mL, 21.50 mmol), (*R*)-2,2′-binaphthol (0.60 g, 3.33 mmol)
A white solid was obtained after recrystallization from cyclohexane. Yield: 180 mg (0.17 mmol, 5 %)
^{1}H NMR: (400 MHz, $CDCl_3$) δ (ppm): 7.89 (d, ^{3}J=8.79 Hz, 2H), 7.86 (d, ^{3}J=8.06 Hz, 2H), 7.65 (d, ^{3}J=9.15 Hz, 2H), 7.55 (dd, ^{3}J=7.69 Hz, ^{4}J=1.83 Hz, 2H), 7.52 (dd, ^{3}J=7.69 Hz, ^{4}J=1.83 Hz, 2H), 7.36 (dt, ^{3}J=7.51 Hz, ^{4}J=1.47 Hz, 2H), 7.29-7.16 (m, 4H), 7.05-6.94 (m, 6H), 6.89 (dt, ^{3}J=7.69 Hz, ^{4}J=1.83 Hz, 2H), 6.66 (d, ^{3}J=8.06 Hz, 2H), 6.52 (d, ^{3}J=8.05 Hz, 2H), 5.55 (s, 2H), 5.51 (s, 2H) 4.04-.92 (m, 8H), 3.69-3.51 (m, 8H), 2.13-1.99 (m, 4H), 1.19 (d, ^{3}J=12.45 Hz, 4H) ^{13}C NMR: (100 MHz, $CDCl_3$) δ (ppm): 148.81, 147.96, 133.91, 130.82, 129.86, 129.81, 129.71, 127.88, 127.26, 127.19, 126.80, 126.13, 125.06, 123.88, 123.82, 121.20 (m), 119.70 (m), 96.7, 67.2, 26.9, 25.7 ^{31}P NMR: (162 MHz, $CDCl_3$) δ (ppm): 130.3 Maldi-TOF: 1061.71 (M^+-1, 100%), 1085.73 (M^++Na, 50%), 1101.73 (M^++K, 60%)

(*R*)-[1,1']Binaphthyl-2,2'-bis(di(*o*-^{t}butylphenyl)phosphite) (L5)

PCl_3 (1.03 g, 7.58 mmol), 2-(^{t}Bu)phenol (2.24 g, 14.92 mmol), Et_3N (6 mL, 43.00 mmol), (*R*)-2,2′-binaphthol (1.07 g, 3.74 mmol)
A white solid was obtained after purification by column chromatography (silica 60, *n*-hexanes/EtOAc (9:1)). Yield: 1.51g (1.60 mmol, 43 %)
^{1}H NMR: (400 MHz, $CDCl_3$) δ (ppm): 7.82 (d, ^{3}J=8.42 Hz, 2H), 7.80 (d, ^{3}J=8.79 Hz, 2H), 7.45 (d, ^{3}J=9.15 Hz, 2H), 7.37-7.32 (m, 2H), 7.23-7.17 (m, 8H), 6.91-6.84 (m, 6H), 6.77-6.67 (m, 6H), 1.20 (s, 18H^{CH3}), 1.18 (s, 18H^{CH3}) ^{13}C NMR: (100 MHz, $CDCl_3$) δ (ppm): 151.1 (d, *J*=4.57 Hz), 139.6, 134.0, 130.8, 129.8, 127.9, 126.9 (d, *J*=3.05 Hz), 126.7 (d, *J*=3.82 Hz), 126.7, 126.1, 124.9, 122.9 (d, *J*=6.86 Hz), 120.8 (d, *J*=5.22 Hz), 120.0 (d, *J*=8.36 Hz), 119.8 (d, *J*=3.91 Hz), 119.6 (d, *J*=9.15 Hz), 34.5 (d, *J*=3.82 Hz, *C*CH_3), 29.9 (s, *C*H_3) ^{31}P NMR: (162 MHz, $CDCl_3$) δ (ppm): 129.4 (s) Maldi-TOF: 941.37 (M^+-1), 965.40 (M^++Na), 981.39 (M^++K) Elemental Analysis: Calculated (Found): %C 76.4 (76.2), %H 6.8 (6.9)

(*R*)-2,2′-Bis(1-ethoxyethoxy))-1,1′-binaphthyl

Azeotropically dried pyridinium *p*-toluenesulfonate (880 mg, 3.49 mmol) was dissolved in 300 mL CH_2Cl_2. Azeotropically dried (*R*)-2,2′-binaphthol (10.0 g, 34.9 mmol) was added to the mixture, followed by dropwise addition of distilled ethyl vinyl ether (10 mL, 104.7 mmol). The mixture was stirred at room temperature for 3 days. All volatiles were evaporated and the residue was purified by column chromatography (Silica 60, EtOAc/hexanes, 1:7). Yield: 10.03 g (23.0 mmol, 66.7 %)
^{1}H NMR: (200 MHz, $CDCl_3$) δ (ppm): 7.85-7.0 (m, 12H), 5.2 (m, 1H), 5.1 (m, 1H), 3.5 (m, 2H), 3.25 (m, 2H), 1.1 (m, 3H), 1.01 (m, 3H), 0.85 (m, 6H)

(*R*)-3-Methyl-2,2′-bis(1-ethoxyethoxy)-1,1′-binaphthyl

To a solution of (*R*)-2,2′-bis(1-ethoxyethoxy))-1,1′-binaphthyl (5.015 g, 11.65 mmol) in 50 mL of THF 12 mL ^{n}BuLi (2.5 M in hexanes) was added at –78 ˚C. The mixture was stirred at –78 ˚C for 3h. Methyl iodide (6.4 g, 45.0 mmol) was added dropwise at –78 ˚C, then the cooling was removed and the mixture was stirred overnight at room temperature. The mixture was concentrated, and the residue was redissolved in CH_2Cl_2 and washed with water. The organic layer was dried over $MgSO_4$ and concentrated. Yield: 4.77 g (10.74 mmol, 92%)
^{1}H NMR: (200 MHz, $CDCl_3$) δ (ppm): 7.92-7.13 (m, 11H), 5.29 (m, 1H), 5.18 (m, 1H), 3.4 (m, 2H), 3.05 (m, 2H), 2.6 (s, 3H), 0.99 (m, 3H), 0.88 (m, 3H), 0.72 (t, 6H)

(*R*)-3-Methyl-2,2′-binaphthol

To a solution of (*R*)-3-Methyl-2,2′-bis(1-ethoxyethoxy)-1,1′-binaphthyl (1.0 g, 2.25 mmol) in a 20 mL benzene and 4 mL methanol, 4 mL of an HCl solution (2.0 M in Et_2O) was added dropwise. The mixture was stirred overnight at room temperature. All volatiles were evaporated and no further purification was necessary. Yield: 676 mg (2.25 mmol, 100%)
^{1}H NMR: (200 MHz, $CDCl_3$) δ (ppm): 8.0-7.1 (m, 11H), 5.1 (s, 1H), 5.06 (s, 1H), 2.5 (s, 3H)

(*R*)-3-Methyl[1,1']binaphthyl-2,2'-bis(di(*o*-isopropylphenyl)phosphite) (L6)

PCl_3 (240 mg, 1.73 mmol), 2-isopropylphenol (413 mg, 3.03 mmol), Et_3N (700 mg, 6.93 mmol) and (*R*)-3-Methyl-2,2′-binaphthol (260 mg, 0.87 mmol)
The residue was purified with column chromatography over silica 60 eluting with EtOAc/hexanes, 1:16. Yield: 0.26 g (0.29 mmol, 33 %)
^{1}H NMR: (400 MHz, $CDCl_3$) δ (ppm):7.80-6.70 (m, 27H), 3.0 (sept, 4H), 2.45 (s, 3H), 1.0 (m, 24H) ^{13}C NMR: (100 MHz, $CDCl_3$) δ (ppm): 149.1, 139.3-119.7 (aromatic signals), 26.6, 22.9, 22.7, 22.6, 22.5, 18.3 ^{31}P NMR: (162 MHz, $CDCl_3$) δ (ppm): 134.3

(d, J_{PP}=24 Hz), 129.8 (d, J_{pp}=24Hz) Maldi-TOF: 899.20 (M^+-1, 100%), 923.21 (M^++Na, 10%)

(*R*)-3-Methyl[1,1']binaphthyl-2,2'-bis(di(*o*-[1,3]-dioxan-2-yl-phenyl)phosphite) (L8)

PCl_3 (915 mg, 6.66 mmol), 2-(1,3-dioxan-2-yl)phenol (2.10 g, 11.66 mmol), Et_3N (2.7 g, 26.64 mmol), (*R*)-3-methyl-2,2′-binaphthol (1 g, 3.33 mmol)

The product was recrystallized from isopropanol/acetone. Yield: 1.31 g (1.22 mmol, 37 %)

^{1}H NMR: (400 MHz, $CDCl_3$) δ (ppm): 7.79-6.94 (m, 27H), 5.57 (s, 1H), 5.45 (s, 1H), 5.43 (s, 1H), 5.22 (s, 1H), 4.0 (m, 8H), 3.56 (m, 8H), 2.49 (s, 3H), 1.22 (m, 8H)

^{13}C NMR: (100 MHz, $CDCl_3$) δ (ppm): 145.0, 144.0, 130.2-120.0 (aromatic signals), 96.7, 67.2, 25.7, 19.1 ^{31}P NMR: (162 MHz, $CDCl_3$) δ (ppm): 132.4 (d, J_{PP}=17 Hz), 129.73 (d, J_{PP}=17 Hz) Maldi-TOF: 1075.52 (M^+-1, 100%), 1099.53 (M^++Na, 25%), 1115.52 (M^++K, 20%) Elemental Analysis: Calculated (Found): %C 67.9 (67.8), %H 5.2 (5.6)

(*R*)-3,3′-Dimethyl-2,2′-bis(1-ethoxyethoxy)-1,1′-binaphthyl

To a solution of (*R*)-2,2′-bis(1-ethoxyethoxy))-1,1′-binaphthyl (2.0 g, 4.65 mmol) in 24 mL of THF 4.64 mL ^{n}BuLi (2.5 M in hexanes) was added at –78 ˚C. The mixture was stirred at 0 ˚C for 3h. Methyl iodide (2.51 g, 17.65 mmol) was added dropwise at –78 ˚C, then the cooling was removed and the mixture was stirred overnight at room temperature.

The mixture was concentrated, and the residue was redissolved in CH_2Cl_2 and washed with water. The organic layer was dried over $MgSO_4$ and concentrated. Yield: 1.90 g (4.14 mmol, 89 %)

^{1}H NMR: (200MHz, $CDCl_3$) δ (ppm): 7.80-7.15 (m, 10H), 4.34 (m, 2H), 3.45 –3.04 (m, 4H), 2.56 (s, 6H), 1.07 (m, 3H), 0.94 (m, 3H), 0.74 (m, 6H)

(*R*)-3,3′-Dimethyl-2,2′-binaphthol

To a solution of (*R*)-3,3′-dimethyl-2,2′-bis(1-ethoxyethoxy)-1,1′-binaphthyl (1.90 g, 4.14 mmol) in a 30 mL benzene and 6 mL methanol, 6 mL of an HCl solution (2.0 M in Et_2O) was added dropwise. The mixture was stirred overnight at room temperature. All volatiles were evaporated and no further purification was necessary. Yield: 1.30 g (4.14 mmol, 100 %)

^{1}H NMR: (200MHz, $CDCl_3$) δ (ppm):7.83-7.1 (m, 10H), 5.1 (s, 2H), 2.5 (s, 6H)

(*R*)-3,3′-Dimethyl[1,1']binaphthyl-2,2'-bis(di(*o*-isopropylphenyl)phosphite) (L7)

PCl_3 (871 mg, 6.36 mmol), 2-isopropylphenol (1.52 g, 11.13 mmol), Et_3N (2.57 g, 25.44 mmol) and (*R*)-3,3′-dimethyl-2,2′-binaphthol (1 g, 3.18 mmol)

The residue was purified with column chromatography over silica 60 eluting with EtOAc/hexanes, 1:20. Yield: 0.43 g (0.47 mmol, 15 %)

^{1}H NMR: (400 MHz, $CDCl_3$) δ (ppm): 7.72-6.56 (m, 26H), 2.94 (sept, 4H), 2.47 (s, 6H), 0.92 (d, 24H, *J*=1.6Hz) ^{13}C NMR: (100 MHz, $CDCl_3$) δ (ppm): 149.2, 148.5, 139.2, 139.1, 133.3, 131.4, 131.0, 130.2, 127.1, 126.5, 126.1, 126.0, 125.5, 124.8, 123.5, 119.9(m), 119.3(m), 26.4, 22.8, 22.7, 22.6, 22.5, 18.2 ^{31}P NMR: (162 MHz, $CDCl_3$) δ (ppm): 133 (s) Maldi-TOF: 913.66 (M^+-1, 20%), 937.66 (M^++Na, 50%)

Elemental Analysis: Calculated (Found): %C 76.1 (76.3), %H 6.6 (6.5)

(*R*)-3,3′-Dimethyl[1,1']binaphthyl-2,2'-bis(di(*o*-[1,3]-dioxan-2-yl-phenyl)phosphite) (L9)

PCl_3 (871 mg, 6.36 mmol), 2-(1,3-dioxan-2-yl)phenol (2.01 g, 11.13 mmol), Et_3N (2.57 g, 25.44 mmol) and (*R*)-3,3′-dimethyl-2,2′-binaphthol (1 g, 3.18 mmol)

The product was crystallized from isopropanol/acetone. Yield: 1.63 g (1.50 mmol, 47 %)

^{1}H NMR: (400 MHz, $CDCl_3$) δ (ppm): 7.90-6.90 (m, 26H), 5.37 (s, 2H), 5.16 (s, 2H), 4.0 (m, 8H), 3.62 (m, 8H), 2.36 (s, 6H), 1.49 (m, 8H) ^{13}C NMR: (100 MHz, $CDCl_3$) δ (ppm): 148.8, 148,4, 133.3, 131.3, 131.0, 130.3, 129.7, 129.5, 129.4, 127.3, 127.2, 127.0, 126.5, 125.7, 125.0, 123.7, 123.5, 119.7(m), 118.8(m), 96.6, 96.3, 67.5, 67.2, 67.1, 66.9, 25.7, 18.2 ^{31}P NMR: (162 MHz, $CDCl_3$) δ (ppm): 131.3 (s) Maldi-TOF: 1089.11 (M^+-1, 100%), 1113.12 (M^++Na, 50%)

L3Ni(cod): 5 mg (0.018 mmol) $Ni(cod)_2$ and 16 mg (0.018 mmol) **L3** were dissolved in 1 mL toluene and stirred for 30 minutes. All volatiles were evaporated and the solids were dissolved in 0.75 mL of benzene-d_6.

^{1}H NMR: (400 MHz, C_6D_6) δ (ppm): 7.83 (d, ^3J=8.06 Hz, 2H), 7.63 (d, ^3J=8.79 Hz, 2H), 7.54 (d, ^3J=8.05 Hz, 2H), 7.46 (d, ^3J=8.78 Hz, 2H), 7.31 (d, ^3J=8.42 Hz, 2H), 7.83 (dd, ^3J=7.69 Hz, ^4J=1.84 Hz, 2H), 7.83 (dt, ^3J=7.51 Hz, ^4J=0.74 Hz, 2H), 6.94-6.83 (m, 6H), 6.80 (dt, ^3J=7.88 Hz, ^4J=1.83 Hz, 2H), 6.74 (dt, ^3J=7.32 Hz, ^4J=1.10 Hz, 2H), 6.47 (dt, ^3J=7.51 Hz, ^4J=1.47 Hz, 2H), 6.41 (d, ^3J=7.33 Hz, 2H), 5.15 (br s, 2H), 4.67 (br s, 2H), 3.79 (sept, ^3J=6.96 Hz, 2H), 2.91 (sept, ^3J=6.96 Hz, 2H), 2.80 (br s, 2H), 2.32 (br s, 2H), 2.20 (br s, 2H), 1.99 (br s, 2H), 1.35 (d, ^3J=6.59 Hz, 6H), 1.21 (d, ^3J=6.59 Hz, 6H), 0.91 (d, ^3J=6.96 Hz, 6H), 0.70 (d, ^3J=7.81 Hz, 6H). ^{31}P NMR: (162 MHz, C_6D_6) δ (ppm): 147.8 (s)

L3$PtCl_2$: 50 mg (13.40 mmol) $Pt(cod)Cl_2$ and 119 mg (13.40 mmol) **L3** in 3 mL CH_2Cl_2 and 2 mL CH_3CN were stirred for 1 hour at 25 ˚C. After 7 days at –30 ˚C crystals were formed suitable for X-ray analysis. Filtration and evaporation of all volatiles gave 123 mg (10.64 mg, 79%) of white crystalline product.
^1H NMR: (400 MHz, $CDCl_3$) δ (ppm): 7.92 (d, ^3J=8.79 Hz, $2H^{napht}$), 7.85 (d, ^3J=8.06 Hz, $2H^{arA}$), 7.78 (d, ^3J=8.06 Hz, $2H^{napht}$), 7.71 (d, ^3J=9.16 Hz, $2H^{napht}$), 7.50 (t, ^3J=7.32 Hz, $2H^{arA}$), 7.34 (t, ^3J=7.69 Hz, $2H^{arA}$), 7.26-7.19 (m), 7.12-7.03 (m), 6.92 (d, ^3J=6.59 Hz, $2H^{arB}$), 6.78 (t, ^3J=7.32 Hz, $2H^{arB}$), 6.14 (t, ^3J=7.69 Hz, $2H^{arB}$), 6.04 (d, ^3J=8.05 Hz, $2H^{arB}$), 3.26 (sept, ^3J=6.95 Hz, $2H^{arA}$), 2.79 (sept, ^3J=6.96 Hz, $2H^{arB}$), 1.10 (d, ^3J=6.96 Hz, $6H^{arA}$), 1.03 (d, ^3J=6.59 Hz, $6H^{arA}$), 0.78 (d, ^3J=6.95 Hz, $6H^{arB}$), 0.68 (d, ^3J=6.96 Hz, $6H^{arB}$). ^{13}C NMR: (100 MHz, $CDCl_3$) δ (ppm): 148.5 (m), 147.9 (m), 139.4, 138.2, 133.5, 131.7, 131.3, 128.5, 127.7, 127.0, 126.4, 126.3, 126.2, 125.9, 125.6, 125.5, 124.7, 123.1, 121.5, 119.4, 118.3, 26.6, 25.6, 23.2, 22.9, 22.6, 22.5 ^{31}P NMR: (162 MHz, $CDCl_3$) δ (ppm): 57.2 (s), 57.2 (d, $^1J_{PtP}$=5782 Hz) Elemental Analysis: calculated for **L3**$PtCl_2.0.5CH_2Cl_2$ (found): %C 58.4 (58.2), %H 4.9 (4.7)
X-ray crystal structure determination of **L3**$PtCl_2$
$C_{56}H_{56}Cl_2O_6P_2Pt \cdot 2.3\ CH_3CN \cdot 0.35\ CH_2Cl_2$, Fw = 1277.09, colourless needle, 0.36 x 0.12 x 0.12 mm^3, triclinic, P1 (no. 1), a = 11.8303(5), b = 11.9100(3), c = 12.1728(3) Å, α = 114.822(1), β = 95.154(4), γ = 98.106(2)°, V = 1519.79(9) $Å^3$, Z = 1, D_x = 1.395 g/cm^3, μ = 2.529 mm^{-1}. 31162 Reflections were measured on a Nonius Kappa CCD diffractometer (sealed tube, graphite monochromator, λ = 0.71073 Å) up to a resolution of $(\sin\theta/\lambda)_{max}$ = 0.65 $Å^{-1}$ at a temperature of 125(2) K. An absorption correction based on multiple measured reflections was applied (0.35-0.74 correction range). 13968 Reflections were unique (R_{int} = 0.0254). The structure was solved with Direct Methods [26] and refined with SHELXL-97 [27] against F^2 of all reflections. Non hydrogen atoms were refined with anisotropic displacement parameters. Hydrogen atoms were introduced in geometrically idealized positions and refined with a riding model. The acetonitrile and dichloromethane solvent molecules were refined with partial occupancies, respectively. 724 Parameters were refined with 189 restraints. R1/wR2 [I > 2σ(I)]: 0.0287/0.0792. R1/wR2 [all refl.]: 0.0289/0.0793. S = 1.135. Refined Flack parameter [28] x = -0.010(4); 99.9% Friedel pair coverage. Residual electron density between -0.41 and 1.69 e/$Å^3$. Geometry calculations and checking for higher symmetry was performed with the PLATON program [29].

General procedure for the hydrocyanation experiments

A solution of 1.1 equiv. (0.020 mmol) of ligand in 500 µL toluene was added to 5 mg (0.018 mmol) $Ni(cod)_2$ in a glovebox (N_2 atmosphere). 200 µL from this stock solution and 100 equiv. (0.73 mmol) of substrate were added with an Eppendorf pipet to a 15 mL reaction Schlenk tube equipped with a teflon coated stirring bar. A round-bottom Schlenk flask was filled with 1 mL toluene and 100 µL hydrogen cyanide, which was taken up in a 5 mL syringe and added to the reaction mixture by syringe pump during 2 hours (closed system). The reaction was stirred for another 2 hours, after which the reaction mixture was cooled to 0 ˚C and purged with a gentle stream of argon for 1 minute to remove traces of HCN. The reaction product was then analyzed by GC.

Yield is defined as (area of product) / (area of substrate + area of product) and was performed on a Shimadzu GC17A with Ultra 2 column (25 m with inner diameter of 0.20 mm) with a variable temperature program which consists of an initial isothermic temperature followed by an increase with 20 ˚C/min to 280 ˚C with a constant velocity pressure program using He as carrier gas.

Substrate	Initial Temp	Time	RT substrate	RT product
Styrene	90 ˚C	3 min	2.80 min	6.25 min
4-MeStyrene	110 ˚C	4 min	2.98 min	6.94 min
Trans-β-MeStyrene	110 ˚C	4 min	3.42 min	6.62 min
Piperylene	90 ˚C	3 min	1.22 min	2.18 min
1,3-cyclohexadiene	90 ˚C	3 min	1.49 min	4.65 min

Enantiomeric excess is defined as (area of enantiomer 1 – area of enantiomer 2) / (area of enantiomer 1 + area of enantiomer 2) and was determined on a Carlo Erba 6000 Vega series 2 GC with Lipodex E column (25 m with inner diameter of 0.25 mm), using an isothermic temperature program with 50 kPa H_2 pressure. The second enantiomer on the chiral GC trace, for all products, is the enantiomer in excess.

Substrate	Isothermic Temp	RT enantiomer 1	RT enantiomer 2
Styrene	150 ˚C	3.24 min	3.50 min
4-MeStyrene	120 ˚C	6.12 min	6.37 min
Trans-β-MeStyrene	130 ˚C	3.38 min	3.67 min
Piperylene	100 ˚C	2.47 min	3.16 min
1,3-cyclohexadiene	130 ˚C	3.30 min	3.46 min

Isomerization of 2M3BN to 3PN

The nickel precursor $Ni(cod)_2$ (5 mg, 0.018 mmol) and 1 equiv. (0.018 mmol) or 3 equiv. (0.054 mmol) of **L** were dissolved in 2 mL of toluene in a Schlenk tube and stirred for 5 minutes. The substrate 2M3BN (0.5 mL, 5.20 mmol) was added and the Schlenk tube was placed in an oil bath at 100 ˚C. Samples for GC analysis were taken over time to determine the TOF.

TOF is defined as formation of 3PN in mole per mole nickel per hour. Yield is defined as (area of product) / (area of substrate + area of product) and was performed on a Shimadzu GC17A with Ultra 2 column (25 m with inner diameter of 0.20 mm) with a variable temperature program that consists of an initial isothermic temperature, 40 ˚C for 5 min followed by an increase of 5 ˚C/min to 60 ˚C followed by an increase of 25 ˚C/min to 280 ˚C with a constant velocity pressure program using He as carrier gas. This resulted in the following retention times: 2M3BN (3.28 min), toluene (5.15 min) and 3PN (5.86 min).

L	TOF (1 equiv.) $\{h^{-1}\}$	TOF (3 equiv.) $\{h^{-1}\}$
L2	78	36
L3	74	85
L5	3	nd

§ 4.7 References

[1] Tolman, C. A., McKinney, R. J., Seidel, W. C., Druliner, J. D. and Stevens, W. R. *Adv. Catal.* **1985**, *33*, 1-46.

[2] Elmes, P. S. and Jackson, W. R. *J. Am. Chem. Soc.* **1979**, *101* (20), 6128-6129.

[3] Wilting, J. and Vogt, D. Asymmetric Hydrocyanation of alkenes. In *Handbook of C-H Transformations*, 1 ed.; Dyker, G., Ed.; Wiley-VCH: Weinheim, 2005; Vol. 1 pp 87-96.

[4] Babin, J. E. and Whiteker, G. T. Asymmetric syntheses using optically active metal-ligand complex catalysts. US US 5,360,938, **Nov 1, 1994.**

[5] Goertz, W., Kamer, P. C. J., Van Leeuwen, P. W. N. M. and Vogt, D. *Chem. Eur. J.* **2001**, *7* (8), 1614-1618.

[6] Yan, M., Xu, Q. Y. and Chan, A. S. C. *Tetrahedron: Asymmetry* **2000**, *11* (4), 845-849.

[7] Casalnuovo, A. L., RajanBabu, T. V., Ayers, T. A. and Warren, T. H. *J. Am. Chem. Soc.* **1994**, *116* (22), 9869-9882.

[8] RajanBabu, T. V. and Casalnuovo, A. L. *J. Am. Chem. Soc.* **1996**, *118* (26), 6325-6326.

[9] Goertz, W., Keim, W., Vogt, D., Englert, U., Boele, M. D. K., Van der Veen, L. A., Kamer, P. C. J. and Van Leeuwen, P. W. N. M. *J. Chem. Soc., Dalton Trans.* **1998**, (18), 2981-2988.

[10] Sakai, N., Nozaki, K., Mashima, K. and Takaya, H. *Tetrahedron: Asymmetry* **1992**, *3* (5), 583-586.

[11] Botteghi, C., Delogu, G., Marchetti, M., Paganelli, S. and Sechi, B. *J. Mol. Cat. A: Chem.* **1999**, *143* (1-3), 311-323.

[12] Tolman, C. A. *Chem. Rev.* **1977**, *77* (3), 313-348.

[13] Baker, M. J., Harrison, K. N., Orpen, A. G., Pringle, P. G. and Shaw, G. *J. Chem. Soc., Chem. Commun.* **1991**, (12), 803-804.

[14] Baker, M. J. and Pringle, P. G. *J. Chem. Soc., Chem. Commun.* **1991**, (18), 1292-1293.

[15] Wilting, J., Müller, C., Hewat, A. C., Ellis, D. D., Tooke, D. M., Spek, A. L. and Vogt, D. *Organometallics* **2005**, *24* (1), 13-15.

[16] Zuidema, E., Van Leeuwen, P. W. N. M. and Bo, C. *Organometallics* **2005**, *24* (15), 3703-3710.

[17] Culkin, D. A. and Hartwig, J. F. *Organometallics* **2004**, *23* (14), 3398-3416.

[18] Caporali, M., Müller, C., Staal, B. B. P., Tooke, D. M., Spek, A. L. and Van Leeuwen, P. W. N. M. *Chem. Commun.* **2005**, (27), 3478-3480.

[19] Dennis, M. R. and Woodward, S. *J. Chem. Soc., Perkin Trans. 1* **1998**, (6), 1081-1086.

[20] Keim, W., Behr, A., Lühr, H. O. and Weisser, J. *J. Catal.* **1982**, *78* (1), 209-216.

[21] Campi, E. M., Elmes, P. S., Jackson, W. R., Lovel, C. G., and Probert, M. K. S. *Aust. J. Chem.* **1987**, *40* (6), 1053-1061.

[22] Bäckvall, J. E. and Andell, O. S. *Organometallics* **1986**, *5* (11), 2350-2355.

[23] Schunn, R. A. *Inorg. Synth.* **1974**, *15*, 5-9.

[24] Clark, H. C. and Manzer, L. E. *J. Organomet. Chem.* **1973**, *59*, 411-428.

[25] Slotta, K. H. *Berichte d. D. Chem. Gesellschaft* **1934**, *67B*, 1028-1030.

[26] Sheldrick, G.M. (1997). SHELXS-97. Program for crystal structure solution. University of Göttingen, Germany.
[27] Sheldrick, G.M. (1997). SHELXL-97. Program for crystal structure refinement. University of Göttingen, Germany.
[28] Flack, H. D. *Acta Crystallogr., Sect. A: Found. Crystallogr.* **1983**, *A39* (6), 876-881.
[29] Spek, A. L. *J. Appl. Crystallogr.* **2003**, *36* (1), 7-13.

Chapter 5

The Enantioselective Step in the Nickel-Catalyzed Hydrocyanation of 1,3-cyclohexadiene

Enantioselective step	
Insertion into M-D bond	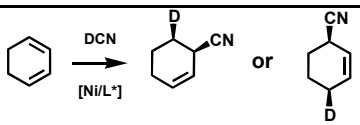
Reductive elimination of the product	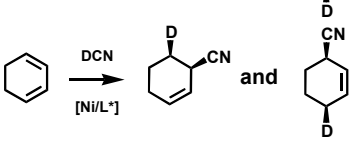

The reductive elimination of the product has been established to be the enantioselective step in the nickel-catalyzed hydrocyanation of 1,3-cyclohexadiene by determining the 1,2-/1,4-product distribution on the basis of deuterium labeling experiments. This result could be achieved by successfully exploiting the rather unique features of this reaction: identical product formation for 1,2- and 1,4-addition, *cis* addition over the diene and high enantiomeric excess.

Parts of the work described in this chapter have been published:

Jos Wilting, Michèle Janssen, Christian Müller and Dieter Vogt. The Enantioselective Step in the Nickel-Catalyzed Hydrocyanation of 1,3-Cyclohexadiene, *J. Am. Chem. Soc.*, **2006**, *128* (35), 11374-11375

§ 5.1 Introduction

The nickel-catalyzed asymmetric hydrocyanation is a useful carbon-carbon bond formation reaction for the production of optically active compounds; yet, the number of contributions in the literature regarding this topic are scarce. [1] Only vinylarenes [2-6] and norborn(adi)ene [6-14] have been applied as prochiral substrates so far. The generally accepted mechanism for the hydrocyanation of dienes as well as vinylarenes is depicted in Figure 1. The reductive elimination of the product is proposed to be the rate determining step, which causes the rate law to be zero order in substrate. [15] In the case of vinylarenes as substrates, Casalnuovo and RajanBabu concluded that the enantioselective step has to be either the substrate insertion into the Ni-H bond and/or the reductive elimination of the product since all diastereoisomers of the intermediate, containing coordinated substrate (stage **II** in Figure 1), were observed spectroscopically and are formed in almost equal amount. [2] They also showed that substrate insertion is reversible, by using a deuterium labeled substrate and that the relative rate of reductive elimination over β-hydride elimination increased when the electron density on phosphorus was reduced by introducing electron withdrawing groups on the ligand. However, so far, little is known about the deactivation pathway as well as the enantioselective step.

The enantioselective step in asymmetric catalytic reactions is intrinsically difficult to determine experimentally, nevertheless it has been studied for multiple reactions. Substrate coordination is commonly believed to be the enantioselective step in biocatalytic transformations. In asymmetric hydrogenation the enantioselectivity is determined during the oxidative addition of H_2 and the consecutive insertion. [16,17] Moreover, there is a delicate balance for kinetic vs. thermodynamic control. [18] In the asymmetric allylic alkylation the attack of the nucleophile on the allyl group is believed to be the enantioselective step. [19] In rhodium and platinum/tin catalyzed hydroformylation the enantioselective step changes with temperature, from olefin insertion into the M-H bond at low temperature to the reductive elimination of the product at high temperature. [20,21]

The main goal of this investigation is the determination of the enantioselective step in the hydrocyanation of 1,3-cyclohexadiene.

§ 5.2 Results

Addition of HCN to 1,3-cyclohexadiene results in the formation of 2-cyclohexene-1-carbonitrile; wherein 1,2- and 1,4-addition both lead to identical products, as at stage (**V**) (Figure 1) a symmetrical allyl fragment is formed in which the positions 2 and 4 cannot be distinguished.

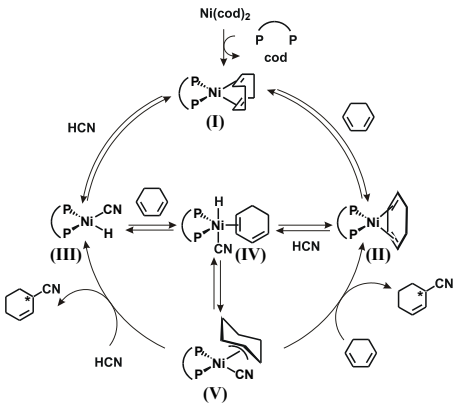

Figure 1 *Catalytic cycle of the Ni-catalyzed hydrocyanation of 1,3-cyclohexadiene*

However, by using DCN instead of HCN one can distinguish between the 1,2- and 1,4-addition products by NMR. Tolman demonstrated that the insertion of cyclopentadiene into $DNiL_4^+$ resulted in a deuterated (π-allyl)nickel complex in which the nickel center and the deuterium atom were located on the same side of the ring. [22] Bäckvall and Andell observed *cis* addition of DCN over the diene in 1,3-cyclohexadiene using $Ni(P(OPh)_3)_4$ as catalyst system. [23] *Cis* addition was further demonstrated by Jackson and Lovel for 4-*tert*-butylcyclohexene with $Pd(DIOP)_2$ as catalyst system. [9]

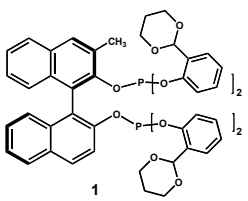

Figure 2 *Asymmetric diphosphite ligand **1***

Even though 1,2- and 1,4-addition results in opposite enantiomers, an enantiomeric excess of 86 % was achieved with the chiral diphosphite ligand **1** (Figure 2 and Chapter 4 of this thesis). This means that the CN-addition takes place at only one terminus of the η^3-allyl fragment. Addition of CN on the *Re* side of the Ni-allyl fragment (Figure 1) results in formation of the (*R*) enantiomer (Eq. 1 and Eq. 2 in Figure 3), while addition on the *Si* side of the Ni-allyl fragment leads to the formation of the (*S*) enantiomer. A series of β-hydrogen elimination -without dissociation of 1,3-cyclohexadiene (**V→IV** in Figure 1)- and subsequent reinsertion reactions could give the intramolecular interconversion of the corresponding two nickel-allyl intermediates (**K2**). If this would take place the 1,3-product would also be formed. However, the 1,3-product was not detected by either ^{13}C or ^{2}H NMR spectroscopy. Intermolecular conversion is excluded since this would lead to *trans* addition.

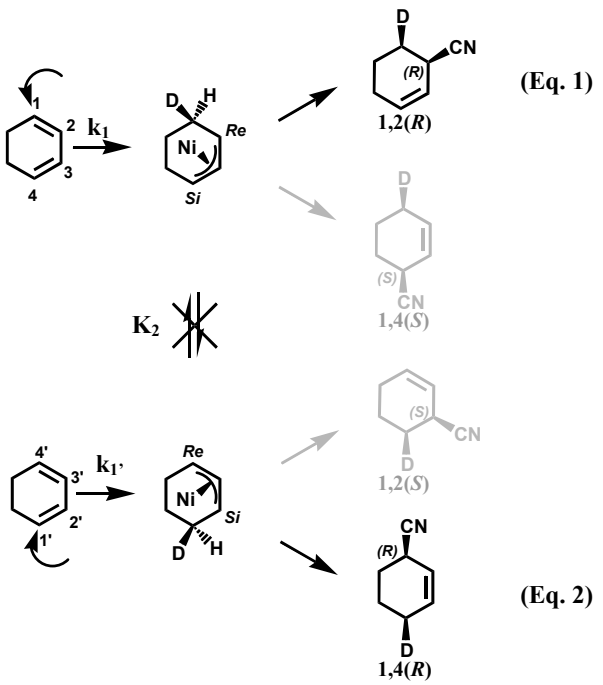

Figure 3 *The enantioselective deuteriocyanation of 1,3-cyclohexadiene*

These three rather unique features give the possibility to distinguish between insertion (**IV→V** in Figure 1) and reductive elimination (**V→II/III** in Figure 1) as the enantioselective step based on product distribution. In the theoretical case of 100 %

ee (*R*), one can expect, depending on the enantioselective step, the following product distributions:

(1) Insertion: The reaction proceeds either via Eq.1 ($\mathbf{k_1 >> k_{1'}}$ in Figure 3) or via Eq. 2 ($\mathbf{k_1 << k_{1'}}$) as 1,3-cyclohexadiene inserts in a specific way. Only one regioisomer will be formed (either **1,2(*R*)** or **1,4(*R*)**).

(2) Reductive elimination: Random insertion ($\mathbf{k_1 = k_{1'}}$) of the substrate will form the regioisomers, **1,2(*R*)** and **1,4(*R*)**, in equal amounts.

(3) Insertion and reductive elimination: *i.e.* Eq. 1 is favored over Eq. 2 by a small factor ($\mathbf{k_1 > k_{1'}}$ or $\mathbf{k_1 < k_{1'}}$), the **1,2(*R*)** and **1,4(*R*)** products will be formed in uneven amounts.

The results obtained for the asymmetric hydrocyanation of 1,3-cyclohexadiene with HCN and DCN at different temperatures are shown in Table 1. From GC-MS measurements it is clear that the product has incorporated one deuterium atom and that the substrate had no detectable deuterium incorporation ($\mathbf{k_1}$ is irreversible).

Table 1 *Hydro- and Deuteriocyanation of 1,3-cyclohexadiene*

Entry	H/D CN	T (˚C)	Y (%)	ee (%)[a]	1,2/1,4[c]	1,2/1,4[d] Red. Elim.	1,2/1,4[d] Insertion	Subs/Ni
1	HCN	60	57	71	-			500
2	DCN	60	50	75[b]	52/48(5)	50/50	87.5/12.5	100
3	HCN	0	45	86	-			500
4	DCN	0	10	85[b]	54/46(10)	50/50	92.5/7.5	100

[a] ee was determined with GC, lipodex E (130 ˚C, 50kPa H_2). [b] ee = {[1,2(*R*)+1,4(*R*)] – [(1,2(*S*) + 1,4(*S*)]} / {[1,2(*R*)+1,4(*R*)] + [(1,2(*S*) + 1,4(*S*)]}. [c] ratio was determined with $^{13}C\{^1H\}$NMR, with estimated error between parentheses [d] theoretical values for 1,2/1,4 ratio

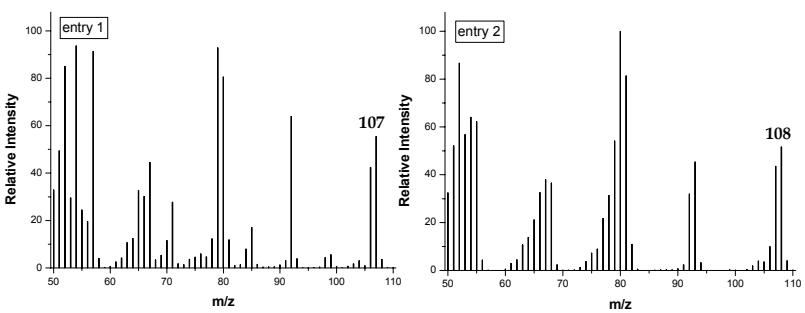

Figure 4 *Mass spectra from GC-MS measurements of HCN(left) and DCN (right) addition to 1,3-cyclohexadiene leading to 2-cyclohexene-1-carbonitrile (M^+ = 107), and 2-cyclohexene-1-carbonitrile-d_1 (M^+ = 108)*

While it is possible to separate both enantiomers with chiral GC, the diastereoisomers **1,2(*R*)** and **1,4(*R*)** as well as **1,2(*S*)** and **1,4(*S*)** could not be separated. However, the product ratio could be determined by means of $^{13}C\{^{1}H\}$ NMR of the nitrile in case of entries 2 and 4 and ^{1}H and ^{2}H NMR of the corresponding amine (entry 2), which was prepared by reduction of the nitrile with $LiAlH_4$.

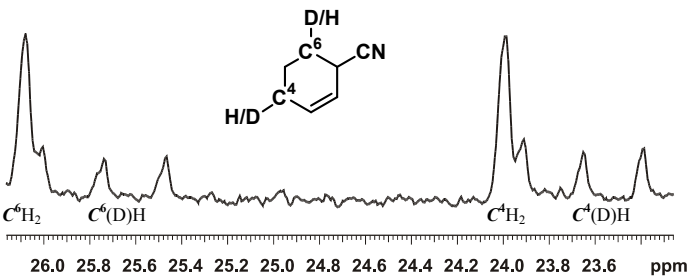

Figure 5 *Excerpt of $^{13}C\{^{1}H\}$ NMR spectrum of the products obtained in entry 2*

The reaction proceeds at 60 °C with an enantiomeric excess of 75 %. This would result in a product distribution of 87.5 / 12.5 when the enantioselectivity is determined during the insertion step and 50 / 50 in case the reductive elimination is the enantioselective step. From Table 1 it is obvious, that equal amounts of 1,2- and 1,4-product were formed when DCN was applied in the hydrocyanation reaction. Therefore, the enantioselective step has to be the reductive elimination. Although the activity is affected (the reported isotope effect is 3.6), no isotope effect was observed on the *ee*, which is in agreement with the observations made by RajanBabu in the hydrocyanation of 6-methoxy-2-vinylnaphthalene. [2]

§ 5.3 Conclusions

The reductive elimination of the product was established to be the enantioselective step in the nickel-catalyzed hydrocyanation of 1,3-cyclohexadiene, on the basis of deuterium labeling experiments and an equal 1,2- / 1,4-product distribution. This could be achieved by successfully exploiting the rather unique features of this reaction: identical product formation for 1,2- and 1,4-addition, *cis* addition over the diene and high enantiomeric excess.

§ 5.4 Experimental

Hydrocyanation experiments

A solution of 1.1 equiv. (0.020 mmol) of ligand in 500 µL of toluene was added to 5 mg (0.018 mmol) $Ni(cod)_2$ in a glovebox (N_2 atmosphere). From this stock solution 200 µL were added with an Eppendorf pipet to a 15 mL reaction Schlenk tube equipped with a teflon coated stirring bar followed by 500 equiv. (350 µL, 3.65 mmol) of 1,3-cyclohexadiene. A round bottom Schlenk flask was filled with 1 mL toluene and 100 µL hydrogen cyanide, which was taken up in a 5 mL syringe and added to the reaction mixture by syringe pump in 2 hours (closed system). The reaction was stirred for another 2 hours, after which the reaction mixture was cooled to 0 ˚C and was flushed with a gentle stream of argon for 1 minute to remove traces of HCN. The reaction product was then analyzed by GC. Filtration over silica/celite and removal of all solvents *in vacuo* left enough sample to be analyzed with NMR spectroscopy.

Deuteriocyanation experiments

To azeotropically (toluene) dried KCN (2 g, 30.8 mmol) was added 5 mL of D_2SO_4 (Aldrich, 98 wt % in D_2O, >99.5 atom % D) by syringe pump at 60 ˚C. The DCN vapour was condensed into 5 mL of toluene.

A solution of 1.1 equiv. (0.020 mmol) of ligand in 500 µL of toluene was added to 5 mg (0.018 mmol) $Ni(cod)_2$ in a glovebox (N_2 atmosphere).This solution and 100 equiv. (200 µL, 1.82 mmol) of substrate were added with an Eppendorf pipet to a 15 mL reaction Schlenk tube equipped with a teflon coated stirring bar. To this reaction mixture was added 2 mL from the DCN solution in toluene by syringe pump during 2 hours (closed system). The reaction was stirred for another 2 hours, after which the reaction mixture was cooled to 0 ˚C and was flushed with a gentle stream of argon for 1 minute to remove traces of DCN. The reaction product was then analyzed by GC. Filtration over silica/celite and removal of all solvents *in vacuo* left enough sample to be analyzed with NMR spectroscopy.

Reduction of 2-cyclohexene-1-carbonitrile-d_1

2-Cyclohexene-1-carbonitrile-d_1 was dissolved in 5 mL dry diethyl ether and $LiAlH_4$ (150 mg, 3.94 mmol) was added slowly. The reaction mixture was stirred for 5 hours at 30 ˚C, 2 mL MeOH was added and the resulting precipitate was filtered off. The ether phase was extracted with 2 M HCl (aqueous). The aqueous phase was extracted with ether, made alkaline with NaOH (aqueous) and extracted with ether. The organic phase was dried ($MgSO_4$), all volatiles were removed *in vacuo* and the product was dissolved in 0.75 mL $CDCl_3$.

Chiral GC

GC:	Carlo Erba 6000 Vega series 2
Column:	Lipodex E (25 m, 0.25 mm inner diameter)
Carrier gas:	Hydrogen 50 kPa
Temperature program:	130 ˚C (isotherm)
Injector:	280 ˚C
Detector:	280 ˚C
Split ratio:	25
Injection volume:	0.25 μL

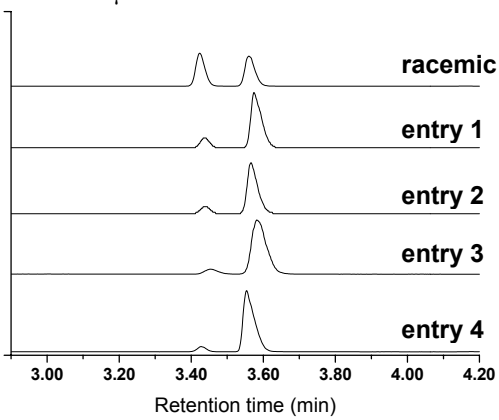

Entry	Area 1 (%)	Area 2 (%)	ee (%)
Racemic	49.94	50.06	0
1	13.10	86.90	74
2	12.36	87.64	75
3	6.51	93.49	86
4	7.74	99.26	85

MS from GC-MS measurement

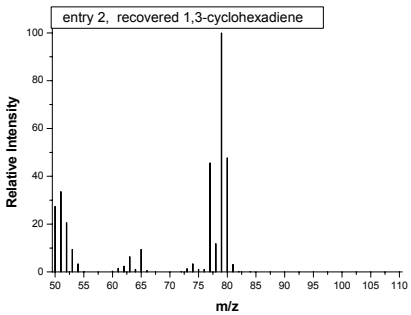

^{1}H and ^{2}H NMR Amine (entry 2)

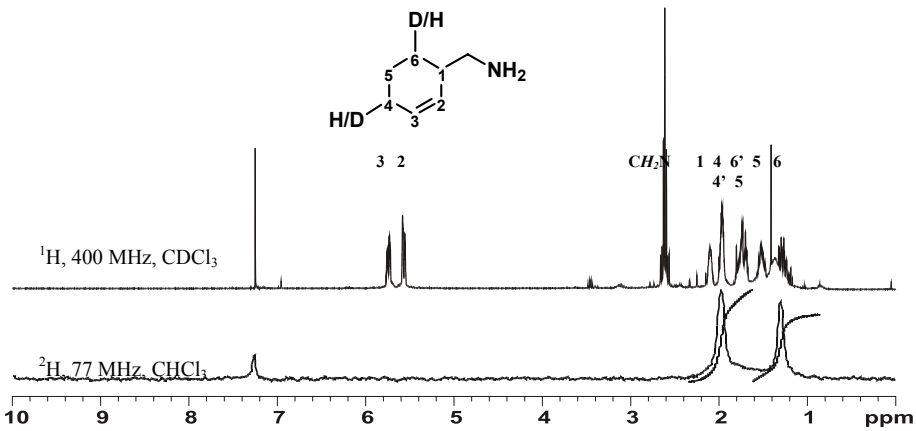

C4/C6 ratio for entries 2 and 4

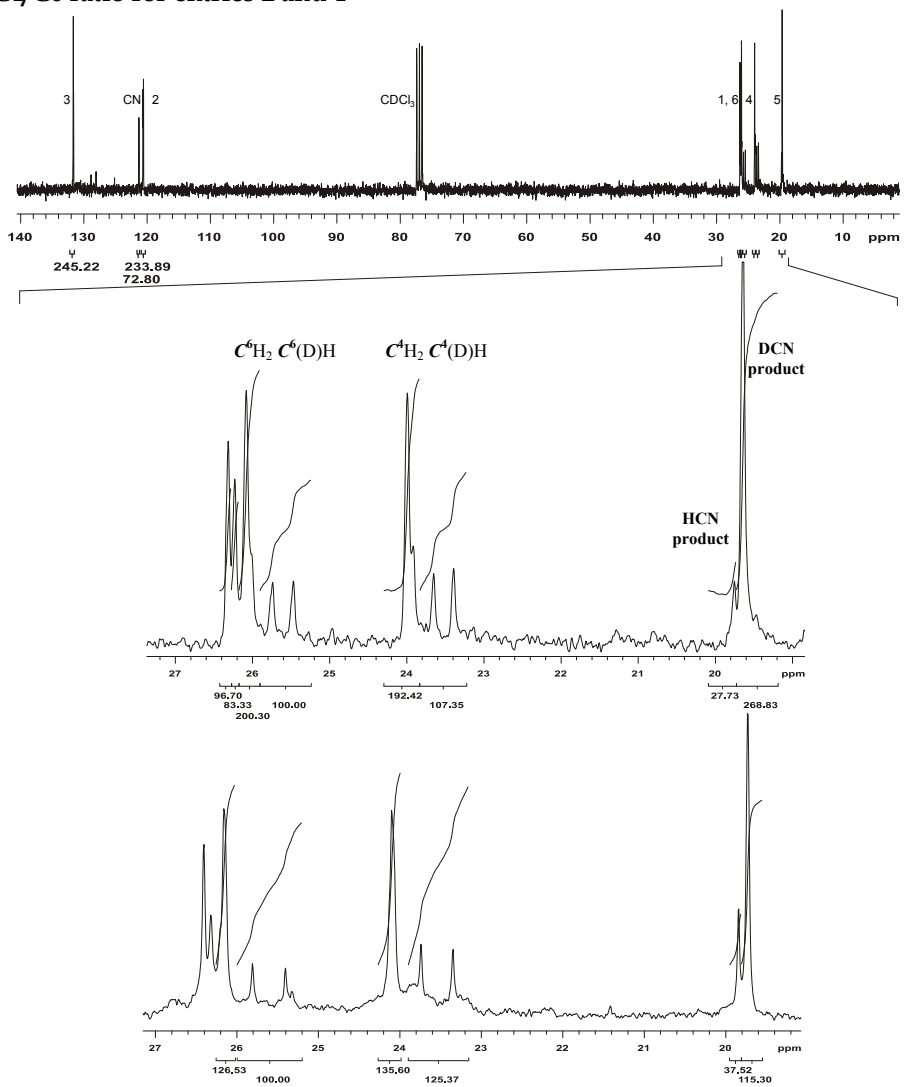

Entry	C	C'	Values	Ratio (%)
2	2/3 C(D)H	2/3 C'(D)H	107.35 / 100.00	51.8
2	C(CN)H	C'(CN)H	96.70 / 83.33	53.7
2	C^6H_2+1/3C'^{6}(D)H	C^4H_2+1/3C'^{4}(D)H	200.30 / 192.42	51.0
4	2/3 C(D)H	2/3 C'(D)H	125.37 / 100.00	55.6
4	C^6H_2+1/3C'^{6}(D)H	C^4H_2+1/3C'^{4}(D)H	135.60 / 126.53	51.7

§ 5.5 References

[1] Wilting, J. and Vogt, D. Asymmetric Hydrocyanation of alkenes. In *Handbook of C-H Transformations*, 1 ed.; Dyker, G., Ed.; Wiley-VCH: Weinheim, 2005; Vol. 1 pp 87-96.

[2] Casalnuovo, A. L., RajanBabu, T. V., Ayers, T. A. and Warren, T. H. *J. Am. Chem. Soc.* **1994**, *116* (22), 9869-9882.

[3] RajanBabu, T. V. and Casalnuovo, A. L. *J. Am. Chem. Soc.* **1996**, *118* (26), 6325-6326.

[4] Goertz, W., Kamer, P. C. J., Van Leeuwen, P. W. N. M. and Vogt, D. *Chem. Eur. J.* **2001**, *7* (8), 1614-1618.

[5] Babin, J. E. and Whiteker, G. T. Asymmetric syntheses using optically active metal-ligand complex catalysts. US 5360938, **1994.** *Chem. Abstr.* **1995,** *122*, 186609.

[6] Yan, M., Xu, Q. Y. and Chan, A. S. C. *Tetrahedron: Asymmetry* **2000**, *11* (4), 845-849.

[7] Elmes, P. S. and Jackson, W. R. *J. Am. Chem. Soc.* **1979**, *101* (20), 6128-6129.

[8] Elmes, P. S. and Jackson, W. R. *Aust. J. Chem.* **1982**, *35* (10), 2041-2051.

[9] Jackson, W. R. and Lovel, C. G. *Aust. J. Chem.* **1982**, *35* (10), 2053-2067.

[10] Hodgson, M. and Parker, D. *J. Organomet. Chem.* **1987**, *325* (1-2), C27-C30.

[11] Hodgson, M., Parker, D., Taylor, R. J. and Ferguson, G. *Organometallics* **1988**, *7* (8), 1761-1766.

[12] Horiuchi, T., Shirakawa, E., Nozaki, K. and Takaya, H. *Tetrahedron: Asymmetry* **1997**, *8* (1), 57-63.

[13] Baker, M. J., Harrison, K. N., Orpen, A. G., Pringle, P. G. and Shaw, G. *J. Chem. Soc., Chem. Commun.* **1991**, (12), 803-804.

[14] Baker, M. J. and Pringle, P. G. *J. Chem. Soc., Chem. Commun.* **1991**, (18), 1292-1293.

[15] Wilting, J., Müller, C., Hewat, A. C., Ellis, D. D., Tooke, D. M., Spek, A. L. and Vogt, D. *Organometallics* **2005**, *24* (1), 13-15.

[16] Knowles, W. S. *Acc. Chem. Res.* **1983**, *16* (3), 106-112.

[17] Noyori, R. *Angew. Chem. Int. Ed.* **2002**, *41* (12), 2008-2022.

[18] Landis, C. R. and Halpern, J. *J. Am. Chem. Soc.* **1987**, *109* (6), 1746-1754.

[19] Helmchen, G. and Pfaltz, A. *Acc. Chem. Res.* **2000**, *33* (6), 336-345.

[20] Horiuchi, T., Shirakawa, E., Nozaki, K. and Takaya, H. *Organometallics* **1997**, *16* (13), 2981-2986.

[21] Casey, C. P., Martins, S. C. and Fagan, M. A. *J. Am. Chem. Soc.* **2004**, *126* (17), 5585-5592.

[22] Tolman, C. A. *J. Am. Chem. Soc.* **1970**, *92* (23), 6785-6790.

[23] Bäckvall, J. E. and Andell, O. S. *Organometallics* **1986**, *5* (11), 2350-2355.

Chapter 6

The Kinetic Resolution of Allylic Nitriles

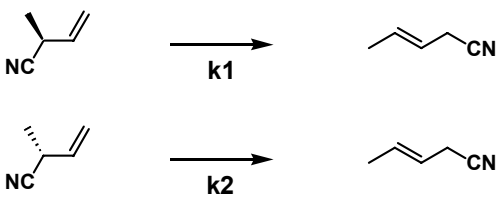

The kinetic resolution of 2-methyl-3-butenenitrile using chiral phosphorus based ligands with $Ni(cod)_2$ was achieved for the first time, with selectivities up to 2.0. Moreover, an interesting switch in enantioselectivity was observed during the kinetic resolution. The kinetic resolution of 2-cyclohexene-1-carbonitrile, synthesized by a preparative hydrocyanation of 1,3-cyclohexadiene, resulted in double bond isomerization to 3-cyclohexene-1-carbonitrile.

§ 6.1 Introduction

Kinetic resolution is the achievement of partial or complete resolution by virtue of unequal rates of reaction of the enantiomers in a racemate with a chiral agent (reagent, catalyst, solvent, etc.). [1]

The Sharpless epoxidation of racemic allylic alcohols is a well-known example of a kinetic resolution with a chiral homogeneous catalyst. In this kinetic resolution allylic alcohols are resolved with the epoxidation catalyst $Ti(O^iPr)_4$, using L-(+)-diisopropyl tartrate as the chiral reagent, together with ^{t}BuOOH as oxidation reagent, with a selectivity up to 138 (Figure 1). [2] Enzymes have also been applied successfully in kinetic resolutions. [3,4]

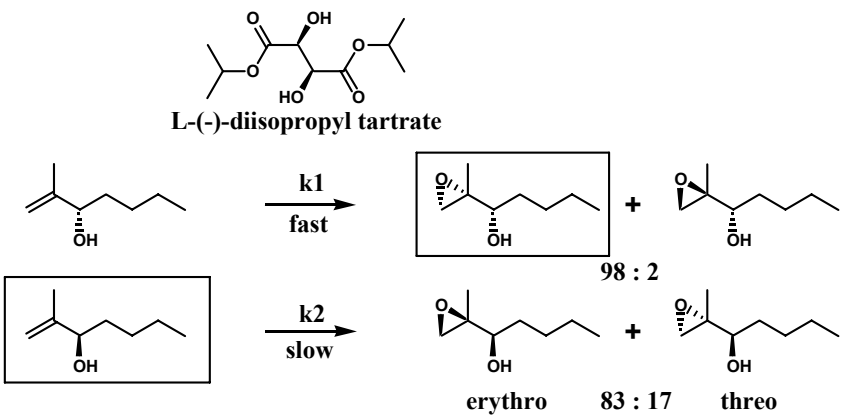

Figure 1 *The Sharpless epoxidation of a racemate of allylic alcohol with the main products in squares*

In order for the kinetic resolution to occur, the rates of reaction of the two enantiomers of the substrate must be different. The selectivity (S) is defined as the ratio of these rates (k1/k2), and can be related to the enantiomeric excess (ee) of the substrate and the conversion (c) by Eq. 1. [5,6]

$$S = \frac{\ln[(1-c)(1-ee)]}{\ln[(1-c)(1+ee)]} \qquad (1)$$

The kinetic resolution is described in Figure 2 for four situations: k1 = k2 (*S*=1), k1 = 1.3k2 (*S*=1.3), k1 = 3k2 (*S*=3) and k1 = 30k2 (*S*=30). Eq. 1 indicates for the Sharpless epoxidation with a selectivity of 138 at 60 % conversion an enantiomeric excess of 99.99999999999%.

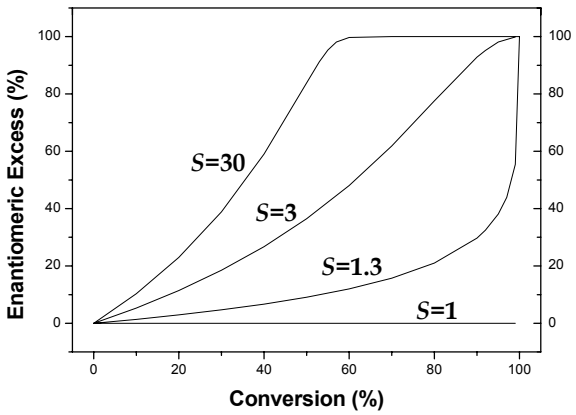

Figure 2 *The theoretical kinetic resolution with different selectivities*

The results described in this chapter regard the kinetic resolution of two allylic nitriles, 2-methyl-3-butenenitrile and 2-cyclohexene-1-carbonitrile. The ideal kinetic resolution of 2-methyl-3-butenenitrile would result in 50 % yield of enantiomerically pure 2M3BN and 50 % 3-pentenenitrile (3PN). The 3PN can be used in the adiponitrile process where adiponitrile is produced in 3 steps, with the last step being the hydrocyanation of 3PN to adiponitrile (see Chapter 1). [7] The ideal kinetic resolution of 2-cyclohexene-1-carbonitrile would result in 100 % enantiomeric pure 2-cyclohexene-1-carbonitrile. [8] In order to achieve the kinetic resolution, a suitable chiral catalyst system is required, which reacts faster with one of the two enantiomers (Figure 3).

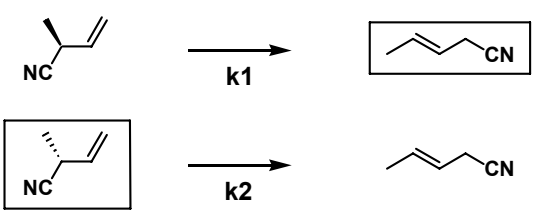

Figure 3 *The kinetic resolution of 2M3BN with the two products in squares if k1>k2*

§ 6.2 Proof of principle

The two enantiomers of 2M3BN can be separated on a chiral GC column (Lipodex E) as is displayed in Figure 4. However, the error in measurement of enantiomeric excess increases during the reaction as the amount of 2M3BN decreases.

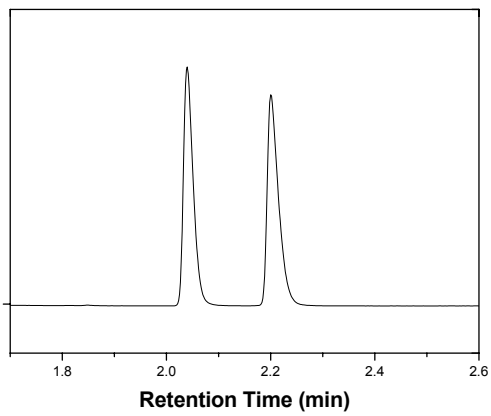

Figure 4 *The separation of both enantiomers of 2M3BN by chiral GC, with integrated area percentages of 49.4 and 50.6*

To achieve kinetic resolution by chemical means, the chiral catalyst system (*S,S*)-BDPP/Ni(cod)$_2$ was selected, as this system proved to be outstanding in turn over frequency (Chapter 3 of this thesis). The reaction was performed at 90 °C in 2 mL of toluene with a substrate to nickel ratio of 142.

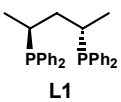

L1

Figure 5 *Ligand (S,S)-BDPP* ***(L1)***

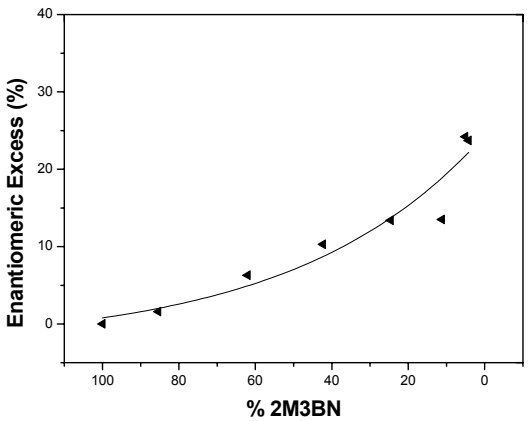

Figure 6 *The kinetic resolution of 2M3BN by **L1**/Ni(0) at 90 °C*

The results of this reaction, displayed in Figure 6, prove that 2M3BN is enantiomerically enriched during the reaction, with a selectivity (k1/k2) of approximately 1.25. This results in an enantiomeric excess of 24 % at the end of the reaction (4% yield in enantiomeric enriched 2M3BN).

§ 6.3 Selection of ligands

The requirements for the ideal catalyst system are both a high k1/k2 ratio and high TOF. However, for this investigation the focus is on the k1/k2 ratio and therefore four different chiral ligands were selected to be screened in the kinetic resolution of 2M3BN, regardless of the activities displayed by the various catalyst systems (Figure 7).

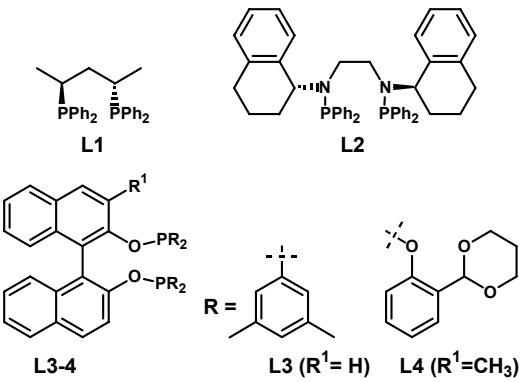

Figure 7 *The selected chiral ligands **L1-L4***

§ 6.4 Kinetic resolution of 2M3BN

Ligands **L1**-**L4** (Figure 7) were applied in the kinetic resolution of 2M3BN in toluene at 90 °C. The results are displayed in Figure 8.

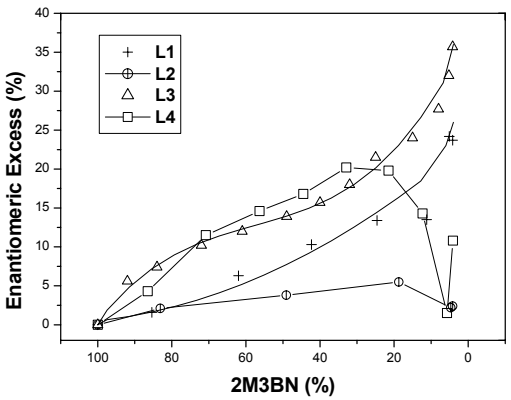

Figure 8 *The kinetic resolution of 2M3BN with **L1**-**L4**/Ni(0)*

The catalyst system based on **L2** gives a maximum enantiomeric excess of 5 %. The highest enantiomeric excess was obtained with ligand **L3**/Ni(0), 37 % at 96 % conversion, which has an estimated selectivity of 1.4. However, the TOF of **L3**/Ni(0) is approximately 30 h^{-1}. With **L1**/Ni(0), the reaction rate is 10 times faster (TOF = 330 h^{-1}) but a somewhat lower enantiomeric excess (25 % at 96 % conversion) was observed. This system was tested at 60 °C, which improves the selectivity from ~1.25 to ~1.4, but the TOF drops to 25 h^{-1} (Figure 9).

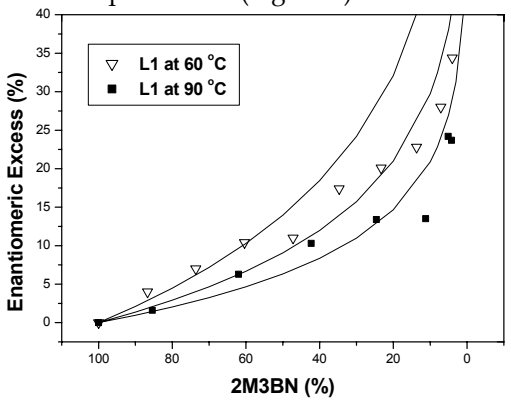

Figure 9 *The kinetic resolution of 2M3BN with **L1** /Ni(0) at 90 and 60 °C, with selectivity lines at S=1.2, 1.3, and 1.5*

Catalytic system **L4**/Ni(0) initially gives the highest selectivity, as at 70 % conversion an enantiomeric excess of 20 % is obtained (Figure 8). However, at this point the selectivity changes towards the other enantiomer, which shows 10 % excess at 96 % conversion. All four systems deviate from the theoretical selectivity lines.

When the conversion is plotted as a function of time zero order kinetics in substrate up to approximately 70 % was observed (Figure 10). Hereafter, the graph deviates from the zero order function. This may be ascribed to the low concentration of 2M3BN over 3PN, which could change the rate-determining step from the reductive elimination to the exchange of the product to the substrate molecule (k1 in Figure 4 in Chapter 3).

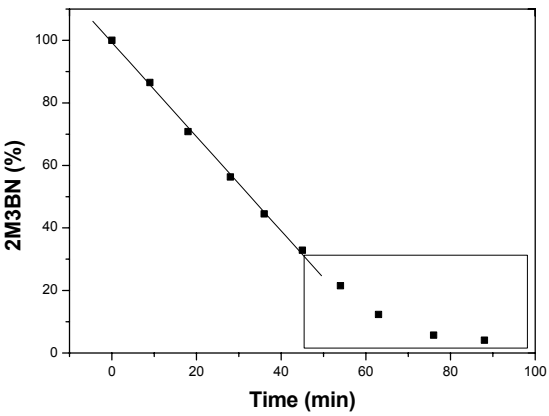

Figure 10 *The isomerization of 2M3BN as function of time with **L4**/Ni(0) at 90 °C, with zero order kinetics up to 70 % (line) and deviation from zero order kinetics (box)*

If the change in enantioselectivity originates from the change in ratio of 2M3BN/3PN, the kinetic resolution of 2M3BN should give a different plot when the reaction is performed with additional 3PN. The results of the two experiments, with and without additional 3PN, are plotted in Figure 11.

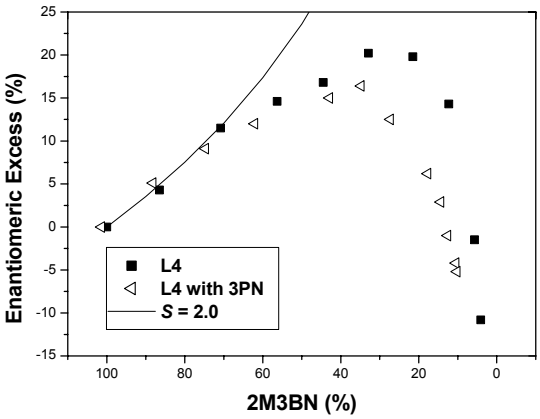

Figure 11 *The kinetic resolution of 2M3BN with **L4**/Ni(0) with different starting ratios of 2M3BN/3PN*

In both experiments the starting concentration of 2M3BN is equal and is set to 100 %. Both experiments give similar results, which proves that the change in enantioselectivity does not originate from the ratio 2M3BN/3PN. However, the origin of the switch in enantioselectivity remains unresolved.

§ 6.4 Kinetic resolution of 2-cyclohexene-1-carbonitrile

In the asymmetric hydrocyanation of 1,3-cyclohexadiene, described in chapter 4, 2-cyclohexene-1-carbonitrile is formed with high enantiomeric excess. Another approach to enantiomeric enriched 2-cyclohexene-1-carbonitrile is to start from the racemic compound and form enantiomerically enriched 2-cyclohexene-1-carbonitrile in a kinetic resolution. Racemic 2-cyclohexene-1-carbonitrile was prepared in a hydrocyanation reaction from 1,3-cyclohexadiene and acetone cyanohydrin. In order for the racemic 2-cyclohexene-1-carbonitrile to be converted into enantiomerically enriched product, the ratio of the rates of oxidative addition of the two enantiomers ($\mathbf{k}^{R}_{oa}/\mathbf{k}^{S}_{oa}$) has to be different from the ratio of reductive elimination ($\mathbf{k}^{R}_{re}/\mathbf{k}^{S}_{re}$), as depicted in Figure 12.

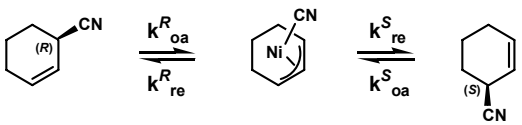

Figure 12 *The kinetic resolution of 2-cyclohexene-1-carbonitrile*

Unfortunately, no kinetic resolution was observed with **L1**/Ni(0) at 90 °C as an isomerization reaction occurs in which 3-cyclohexene-1-carbonitrile is formed (Figure 13).

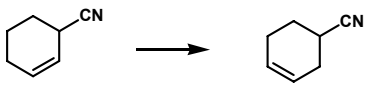

Figure 13 *Isomerization to 3-cyclohexene-1-carbonitrile*

§ 6.5 Conclusions

The kinetic resolution of 2M3BN is possible, however the selectivity needs to be improved as systems **L1**/Ni(0) and **L3**/Ni(0) gave a selectivity of ~1.5. Moreover, for industrial application the kinetic resolution is only feasible with high TOF, whereas these systems react with a modest TOF of ~25 h^{-1}. The kinetic resolution might be preceded by asymmetric hydrocyanation of 1,3-butadiene to increase the enantiomeric excess of the starting material.

None of the 4 tested chiral catalytic systems followed the theoretical selectivity described by Eq. 1. Catalytic system **L4**/Ni(0) showed a switch in enantioselectivity during the kinetic resolution. The origin of this switch remains unresolved but underlines the fact that our understanding of this reaction is still incomplete.

Kinetic resolution of 2-cyclohexene-1-carbonitrile failed as the unwanted isomerization to 3-cyclohexene-1-carbonitrile was observed. However, 2-cyclohexene-1-carbonitrile can be formed with high enantiomeric excess in an asymmetric hydrocyanation reaction as described earlier in chapters 4 and 5.

§ 6.6 Experimental

Typical kinetic resolution of 2M3BN to 3PN

In a nitrogen filled glovebox, a solution of 1.1 equiv. (0.020 mmol) of ligand in 2.0 mL of toluene was added to 5.0 mg (0.018 mmol) $Ni(cod)_2$ in a Schlenk tube and then stirred for 5 minutes. To this solution 0.25 mL (2.60 mmol) 2M3BN was added and the Schlenk tube was placed in an oil bath. Samples for GC analysis were taken over time to determine the TOF (h^{-1}) on a Shimadzu GC-2010 and the enantiomeric excess on a Carlo Erba 6000 Vega series 2.

2-Cyclohexene-1-carbonitrile

To 3.5 mL (35.7 mmol) 1,3-cyclohexadiene was added 20 mg (0.073 mmol) $Ni(cod)_2$ and 68 mg (0.076 mmol) racemic-[1,1']-binaphthyl-2,2'-bis(di(*o*-isopropyl-phenyl)phosphite) and stirred for 10 minutes. Acetone cyanohydrin (4.5 mL, 49.3 mmol) was added and the flask was heated in an oil bath for 6h at 95 ˚C. The reaction was stopped at approximately 90% conversion. Argon was purged through the solution for 5 minutes. Filtration over silica with n-hexanes as eluent followed by evaporation of the volatiles yielded 2.3 g (21.2 mmol, 60 %) of a clear liquid.
^{1}H NMR (200 Mhz, $CDCl_3$): 5.93 (m, 1H), 5.61 (m, 1H), 3.22 (m, CHCN, 1H), 2.12-1.59 (m, 6H), $^{13}C\{^{1}H\}$ NMR (50 Mhz, $CDCl_3$): 131.8, 120.6, 26.4, 26.2, 14.1, 19.9
GC (Lipodex E , 130˚C): 3.30 (49.9%), 3.46 (50.1%)

Kinetic resolution of 2-cyclohexene-1-carbonitrile

In a nitrogen filled glovebox, a solution of 16.0 mg (0.036 mmol) of **L1** in 2.0 mL of toluene was added to 5.0 mg (0.018 mmol) $Ni(cod)_2$ in a Schlenk tube and was stirred for 5 minutes. To this solution 0.25 mL (2.26 mmol) 2-cyclohexene-1-carbonitrile was added and the Schlenk tube was placed in an oil bath. Samples for GC analysis were taken and analyzed on a Carlo Erba 6000 Vega series 2. The main product was identified as 3-cyclohexene-1-carbonitrile by ^{1}H NMR (200 Mhz, $CDCl_3$): 5.73 (m, 1H), 5.61 (m, 1H), 2.80 (m, CHCN, 1H), 2,4-1,8 (m, 6H)

GC analysis

GC:	Shimadzu GC-2010
Column:	DB1 (30 m, 0.32 mm inner diameter)
Carrier gas:	Helium 58.2 kPa
Temperature program:	80 ˚C (8 min), 25 ˚C/min to 250 ˚C
Injector:	280 ˚C
Detector:	270 ˚C
Split ratio:	200
Injection volume:	1.0 μL

Table 1 *Retention times*

Compound	Retention time (min)
2M3BN	3.77
tr-3PN	5.21
2M2BN	4.20, 5.13
2PN	4.38
Toluene	5.53

Chiral GC

GC:	Carlo Erba 6000 Vega series 2
Column:	Lipodex E (25 m, 0.25 mm inner diameter)
Carrier gas:	Hydrogen 50 kPa
Temperature program:	2.5 min at 95 ˚C, 17.5 ˚C/min to 140 C
Injector:	280 ˚C
Detector:	280 ˚C
Split ratio:	25
Injection volume:	0.25 μL

Table 2 *Retention times*

Compound	Retention time (min)
toluene	1.50
2M3BN	2.03, 2.21
2M2BN	2.16, 2.68
tr-3PN	2.80

§ 6.7 References

[1] Moss, G. P. *Pure Appl. Chem.* **1996**, *68* (12), 2193-2222.
[2] Martin, V. S., Woodard, S. S., Katsuki, T., Yamada, Y., Ikeda, M., and Sharpless, K. B. *J. Am. Chem. Soc.* **1981**, *103* (20), 6237-6240.
[3] Whitesides, G. M. and Wong, C. H. *Angew. Chem.* **1985**, *97* (8), 617-638.
[4] Jones, J. B. *Tetrahedron* **1986**, *42* (13), 3351-3403.
[5] Kagan, H. B. and Fiaud, J. C. *Top. Stereochem.* **1988**, *18*, 249-330.
[6] Goodman, J. M., Kohler, A. K., and Alderton, S. C. M. *Tetrahedron Lett.* **1999**, *40* (49), 8715-8718.
[7] Tolman, C. A., McKinney, R. J., Seidel, W. C., Druliner, J. D. and Stevens, W. R. *Adv. Catal.* **1985**, *33*, 1-46.
[8] Gruber, C. C., Lavandera, I., Faber, K., and Kroutil, W. *Adv. Synth. Catal.* **2006**, *348* (14), 1789-1805.

Summary

The Nickel-Catalyzed Hydrocyanation of Vinylarenes and Dienes
Mechanism and Application

The nickel-catalyzed hydrocyanation of olefins is an elegant carbon-carbon bond formation reaction resulting in nitrile products, which are suitable for transformation into a variety of other functional groups. The adiponitrile process, developed in the 1970s, is one of the largest industrial homogeneously catalyzed reactions. The state of the art of the nickel-catalyzed hydrocyanation has been described in Chapter 1.

The isomerization of the branched 2-methyl-3-butenenitrile (2M3BN) to the linear 3-pentenenitrile (3PN) by a DPEphosNi-species has been investigated as a model reaction for the hydrocyanation in Chapter 2. The catalyst precursor DPEphosNi(cod) has been characterized by X-ray diffraction and its reactivity has been investigated. An intermediate in this reaction, which is formed via carbon-carbon bond activation, could be trapped by addition of $ZnCl_2$ and the molecular structure of the corresponding Ni(II)-complex has been determined crystallographically. A range of diphosphine ligands was applied in the isomerization of 2M3BN and in the hydrocyanation of styrene, with (*S*,*S*)-BDPP being the superior ligand in TOF for the isomerization and conversion for the hydrocyanation.

In Chapter 3, the isomerization of the branched unsaturated nitrile 2M3BN to the linear analogue 3PN has been investigated kinetically, using an automated experimental set-up. The equilibrium of the active catalyst with all other nickel-complexes proved to be important in order to determine the activation parameters $\Delta H^{\ddagger}$, $\Delta S^{\ddagger}$. Unfortunately, the equilibrium constant could not be determined. Therefore, a simplified but still informative parameter was introduced and studied: the combined initial concentration of nickel-precursor and ligand, $[Ni(cod)_2, L]_i$. It is shown that the reaction rate law order in $[Ni(cod)_2, L]_i$ is dependent on the ligand

system. This indicates that a two-reaction pathway is more probable than a catalytic cycle based on a mononuclear complex.

In Chapter 4, a series of chiral (*R*)-binaphthol-based diphosphite ligands with different substituents were prepared and applied in the asymmetric hydrocyanation of styrene and 1,3-cyclohexadiene, to investigate the influence of their steric properties. The optimal steric properties for the ligands used in the hydrocyanation reaction are defined within a narrow window. With the optimized ligand, hydrocyanation of styrene gave full conversion (Subs/Ni = 100) with 49 % ee, and the TON was determined to be 600. Hydrocyanation of 1,3-cyclohexadiene gave 50 % conversion (Subs/Ni = 500) with an excellent ee of 86 %. This demonstrates that high ee's are not only accessible for vinyl arenes but also for conjugated dienes in the asymmetric nickel-catalyzed hydrocyanation.

The reductive elimination of the product has been established to be the enantioselective step in the nickel-catalyzed hydrocyanation of 1,3-cyclohexadiene by determining the 1,2-/1,4-product distribution on the basis of deuterium labeling experiments, which is described in Chapter 5. This result could be achieved by successfully exploiting the rather unique features of this reaction: identical product formation for 1,2- and 1,4-addition, *cis*-addition over the diene and high enantiomeric excess.

Finally, the kinetic resolution of 2-methyl-3-butenenitrile using chiral phosphorus based ligands with $Ni(cod)_2$ is described in Chapter 6, with selectivities up to 2.0. Moreover, an interesting switch in enantioselectivity was observed during the kinetic resolution. The kinetic resolution of 2-cyclohexene-1-carbonitrile, synthesized by a preparative hydrocyanation of 1,3-cyclohexadiene, resulted in double bond isomerization to 3-cyclohexene-1-carbonitrile.

Samenvatting

De Nikkel Gekatalyseerde Hydrocyanering van Vinylarenen en Dienen Mechanisme en Toepassing

De nikkel gekatalyseerde hydrocyanering van olefines is een elegante reactie waarin een koolstof-koolstof binding wordt gevormd. Dit resulteert in nitril gefunctionaliseerde producten, die omgezet kunnen worden in een groot aantal verschillende verbindingen. Het adiponitril proces, ontwikkeld in the 70'er jaren van de vorige eeuw, is één van de grootste industrieel gebruikte homogeen gekatalyseerde reacties. De stand van zaken op het gebied van de nikkel gekatalyseerde hydrocyanering is beschreven in Hoofdstuk 1.

De isomerisatie van het vertakte 2-methyl-3-buteennitril (2M3BN) naar het lineaire 3-penteennitril (3PN) door een DPEphosNi-complex, gebruikt als modelreactie voor de hydrocyanering, is beschreven in Hoofdstuk 2. De precursor van de katalysator, DPEphosNi(cod), is gekarakteriseerd door middel van röntgen diffractie en de reactiviteit ervan is onderzocht. Een intermediair in deze reactie, dat wordt gevormd door activering van een koolstof-koolstof binding, kon worden geïsoleerd door toevoeging van $ZnCl_2$ en de moleculaire structuur is kristallografisch bepaald. Een aantal difosfine liganden zijn getest in de isomerisatie van 2M3BN en in de hydrocyanering van styreen. Van de geteste liganden gaf (*S*,*S*)-BDPP de hoogste snelheid in de isomerisatie en de hoogste conversie in de hydrocyanering van styreen.

De isomerisatie van het vertakte onverzadigde nitril 2M3BN naar het lineaire 3PN is kinetisch onderzocht, door gebruik te maken van geautomatiseerde technieken en beschreven in Hoofdstuk 3. Het evenwicht van de katalysator met de overige nikkel verbindingen bleek belangrijk te zijn om de activerings parameters $\Delta H^{\ddagger}$, $\Delta S^{\ddagger}$ te bepalen. De evenwichtsconstante kon helaas niet worden bepaald. Daarom is er een andere parameter geïntroduceerd en bestudeerd: de gecombineerde concentratie van nikkel precursor en ligand, $[Ni(cod)_2, L]_i$. Het blijkt dat de orde van de reactie snelheids vergelijking afhankelijk is van het ligand

systeem. Hieruit volgt dat het meer waarschijnlijk is dat de reactie via twee reactiepaden verloopt dan een katalytische cyclus die alleen gebaseerd is op een mononuclear complex.

In Hoofdstuk 4 zijn een aantal chirale difosfiet liganden, gebaseerd op (*R*)-binaphthol met verschillende substituenten gesynthetiseerd en toegepast in de asymmetrische hydrocyanering van styreen en 1,3-cyclohexadieen. Dit om te onderzoeken hoe de sterische eigenschappen van het ligand de reactie beïnvloeden. De optimale sterische eigenschappen voor de hydrocyanering bevinden zich binnen kleine marges. Het geoptimaliseerde ligand gaf in de hydrocyanering van styreen volledige conversie (Styreen/Ni = 100) met 49 % ee, de maximale TON was 600. Hydrocyanering van 1,3-cyclohexadieen gaf 50 % conversie (1,3-Cyclohexadieen/Ni = 500) met een excellente ee van 86 %. Dit demonstreert dat hoge ee's niet alleen mogelijk zijn voor vinyl arenen maar ook voor geconjugeerde dienen in de asymmetrische nikkel gekatalyseerde hydrocyanering.

Door het bepalen van de 1,2-/1,4-product verhouding kan worden geconcludeerd dat de reductieve eliminatie van het product de enantioselectieve stap is in de nikkel gekatalyseerde hydrocyanering van 1,3-cyclohexadieen. Dit, beschreven in Hoofdstuk 5, kon worden bepaald door de reactie uit te voeren met deuterium cyanide. Deze conclusie kon worden getrokken door succesvol gebruik te maken van de unieke eigenschappen van deze reactie: gelijke product vorming van de 1,2- en 1,4-product, *cis*-additie over het dieen en hoge ee.

Ten slotte is in Hoofdstuk 6 de kinetische resolutie van 2M3BN beschreven met katalysatoren, bestaande uit een chiraal op fosfor gebaseerd ligand en $Ni(cod)_2$, met selectiviteiten tot 2.0. Hierbij is een interessante verandering in enantioselectiviteit waargenomen. De kinetische resolutie van 2-cyclohexeen-1-carbonitril, gesynthetiseerd door hydrocyanering van 1,3-cyclohexadieen, resulteerde in een isomerisatie van de dubbele binding naar 3-cyclohexeen-1-carbonitril.

Dankwoord

Na 4 vooral leuke jaren me te hebben toegelegd op mijn promotieonderzoek wil ik nu eindelijk alle mensen die me hebben geholpen bedanken. Mocht U niet genoemd worden terwijl U dit wel verwacht zal dit waarschijnlijk betekenen dat U de schrijver van dit proefschrift op een grove fout heeft betrapt waarvoor ik mij dan ook onmiddellijk wil en moet excuseren. Wellicht dat het niet verkeerd is om hier te melden dat een wetenschapper ook maar een mens is.

Tijdens de start denk je als naïve beginnende aio dat je alles zelf wel kunt, maar al snel kom je er achter dat je niet zonder je mede aio's en postdocs zoals Vincent, Jarl, Niek, Ruben, Eric, Mabel, Michiel, Rafael en Gijsbert, en zeker niet zonder je technische collegas kunt. Vaak ben je er dan ook van overtuigd dat zij, vooral Ton en Wout (maar ook Robert, Tiny en Frans), belangrijker zijn voor de afdeling dan de wetenschappelijke staf. Maar de wetenschappelijke staf, Christian, Erik en Dieter, heeft ook zeker zijn positieve inbreng gehad, vaak met wilde ideeën, soms met pasklare antwoorden en regelmatig met een koffietje.

Door de nieuwe lichting aio's realiseer je hoeveel dank je verschuldigd bent aan de aio's die je op gang hebben geholpen wat een hoop moeite kost, maar als een ieder dan zijn/haar draai heeft gevonden, lijkt het alsof er niets is veranderd en blijft de bierconsumptie onveranderd hoog tijdens de vele borrels. Zij die regelmatig bij de koffie of borrel aanwezig waren, of zelfs mee gingen op ski-vakantie, danwel af en toe mee bier gingen halen, Thijs, Joost, Dilip, Patrick, Jarno, Paul, Leandra, Daniel, Jose, Bart, Peter, Bouke, Willi, Esther, Chrétien, Sander, Laura, Neelesh, Nollaig, Emiel, Maria, Han, Davy, Zhang, Gilbère, Barry en Evgeny worden dan ook van harte bedankt.

De sfeer op de afdeling was eigenlijk altijd goed, regelmatig gingen we naar de bios, eens per jaar op groepsweekend (waar we de koppen weer dezelfde richting in probeerden te zetten), naar de Binodrome een filmpje kijken met een gecaterd diner, danwel een bezoekje aan de Effenaar, het terras, of gewoon naar Stratum. Het maakte niet uit, gezelligheid was troef. Zelfs als we meerdere wedstrijden verloren tijdens het NIOK voetbaltoernooi (gelukkig was ik er al bij toen we de cup mee naar

Eindhoven mochten nemen). Voetbal kijken deed ik (jammergenoeg) veel vaker dan voetballen. Thijs moet ik dan ook enorm bedanken vanwege de vele gezellige en voedzame PSV-Championsleague avonden, gelukkig vaak met goede afloop. En ook Tiny voor het organiseren van de SKA-PSV beker wedstrijden.

Als ik dan weer naar huis ging na een dag van werken waren er gelukkig ook daar weer mensen waar je je eventuele opgelopen frustraties (het was natuurlijk niet altijd even gezellig, vooral wanneer de moleculen zich wat opstandig gedroegen) danwel blijdschappen bij kwijt kon onder het genot van een flesje wijn of een lekker glaasje vodka, Paul, Bart (ook voor het regelmatig rennen) en Geert bedankt! Het relativerend vermogen van het huis werd vooral duidelijk toen anderen probeerden hun frustraties te botvieren op ons huis (of eigenlijk op de school tegenover).

Dan is er natuurlijk 't Huukske, met De D, de Pool, Nico, Magic, BartverH, Krul, Flo, Renoud, Q, en de Geus als members, waar onder het genot van genoeg bier alles zorgenloos geschreeuwd en soms gevoetbald mag worden. Huukskedag tijdens de zomerfeesten staat natuurlijk altijd weer voor dolle pret, en hopelijk krijgt het Huukske weekend een passend vervolg.

Voor de meer serieuze gesprekken waren daar dan weer anderen zoals Bas, Monique en Marleen. U alle drie succes met uw nieuwe huis met oppas danwel uw appartement. Omdat promoveren door velen als serieuze bezigheid wordt gezien zal het niemand verbazen dat Bas en Marleen mij zullen bijstaan als paranimfen tijdens de openbare verdediging van dit proefschrift.

Veel studenten hebben we niet op de afdeling, waarschijnlijk omdat we chemische technologie vanuit de chemie benaderen en de meeste studenten in Eindhoven toch liever vanuit de technologie denken. Die ene studente die ik dan heb mogen begeleiden kwam dan ook niet van de Technische Universiteit Eindhoven maar van de Radboud Universiteit te Nijmegen. Ze heeft het gelukkig erg goed gedaan en ze mocht dan ook gelijk bij ons op de afdeling aio worden, hopelijk met veel succes. Verder is ze als persoon gewoon geweldig en verdient ze zelfs heel veel dank.

Ook was ik altijd weer blij als mijn ouders mij weer eens een 3-gangen diner voor schotelden waar ik dan steeds (tevergeefs?) probeerde uit te leggen waar ik toch precies mee bezig was. Nu jullie net zijn afgewerkt hoop ik dat jullie heel veel plezier gaan beleven tijdens jullie pensioen!

Tot slot moet ik Michèle, Jarl, Vincent, EZ, Christian en Dieter bedanken voor het corrigeren van mijn proefschrift, in een vroeg danwel allerlaatst stadium, en mijn vader voor de opmaak van de kaft.

Zonder al jullie hulp was deze wetenschappelijke proeve op het gebied van de nikkel gekatalyseerde hydrocyanering zeker en vast op niets uitgelopen.

Nogmaals bedankt!

Jos

Publications

Jos Wilting, Michèle Janssen, Christian Müller, Martin Lutz, Anthony L. Spek and Dieter Vogt. Binaphthol-Based Diphosphite Ligands in Asymmetric Hydrocyanation of Styrene and 1,3-Cyclohexadiene: Influence of Steric Properties, *Advanced Synthesis & Catalysis* **2006**, *accepted for publication*

Jos Wilting, Michèle Janssen, Christian Müller, Dieter Vogt. The Enantioselective Step in the Nickel-Catalyzed Hydrocyanation of 1,3-Cyclohexadiene. *Journal of the American Chemical Society* **2006**, 128 (35), 11374-11375

Jos Wilting, Dieter Vogt. Asymmetric Hydrocyanation of Alkenes. In *Handbook of C-H Transformations*, 1st ed.; Dyker, G., Ed.; Wiley-VCH: Weinheim, **2005**; Vol. 1 pp 87-96.

Jos Wilting, Christian Müller, Alison C. Hewat, Dianne. D. Ellis, Duncan M. Tooke. Anthony L. Spek, Dieter Vogt. Nickel-Catalyzed Isomerization of 2-Methyl-3-butenenitrile. *Organometallics* **2005**, *24* (1), 13-15.

Duncan M. Tooke, Jos Wilting, Dieter Vogt, Anthony L. Spek. 2-(Diphenylphosphino)phenyl-2-(diphenylphosphinoyl)phenyl ether. *Acta Crystallographica, Section E: Structure Reports Online* **2005**, *E61* (8), o2406-o2407.

Bas de Bruin, Theo P.J. Peters, Jos B.M. Wilting, Simone Thewissen, Jan M.M. Smits, Anton W. Gal. Dioxygenation of Sterically Hindered (Ethene)Rh(I) and –Ir(I) Complexes to (Peroxo)Rh(III) and (Ethene)(Peroxo)Ir(III) Complexes. *European Journal of Inorganic Chemistry* **2002**, (10), 2671-2680.

Bas de Bruin, Theo P.J. Peters, Simone Thewissen, Arno N.J. Blok, Jos B.M. Wilting, Rene de Gelder, Jan M.M. Smits, Anton W. Gal. Dioxygen Activation by a Mononuclear Ir(II)-ethene Complex. *Angewandte Chemie, International Edition* **2002**, *41* (12), 2135-2138.

Curriculum Vitae

Jos Wilting was born in Hoogeloon, the Netherlands, on the 8th of January 1979. In 1997 he graduated from the Pius X college in Bladel and started his chemistry studies at the Radboud University in Nijmegen. His graduation project was in the metal organic chemistry group of Prof.dr. A.W. Gal under supervision of Dr. Bas de Bruin concerning oxidation of iridium complexes by molecular dioxygen. Hereafter, he visited the group of Prof.dr. K. Wieghardt at the Max Planck Institute for bioinorganic chemistry in Mülheim a/d Ruhr for a research project on N2S2-iron complexes. In 2002, he started his PhD research in the group of Prof.dr. Dieter Vogt, at Eindhoven University of Technology, on Nickel-catalyzed hydrocyanation, which resulted in this thesis. He is currently working for Hybrid Catalysis B.V. as scientist high-throughput experimentation.

Jos Wilting werd in Hoogeloon geboren op 8 januari 1979. In 1997 behaalde hij zijn VWO diploma aan het Pius X college te Bladel en begon aan de studie scheikunde aan de Radboud Universiteit Nijmegen. Zijn afstudeerstage werd in de metaal organische chemie groep van Prof.dr. A.W. Gal volbracht onder begeleiding van Dr. Bas de Bruin. Deze stage betrof de oxidatie van iridium complexen door moleculair zuurstof. Hierna heeft hij in de group van Prof.dr. K. Wieghardt aan het Max Planck Insituut voor bio-anorganische chemie in Mülheim a/d Ruhr een onderzoeks project gedaan betreffende N2S2-ijzer complexen. In 2002 is hij begonnen als promovendus in de groep van Prof.dr. Dieter Vogt, aan de Technische Universiteit Eindhoven, op het onderwerp nikkel gekatalyseerde hydrocyanering, wat heeft geresulteerd in dit proefschrift. Momenteel is hij werkzaam voor Hybrid Catalysis B.V.